

**International
Progress Report**

IPR-04-53

Äspö Hard Rock Laboratory

Canister Retrieval Test

**Sensors data report
(Period 001026-041101)
Report No:9**

Reza Goudarzi
Lennart Börgesson
Clay Technology AB

Kennert Röshoff
Martin Edelman

BBK

November 2004

Svensk Kärnbränslehantering AB

Swedish Nuclear Fuel
and Waste Management Co
Box 5864
SE-102 40 Stockholm Sweden
Tel 08-459 84 00
+46 8 459 84 00
Fax 08-661 57 19
+46 8 661 57 19



**Äspö Hard Rock
Laboratory**

Report no.	No.
IPR-04-53	F69K
Author	Date
Reza Goudarzi	Nov. 2004
Lennart Börgesson	
Kennert Röshoff	
Martin Edelman	
Checked by	Date
Lennart Börgesson	2004-12-29
Approved	Date
Christer Svemar	2005-01-12

Äspö Hard Rock Laboratory

Canister Retrieval Test

Sensors data report (Period 001026-041101) Report No:9

Reza Goudarzi
Lennart Börgesson
Clay Technology AB

Kennert Röshoff
Martin Edelman
BBK

November 2004

Keywords: Buffer, Bentonite, Rock, Temperature, Stress, Strain, Test, Measurements, Swelling, Full scale, In-situ

This report concerns a study which was conducted for SKB. The conclusions and viewpoints presented in the report are those of the author(s) and do not necessarily coincide with those of the client.

Abstract

This report presents data from the measurements in the Canister Retrieval Test from 001026 to 041101.

The following measurements are made in the bentonite: Temperature is measured in 32 points, total pressure in 27 points, pore water pressure in 14 points and relative humidity in 55 points. Temperature is also measured by all relative humidity gauges. The positions of the measuring points in the bentonite are related to a coordinate system in the deposition hole.

The following measurements are made in the rock: Temperature is measured in 40 points, stresses are measured in 8 points and strain is measured in 9 points. Stresses and strains are also measured in the rock around the empty deposition hole located 6 m south of the test hole.

The following measurements are made in the canister: Temperature is measured every meter along two fiber optic cables and strain is measured in 76 points on the surface of the copper envelop. Temperature is measured in the steel insert in 18 points.

The following measurements are made on the plug: Force is measured in 3 of the 9 anchors and vertical displacement is measured in three points.

The water inflow to the filter mats on the rock surface is also measured.

The general conclusion is that the measuring systems and transducers seem to work well except for the transducers inside the canister and Kulite pressure transducers. The following problems have been noted: The strain measurements in the canister are not reported due to question marks regarding the relevance of the results. Most Vaisala relative humidity transducers have failed due to water saturation. Five out of six Kulite total pressure transducers seem to yield erroneous results. All temperature sensors inside the canister except one have stopped functioning.

Some heaters in the canister failed in December 2003. In order to reduce the risk of further problems the power was decreased to 1600 W.

Some heaters in the canister failed again during this half year (in September and October) but power is still 1600 W.

The wetting has continued during and partly been accelerated due to the applied high water pressure in the mats and the relative humidity sensors indicate that the bentonite between the rock and the canister is close to water saturation although the wetting still seems to be somewhat uneven and the total pressure has not reached the expected values yet. Some clogging of the filters may explain the inhomogeneous appearance. The influence of the neighboring test TBT is seen with increasing temperatures but the reduced power has affected both the temperature and the measured total pressure and the temperature has been constant in almost all transducers during the last half-year.

Sammanfattning

I denna rapport presenteras data från mätningar i Återtag under perioden 001026-041101.

Följande mätningar görs i bentoniten: Temperaturen mäts i 32 punkter, totaltryck i 27 punkter, porvattentryck i 14 punkter och relativa fuktigheten i 55 punkter. Temperaturen mäts även i alla relativa fuktighetsmätare. Varje mätpunkt relateras till ett koordinatsystem i deponeringshålet.

Följande mätningar görs i berget: Temperaturen mäts i 40 punkter, bergspänningar mäts i 8 punkter och töjningar i 9 punkter. Bergspänningar och töjningar mäts också i berget runt det tomma deponeringshålet 6 m söder om försökshålet.

Följande mätningar görs på ytan i kapselns kopparhölje: Temperaturen mäts varje meter längs två fiberoptiska kablar och töjning mäts i 76 punkter. Temperaturen mäts i stålinsatsen i kanistern i 18 punkter.

Följande mätningar görs på pluggen: Kraften mäts i 3 av de 9 stagen och vertikala förskjutningen mäts i tre punkter.

Vatteninflödet till filtermattorna mäts också.

En generell slutsats är att mätsystemen och givarna tycks fungera bra förutom givarna inuti kapseln och Kulites givare. Följande problem har noterats: Töjningsmätningarna i kapseln har inte redovisats p. g. a frågetecken beträffande mätresultatens relevans. De flesta av Visalas relativa fuktighetsmätare, har slutat fungera p. g. a. hög vattenmättnadsgrad. Fem av sex Kulite totaltrycksgivare tycks ge felaktiga resultat idag. Alla temperaturgivare inuti kapseln har slutat fungera.

Fel uppstod på några värmare i kapseln i december 2003. För att minska risken för ytterligare problem sänktes effekten till 1600 W.

Fel uppstod återigen på några värmare i kapseln två gånger under det senaste halvåret (september och oktober) men effekten är fortfarande 1600 W.

Bevätningen har fortsatt och delvis accelerats pga det pålagda vattentrycket i mattorna och fuktighetsmätarna indikerar att bentoniten mellan berget och kapseln är nära vattenmättad, fastän bevätningen fortfarande tycks vara något ojämn och totaltrycket ännu inte har nått de förväntade värdena. En viss igensättning av filterna kan förklara det inhomogena uppförandet. En fortgående höjning av temperaturerna noteras under det senaste året p.g.a.påverkan från det initilliggande försöket TBT, men den sänkta effekten har påverkat både temperaturerna och det mätta trycket och temperaturen har varit konstant i så gott som samtliga givare under det senaste halvåret.

Contents

1	Introduction	9
2	Comments	11
2.1	General	11
2.2	Total pressure, Geokon (App. A pages 35-38)	12
2.3	Total Pressure, Kulite (App. A page 39)	12
2.4	Suction, Wescore Psychrometers (App. A pages 40-49)	12
2.5	Relative humidity, Vaisala (App. A pages 50-54)	13
2.6	Pore water pressure, Geokon (App. A pages 55-56)	13
2.7	Pore water pressure, Kulite (App. A page 57)	13
2.8	Water flow into the filters (App. A page 58)	13
2.9	Forces on the plug (App. A page 59)	14
2.10	Displacement of the plug (App. A page 60)	14
2.11	Canister power (App. A page 61)	14
2.12	Temperature in the buffer (App. A pages 62-66)	14
2.13	Temperature in the rock (App. A pages 67-70)	15
2.14	Temperature on the canister surface, Optical fiber cables (App. A pages 71-72)	15
2.15	Temperature inside the canister (App. A pages 73-75)	15
2.16	Strain in the canister	15
2.17	Rock stresses and strains	15
3	Geometry	17
4	Location of instruments	19
4.1	Brief description of the instruments	19
4.2	Strategy for describing the position of each device	20
4.3	Position of each instrument in the bentonite	21
4.4	Instruments in the rock	26
4.5	Instruments in the canister	27
4.6	Instruments at the plug	30
	References	31
	Appendix A: Results	33
	Appendix B: Stress and strain measurements of the rock mass	77

1 Introduction

The installation of the Canister Retrieval Test was made during autumn 2000. In general the data in this report are presented in diagrams covering the time period 2000-10-26 to 2004-11-01. The time axis in the diagrams represents days from 2000-10-26. The diagrams are attached in Appendix A. The stress and strain measurements in the rock are reported separately by BBK. That report is attached as Appendix B.

A test overview with the positions of the measuring points and a brief description of the instruments is also presented in this report (chapters 3 and 4).

General comments concerning the collected data are given in chapter 2.

2 Comments

2.1 General

In this chapter short comments on general trends in the measurements are given. Sensors that are not delivering reliable data or no data at all are noted and comments on the data in general are given.

The slot between rock and bentonite block was filled with bentonite pellets and water on 001026. This date is also marked as start date. 1 m water head in the water supply tank was connected to the filters on 001102.

The heating of the canister started with an initially applied constant power of 700 W at 001027 that is one day after test start. The power was raised to 1700 W on 001113. The power was further raised to 2600 W on 010213.

At the end of 2001 two of the 36 electrical heaters failed due to short circuit to earth and no power was generated during one day between November 5 and 6, 2001 (day 375). The heaters were also shut off during one week between March 4 and 11 2002 (days 495 to 502) for control measurements. The water pressure in the mats was stepwise increased to 800 kPa in the period 5/9 – 10/10 2002 (days 687-713). The power of the heaters in the canister was reduced to 2100 W on day 683 (10/9 –02) and to 1600 W on day 1135 (4/12 –03). The later reduction was done after another heater failure that took place on day 1134 (3/12 –03). The power was down for about a day.

There were problems with the heaters resulting in short power failures at two occasions in this measuring period: (2004-09-07 (day 1412) and 2004-10-03 (day 1438)).

The water pressure was temporarily reduced to 100 kPa during the period 5/12 2002 – 9/1 2003 (days 770-805) and to 400 kPa during the period 9/1 2003 – 23/1 2003 (days 805-819).

The following events, which may be important for understanding the results, have occurred during this reporting half-year period:

- 040822: The mats were back flushed.
- 041013: The mats were back flushed.

It should also be mentioned that the actual power from start until the latest heater failure (day 1135) has been higher than indicated by the measurements. See chapter 2.11.

The eighth report covered the period up to 040501. This report is the ninth one and covers the results up to 041101.

2.2 Total pressure, Geokon (App. A pages 35-38)

The measured pressure range is from 0 to 7.0 MPa. The highest pressure is indicated in the periphery of the bottom block (C1) and the center ring (R5), where all transducers yield a pressure between 3.4 and 7.0 MPa. All sensors situated outside the canister radius, yield a swelling pressure higher than 2.0 MPa. The influence of the reduced power and subsequent temperature decrease was reflected in a pressure reduction of several MPa and the pressure has now after long time finally reached the earlier level.

Sensor P104 was not installed. U106 was originally intended to be a pore pressure sensor but was replaced by a total pressure sensor. One of 21 sensors is out of order.

2.3 Total Pressure, Kulite (App. A page 39)

Six Kulite total pressure transducers are installed in the bentonite blocks. Unfortunately they don't work properly. The reason for the malfunction is probably brakeage of the transducer connections at high pressures.

One sensor (P221) did not work from start 3 stopped working earlier and the two remaining transducers are having problems and did not yield reliable values during about one year period. One of them (P217) started to work again during measuring period (1300 KPa) and the other (P227) started to work again during last measuring period (900 KPa) but these two sensors are placed in then centre above the canister and yield low measured pressure.

2.4 Suction, Wescor Psychrometers (App. A pages 40-49)

Wescor psychrometers are only working at suction below 5000 kPa, which correspond to high relative humidity (above about 96%). 23 out of 26 transducer yield values that can or could be evaluated and have thus a high relative humidity. 9 out of these 23 are drowned meaning that the sensors are probably filled with water. The remaining three sensors (of all 26) have not yet a high enough relative humidity to yield readable values. The interpretation of the values should be done with care since the evaluation is done with an automatic technique and the plateau required for proper evaluation not always formed. This explains why most transducers start their appearance from very low value. These low values are not correct but only an indication of that the relative humidity or suction is getting close to the measuring range. All diagrams are included (also diagrams with no evaluated values).

In Ring 5 eight out of nine transducers are indicating a high relative humidity (measurable suction), which confirm the total pressure measurements. In ring 10 all eight transducers indicate a high relative humidity.

2.5 Relative humidity, Vaisala (App. A pages 50-54)

Relative humidity and temperature are also measured with Vaisala transducers. The relative humidity results and the temperature results in ring 10 have been split into two diagrams (pages 52 and 53) since the data were interfering with each other.

All transducers in Cyl.1, Ring5 and Ring10 had stopped to work. However, W101 placed in the centre below the canister started to work after 850 days and the three dry transducers placed centrally above the canister have started to function again. The wetting has reached these positions and the drying has turned into a wetting that now has passed the original RH.

The reason for the successive malfunction is not clear but the transducers do not work very well at high relative humidity. All transducers between the rock and the canister in rings 5 and 10 indicate a high degree of saturation, which confirm the results of the Wescor psychrometers.

1 of the sensors that were malfunctioning has started to work again during this measuring period.

17 out of 25 sensors are out of order. The major reason for malfunction is high degree of saturation.

2.6 Pore water pressure, Geokon (App. A pages 55-56)

Four transducers in Ring 5 yield a water pressure of between 750 and 1300 kPa. One transducer (U104) in Cyl.1 yields water pressure of about 560 kPa. The remaining sensors of this type show low pressure (0-220 kPa). The influence of the temperature decrease after the power failure on day 1135 is strong.

U106 is replaced by a total pressure sensor.

1 out of 11 sensors is out of order.

2.7 Pore water pressure, Kulite (App. A page 57)

There are only one sensor of this type in Ring 10 and one in Cylinder 4. None of them have shown any increase in pore pressure.

2.8 Water flow into the filters (App. A page 58)

Measurement of water inflow into the filters started at 001102. The total inflow to the filters has since that date been 639 liter.

The inflow rate has strongly increased after start pressurizing the water in the mats at 020905 (day 678). The inflow is at present about 0.30 l/day.

2.9 Forces on the plug (App. A page 59)

The forces on the plug have been measured since 001106. The total force is about 8505 kN on 041101 and is steadily increasing.

During the first about 50 days the plug was only fixed with 3 rods. When the total force exceeded 1500 kN the rest of the 9 rods were fixed in a prescribed manner. This procedure took place 12-14 December 2000 that is 46-48 days after test start. From that time only every third anchor is measured and the results should thus be multiplied with 3. The diagram shows both the actual measurements and after multiplication with 3.

2.10 Displacement of the plug (App. A page 60)

One transducer shows a logical steady upwards displacement of the plug, while two transducers act strangely.

2.11 Canister power (App. A page 61)

The power 1600 W has been kept constant since the reduction on day 1135.

The power 2100 W was measured by direct measurement regularly. However, an alternative technique for measuring the power showed for some canisters in the Prototype Repository a different power. This technique, which consists in measurement of the entire energy consumed by the canister, was used to measure the average power of the canister in CTR during four weeks (45-48). The result was a conclusion that the average power was not 2100 W but 2220 W. This difference seems to have endured up to the latest power failure. After reduction in power to 1600W the two techniques agree. The new equipment for continuous measurement and calculation of the entire energy consumed by the canister was installed on 2004-01-28.

There were problems with the heaters at two occasions (2004-09-07 (day 1412) and 2004-10-03 (day 1438)). Additional heater elements were lost at those occasions. Now there are 16 functioning elements out of 36. 7 elements are needed to keep the power.

2.12 Temperature in the buffer (App. A pages 62-66)

After reduction of power at 031204 (day 1135) from 2200 W to 1600 W the highest measured temperature near the canister in Ring 5 has decreased from 78 °C to 64 °C. The temperatures have been rather constant during the last half year.

The highest temperature gradient is about 0.50 degrees/cm (ring 5).

2.13 Temperature in the rock (App. A pages 67-70)

The maximum temperature measured in the rock (53 degrees) is measured in the central section on the surface of the deposition hole. There was an almost complete axial symmetry of the temperature measured in the rock until day 880. The late disturbance of this trend with mainly increasing temperature in direction A (north) is caused by the neighboring experiment TBT that started its heating at 030326. However, during the last half year also these temperatures have been constant.

2.14 Temperature on the canister surface, Optical fiber cables (App. A pages 71-72)

The first diagram shows the maximum temperature plotted as a function of time. The maximum temperature measured on the canister surface is presently between 66 and 69 °C. The second diagram shows the distribution of the temperature along the cables at 041101. The length of the cable on the canister surface is only about 20 m and close to the entrances the lower surrounding temperatures have an influence on the measured temperature.

2.15 Temperature inside the canister (App. A pages 73-75)

All sensors have been lost.

2.16 Strain in the canister

Continuous measurements have been made but so far no results have been produced due to evaluation problems.

2.17 Rock stresses and strains

Rock stresses and strains are reported in Appendix B.

3 Geometry

The test installation consists of a full-scale deposition hole, a copper canister equipped with electrical heaters and bentonite blocks (cylindrical and ring shaped). A plug of concrete and steel is anchored to the rock on top of the bentonite.

The saturation of the bentonite is attained artificially by vertical filter stripes. 16 stripes with a width of 0.1 meters and a length of 5.5 meters are applied on the surrounding rock.

Measurements are made in four vertical sections A, B, C and D according to Figure 3-1. Direction A-B is parallel to the tunnels axial with A headed almost against north.

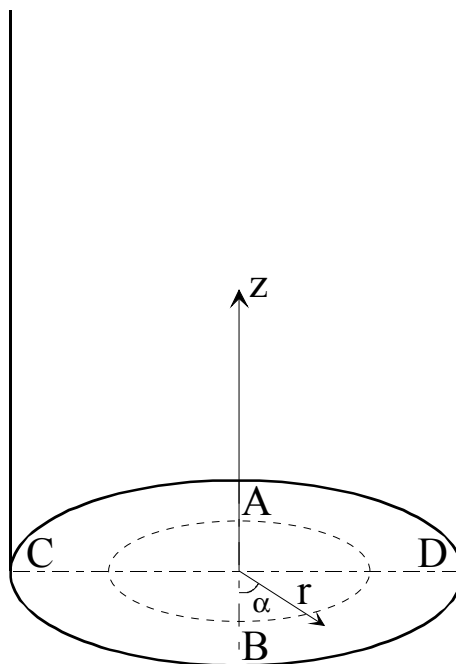


Figure 3-1. Figure describing the instrument planes (A-D) and the coordinate system used when describing the instrument positions.

4 Location of instruments

4.1 Brief description of the instruments

The different instruments that are used in the experiment are briefly described in this chapter.

Measurements of temperature

Buffer

Thermocouples from BICC have been installed for measuring temperature in the buffer. Measurements are done in 32 points in the test hole. In addition, temperature gauges are built in into the capacitive relative humidity sensors (29 sensors) as well as in the pressure gauges of vibrating wire type (13 gauges). Temperature is also measured in the psychrometers.

Canister

Temperature is measured inside the canister (on the insert) in 19 points with PT-100 gauges. In addition temperature is measured on the surface of the canister with optical fiber cables. An optical measuring system called FTR (Fiber Temperature Laser Radar) from BICC is used.

Rock

Temperature in the rock and on the rock surface of the hole is measured in 40 points with thermocouples from BICC.

Measurement of total pressure in the buffer

Total pressure is the sum of the swelling pressure and the pore water pressure. It is measured with the following instrument types:

- Geocon total pressure cells with vibrating wire transducers. 15 cells of this type have been installed.
- Kulite total pressure cells with piezo resistive transducers. 6 cells of this type have been installed.

Measurement of pore water pressure in the buffer

Pore water pressure is measured with the following instrument types:

- Geocon pore pressure cells with vibrating wire transducer. 13 cells of this type have been installed.
- Kulite pore pressure cells with piezo resistive transducer. 2 cells of this type have been installed.

Measurement of the water saturation process

The water saturation process is recorded by measuring the relative humidity in the pore system, which can be converted into water ratio or total suction (negative water pressure). The following techniques and devices are used:

- Vaisala relative humidity sensor of capacitive type. 29 cells of this type have been installed. The measuring range is 0-100 % RH.
- Wescor psychrometers model PST-55. The devices measure the relative humidity in the pore system. The measuring range is 95.5-99.6 % RH corresponding to the pore water pressure -0.5 to -6MPa. 26 cells of this type have been installed.

Measurements of strain in the Canister

These measurements are not reported.

Measurements of stresses and strain in the rock

These measurements are not reported.

Measurements of forces on the plug

The force on the plug caused by the swelling pressure of the bentonite is measured in 3 of the 9 anchors. The force transducers are of the type GLÖTZL.

Measurements of plug displacement

Due to straining of the anchors the swelling pressure of the bentonite will cause not only a force on the plug but also displacement of the plug. The displacement is measured in three points with transducers of the type LVDT with the range 0 – 50 mm.

Measurement of water flow into the permeable mats

Water is supplied to the bentonite with filter strips attached to the rock surface. The water flow into these mats is measured by measuring the water volume in the supply tank with a differential pressure transmitter that measures the difference in pressure between the nitrogen in the top of the tank and the water in the bottom of the tank.

4.2 Strategy for describing the position of each device

Every instrument is named with a short unique name consisting of 1-2 letters describing the type of measurement and 3 figures numbering the device. Every instrument position in the buffer and rock is described with three coordinates according to Figure 3-1.

The r-coordinate is the horizontal distance from the center of the hole and the z-coordinate is the height from the bottom of the hole (the block height is set to 500 mm). The α -coordinate is the angle from the vertical direction B (almost south).

The short description of the positions in the diagrams differs between the buffer and the rock.

Buffer: Three positions with the following meaning: (bentonite block or cylinder number counted from the bottom \ direction A, B, C, or D \ radius in mm from center line)

Rock: Three positions with the following meaning: (distance in meters from the bottom \ α according to Fig 3-1 \ distance in meters from the hole surface)

The bentonite blocks are called cylinders and rings. The cylinders are numbered C1-C4 and the rings R1-R10 respectively (Figure 4-1).

4.3 Position of each instrument in the bentonite

Measurements are done in four vertical sections A, B, C and D according to Figure 3-1. Direction A and B are placed in the tunnels axial direction.

An overview of the positions of the instruments is shown in Fig 4-1. Exact positions are described in Tables 4-1 to 4-4.

The instruments are located in two main levels in the blocks, 50 mm and 160 mm, from the upper surface. The thermocouples have mostly placed in the 50mm level and the other gauges in the 160 mm level.

- pore water pressure + temp.
- total pressure + temp.
- × temp.
- △ relative humidity (+ temp.)

1m

A

B+C

D

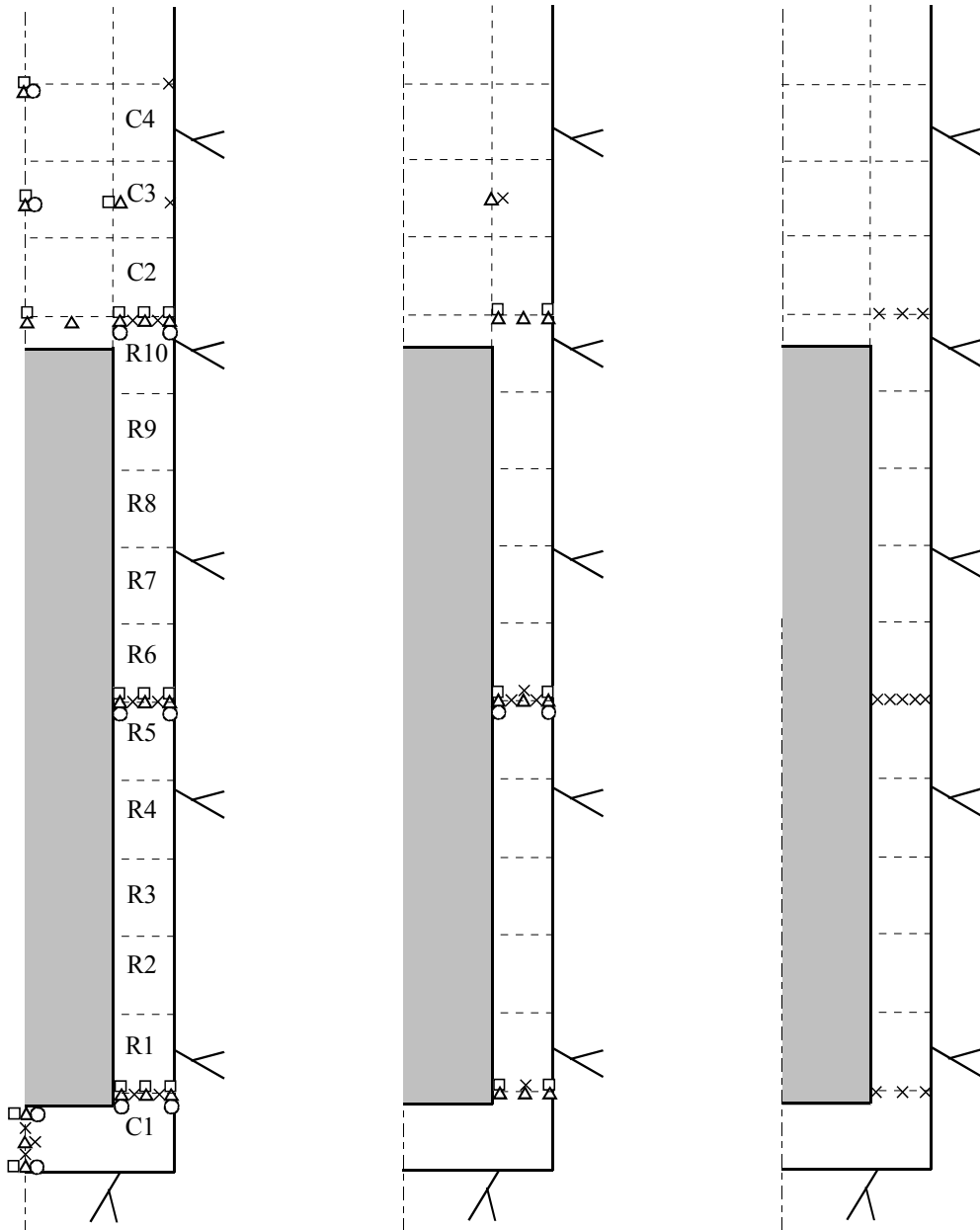


Figure 4-1 Schematic view over the instruments in four vertical sections and the block designation.

Table 4-1 Numbering and position of instruments for measuring temperature (T)

Type and number	Block	Instrument position in block				Cable pos.		Fabricate	Remark
		Direction	α	r	Z	α			
T101	Cyl. 1	Center	90	50	50	242	BICC		
T102	Cyl. 1	Center	90	50	250	238	BICC		
T103	Cyl. 1	Center	90	50	450	230	BICC		
T104	Cyl. 1	A	180	635	450	206	BICC		
T105	Cyl. 1	A	180	735	450	202	BICC		
T106	Cyl. 1	B	365	685	450	38	BICC		
T107	Cyl. 1	C	275	685	450	274	BICC		
T108	Cyl. 1	D	90	585	450	96	BICC		
T109	Cyl. 1	D	90	685	450	94	BICC		
T110	Cyl. 1	D	90	785	450	92	BICC		
T111	Ring 5	A	180	635	2950	224	BICC		
T112	Ring 5	A	180	735	2950	218	BICC		
T113	Ring 5	B	360	610	2950	318	BICC		
T114	Ring 5	B	360	685	2950	322	BICC		
T115	Ring 5	B	360	735	2950	324	BICC		
T116	Ring 5	C	270	610	2950	258	BICC		
T117	Ring 5	C	270	685	2950	260	BICC		
T118	Ring 5	C	270	735	2950	262	BICC		
T119	Ring 5	D	90	585	2950	44	BICC		
T120	Ring 5	D	90	635	2950	46	BICC		
T121	Ring 5	D	90	685	2950	48	BICC		
T122	Ring 5	D	90	735	2950	50	BICC		
T123	Ring 5	D	90	785	2950	52	BICC		
T124	Ring 10	A	180	635	5450	200	BICC		
T125	Ring 10	A	180	735	5450	194	BICC		
T126	Ring 10	D	90	585	5450	54	BICC		
T127	Ring 10	D	90	685	5450	56	BICC		
T128	Ring 10	D	90	785	5450	58	BICC		
T129	Cyl. 3	A	180	785	6250	166	BICC		
T130	Cyl. 3	B	365	585	6250	358	BICC		
T131	Cyl. 3	C	275	585	6250	280	BICC		
T132	Cyl. 4	A	180	785	6950	66	BICC		

Table 4-2 Numbering and position of instruments for measuring total pressure (P)

Type and number	Block	Instrument position in block			Z(mm)	Cable pos.		Fabricate	Remark
		Direction	α	r(mm)		α			
P101	Cyl. 1	Center	180	50	0	244	Kulite		
P102	Cyl. 1	Center	180	50	450	232	Kulite		
P103	Cyl. 1	A	185	585	340	208	Geokon		
P104	Cyl. 1	A	185	685	340	204	Geokon		
P105	Cyl. 1	A	185	785	340	186	Geokon		
P106	Cyl. 1	B	365	585	340	40	Geokon		
P107	Cyl. 1	B	365	785	340	2	Geokon		
P108	Cyl. 1	C	275	585	340	278	Geokon		
P109	Cyl. 1	C	275	785	340	270	Geokon		
P110	Ring 5	A	185	585	2840	228	Geokon		
P111	Ring 5	A	185	685	2840	222	Geokon		
P112	Ring 5	A	185	785	2840	188	Geokon		
P113	Ring 5	B	365	535	2840	36	Geokon		
P114	Ring 5	B	365	825	2840	16	Geokon		
P115	Ring 5	C	275	585	2840	296	Geokon		
P116	Ring 5	C	275	785	2840	290	Geokon		
P117	Ring 10	Center	180	50	5340	24	Kulite		
P118	Ring 10	A	180	585	5340	216	Geokon		
P119	Ring 10	A	180	685	5340	198	Geokon		
P120	Ring 10	A	180	785	5340	192	Geokon		
P121	Ring 10	B	365	585	5340	20	Kulite		
P122	Ring 10	B	365	785	5340	18	Kulite		
P123	Ring 10	C	275	585	5340	286	Kulite		
P124	Ring 10	C	275	785	5340	284	Kulite		
P125	Cyl. 3	Center	180	50	6250	158	Geokon		
P126	Cyl. 3	A	180	585	6250	162	Geokon		
P127	Cyl. 4	Center	180	50	6840	64	Kulite		

Table 4-3 Numbering and position of instruments for measuring pore water pressure (U)

Type and number	Block	Instrument position in block			Z(mm)	Cable pos.		Fabricate	Remark
		Direction	α	r(mm)		α			
U101	Cyl. 1	Center	270	50	50	246	Geokon		
U102	Cyl. 1	Center	270	50	450	236	Geokon	Horizontal	
U103	Cyl. 1	A	175	585	340	126	Geokon		
U104	Cyl. 1	A	175	785	340	178	Geokon		
U105	Ring 5	A	175	585	2840	138	Geokon		
U106	Ring 5	A	175	785	2840	180	Geokon		
U107	Ring 5	B	355	535	2840	314	Geokon	In the slot	
U108	Ring 5	B	355	825	2840	348	Geokon	In the slot	
U109	Ring 5	C	265	585	2840	256	Geokon		
U110	Ring 5	C	265	825	2840	264	Geokon	In the slot	
U111	Ring 10	A	175	585	5340	146	Geokon		
U112	Ring 10	A	175	785	5340	152	Geokon		
U113	Cyl. 3	Center	270	50	6250	156	Geokon		
U114	Cyl. 4	Center	270	50	6950	62	Kulite		

Table 4-4 Numbering and position of instruments for measuring water content (W)

Type and number	Block	Instrument position in block				Cable pos.		Fabricate	Remark
		Direction	α	r	Z	α			
W101	Cyl. 1	Center	360	50	50	248	Vaisala		
W102	Cyl. 1	Center	360	400	160	240	Vaisala		
W103	Cyl. 1	Center	360	50	450	234	Vaisala	Horizontal	
W104	Cyl. 1	A	180	585	340	128	Vaisala		
W105	Cyl. 1	A	180	685	340	132	Vaisala		
W106	Cyl. 1	A	180	785	340	184	Vaisala		
W107	Cyl. 1	A	170	585	340	124	Wescor		
W108	Cyl. 1	A	170	685	340	130	Wescor		
W109	Cyl. 1	A	170	785	340	134	Wescor		
W110	Cyl. 1	B	360	585	340	304	Vaisala		
W111	Cyl. 1	B	360	785	340	360	Vaisala		
W112	Cyl. 1	B	360	685	340	308	Vaisala		
W113	Cyl. 1	B	355	585	340	302	Wescor		
W114	Cyl. 1	B	355	685	340	306	Wescor		
W115	Cyl. 1	B	355	785	340	310	Wescor		
W116	Cyl. 1	C	270	585	340	250	Wescor		
W117	Cyl. 1	C	270	685	340	252	Wescor		
W118	Cyl. 1	C	270	785	340	254	Vaisala		
W119	Ring 5	A	180	585	2840	226	Vaisala		
W120	Ring 5	A	180	685	2840	220	Vaisala		
W121	Ring 5	A	180	785	2840	182	Vaisala		
W122	Ring 5	A	170	585	2840	136	Wescor		
W123	Ring 5	A	170	685	2840	140	Wescor		
W124	Ring 5	A	170	785	2840	142	Wescor		
W125	Ring 5	B	360	535	2840	316	Vaisala	In the slot	
W126	Ring 5	B	360	685	2840	34	Vaisala		
W127	Ring 5	B	360	785	2840	350	Vaisala		
W128	Ring 5	B	350	535	2840	312	Wescor	In the slot	
W129	Ring 5	B	350	685	2840	320	Wescor		
W130	Ring 5	B	350	785	2840	346	Wescor		
W131	Ring 5	C	270	585	2840	294	Wescor	In the slot	
W132	Ring 5	C	275	685	2840	292	Wescor		
W133	Ring 5	C	270	785	2840	288	Wescor		
W134	Ring 10	Center	360	50	5340	22	Vaisala		
W135	Ring 10	A	180	262	5340	26	Vaisala		
W136	Ring 10	A	180	585	5340	214	Vaisala		
W137	Ring 10	A	180	685	5340	196	Vaisala		
W138	Ring 10	A	180	785	5340	190	Vaisala		
W139	Ring 10	A	170	585	5340	144	Wescor		
W140	Ring 10	A	170	685	5340	148	Wescor		
W141	Ring 10	A	170	785	5340	150	Wescor		
W142	Ring 10	B	360	585	5340	328	Vaisala		
W143	Ring 10	B	360	685	5340	332	Vaisala		
W144	Ring 10	B	360	785	5340	336	Vaisala		
W145	Ring 10	B	355	585	5340	326	Wescor		
W146	Ring 10	B	355	685	5340	330	Wescor		
W147	Ring 10	B	355	785	5340	334	Wescor		
W148	Ring 10	C	270	585	5340	266	Wescor		
W149	Ring 10	C	270	685	5340	268	Wescor		
W150	Ring 10	C	270	785	5340	272	Vaisala		
W151	Cyl. 3	Center	360	50	6250	154	Vaisala		
W152	Cyl. 3	A	180	585	6250	160	Vaisala		
W153	Cyl. 3	B	360	585	6250	356	Vaisala		
W154	Cyl. 3	C	270	585	6250	276	Wescor		
W155	Cyl. 4	Center	360	50	6840	60	Vaisala		

4.4 Instruments in the rock

Temperature measurements

40 thermocouples are placed in the rock and on the rock surface of the deposition hole. Holes have been bored in three directions on three levels and one additional hole has been bored in the bottom of the deposition hole i.e. totally 10 holes. They are led from the rock, over the gap between rock and bentonite and up along the bentonite block periphery. The position of the thermocouples in the rock is shown in Table 4-5.

Table 4-5 Numbering and positions of thermocouples in the rock

Type and number	Level	Direction	Distance from rock surface	Cable pos. α	Fabricate	Remark
TR101	0	Center	0.000	70°-90°	BICC	
TR102	0	Center	0.375	70°-90°	BICC	
TR103	0	Center	0.750	70°-90°	BICC	
TR104	0	Center	1.500	70°-90°	BICC	
TR105	0.61	10°	0.000	4°-14°	BICC	
TR106	0.61	10°	0.375	4°-14°	BICC	
TR107	0.61	10°	0.750	4°-14°	BICC	
TR108	0.61	10°	1.500	4°-14°	BICC	
TR109	0.61	80°	0.000	70°-90°	BICC	
TR110	0.61	80°	0.375	70°-90°	BICC	
TR111	0.61	80°	0.750	70°-90°	BICC	
TR112	0.61	80°	1.500	70°-90°	BICC	
TR113	0.61	170°	0.000	168°-176°	BICC	
TR114	0.61	170°	0.375	168°-176°	BICC	
TR115	0.61	170°	0.750	168°-176°	BICC	
TR116	0.61	170°	1.500	168°-176°	BICC	
TR117	3.01	10°	0.000	4°-14°	BICC	
TR118	3.01	10°	0.375	4°-14°	BICC	
TR119	3.01	10°	0.750	4°-14°	BICC	
TR120	3.01	10°	1.500	4°-14°	BICC	
TR121	3.01	80°	0.000	70°-90°	BICC	
TR122	3.01	80°	0.375	70°-90°	BICC	
TR123	3.01	80°	0.750	70°-90°	BICC	
TR124	3.01	80°	1.500	70°-90°	BICC	
TR125	3.01	170°	0.000	168°-176°	BICC	
TR126	3.01	170°	0.375	168°-176°	BICC	
TR127	3.01	170°	0.750	168°-176°	BICC	
TR128	3.01	170°	1.500	168°-176°	BICC	
TR129	5.41	10°	0.000	4°-14°	BICC	
TR130	5.41	10°	0.375	4°-14°	BICC	
TR131	5.41	10°	0.750	4°-14°	BICC	
TR132	5.41	10°	1.500	4°-14°	BICC	
TR133	5.41	80°	0.000	70°-90°	BICC	
TR134	5.41	80°	0.375	70°-90°	BICC	
TR135	5.41	80°	0.750	70°-90°	BICC	
TR136	5.41	80°	1.500	70°-90°	BICC	
TR137	5.41	170°	0.000	168°-176°	BICC	
TR138	5.41	170°	0.375	168°-176°	BICC	
TR139	5.41	170°	0.750	168°-176°	BICC	
TR140	5.41	170°	1.500	168°-176°	BICC	

Stress and strain measurements

See Appendix B .

4.5 Instruments in the canister

The canister is instrumented with optical fiber cables on the copper surface, thermocouples in the steel insert and strain gauges on the inner and outer surface of the copper envelop in canister.

Optical fiber cables

Figure 4-2 shows how the two optical fiber cables are placed on the canister surface. Both ends of a cable are used for measurements. This means that the two cables are used as four measuring channels as described in Table 4-6.

With this laying the cable will enter and exit the surface at almost the same position. Curvatures are shaped as a quarter circle with a radius of 20 cm. The cable is placed in a milled out channel on the surface. The channel has a width and a depth of just above 2 mm

Table 4-6. Combination of cables and channels

Channel 1	Outlet of cable 1
Channel 2	Inlet of cable 1
Channel 3	Outlet of cable 2
Channel 4	Inlet of cable 2

Figure 4-3 shows the location of the thermocouples on the steel insert inside the canister.

Thermocouple, PT100

Temperature in the steel insert measured at 18 point of measuring with. thermocouple of type PT100. Figure 4-4 shows how these thermocouple are placed

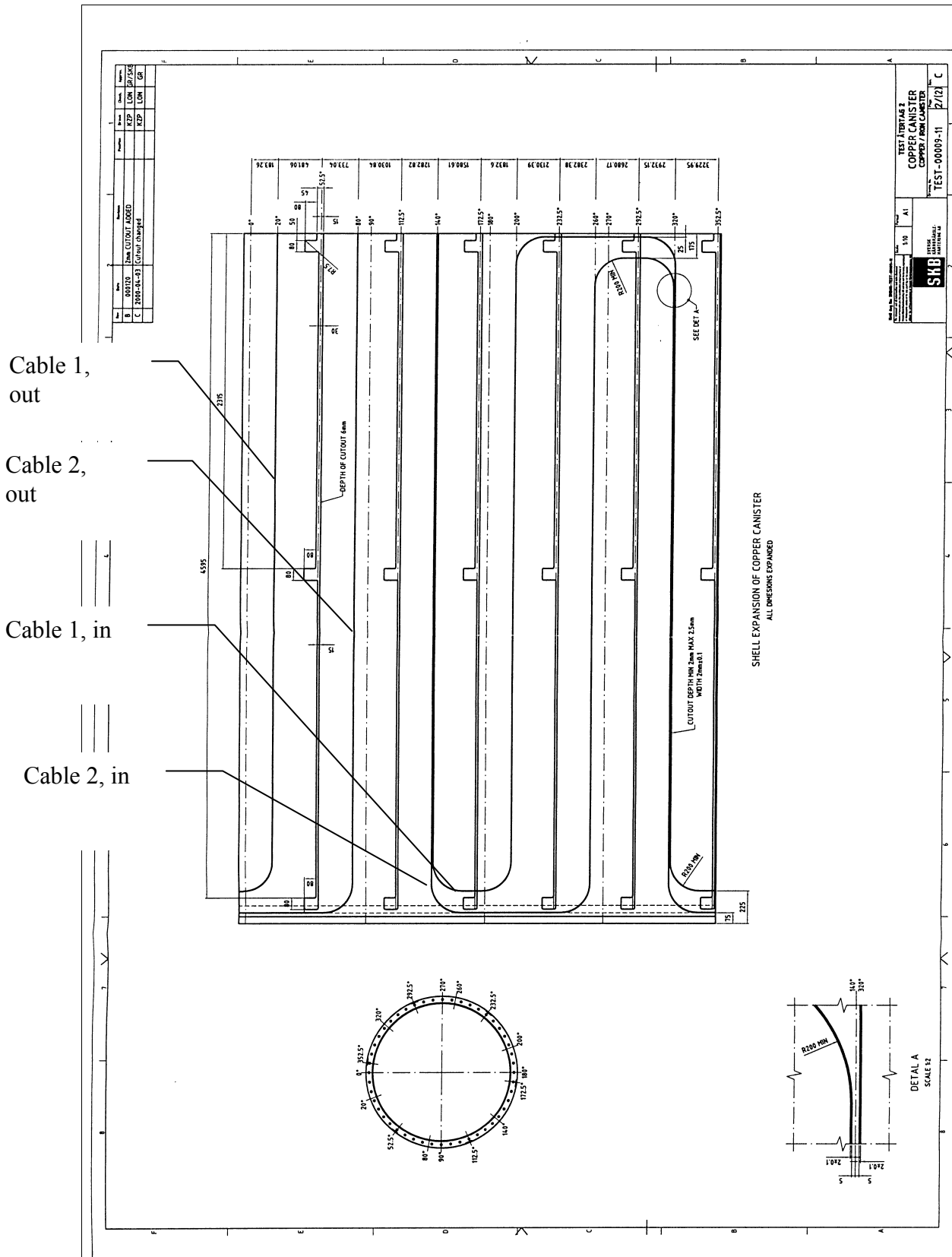
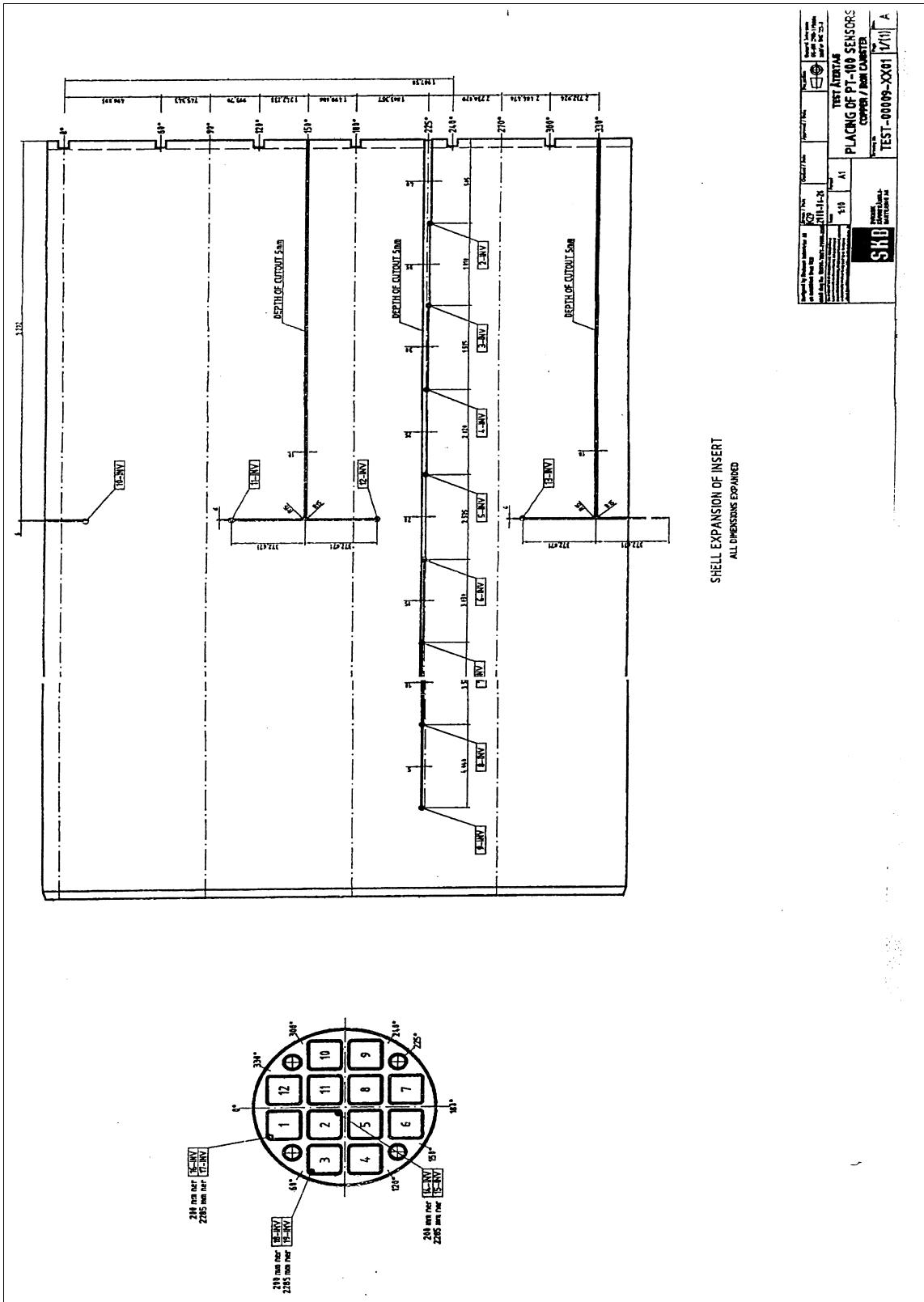


Figure 4-2. Laying of two optical fibre cables with protection tube of Inconel 625 (outer diameter 2 mm) for measurement of the canister surface temperature (surface unfolded).



Figur 4-3. Location of thermocouples inside the canister

4.6 Instruments at the plug

Three force transducers and three displacement transducers have been placed on the plug to measure the force of the anchors and the displacement of the plug. The location of these transducers can be described in relation to Fig 4-4, which shows a schematic view of the plug with the slots, rods and cables.

The rods are numbered 1-9 anti-clockwise and number 1 is assumed to be the northern rod in direction A. The force transducers are placed on rods 3, 6, and 9. The displacement transducers are placed between the rods 5 cm from the rock surface of the hole and according to Table 4-6. They are fixed on the rock surface and measure thus the displacement relative the rock.

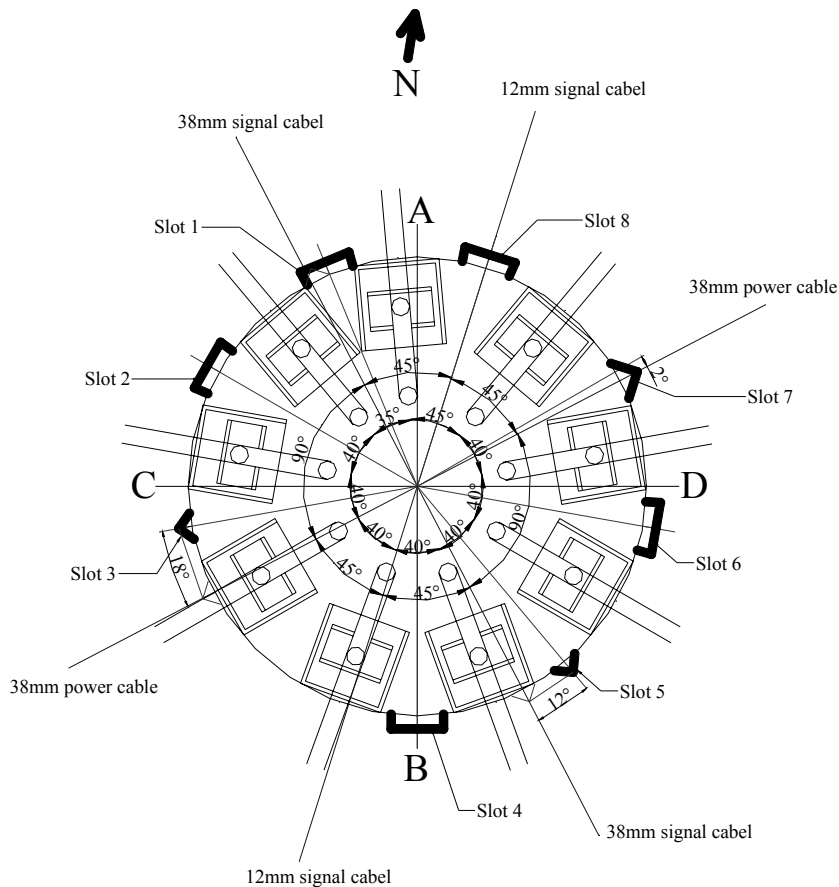


Figure 4-4. Schematic view of the deposition hole, showing the position of the slots, the rods and the cables from the canister.

Table 4-6. Location of displacement transducers

Transducer No.	Located between rods No.
1	4 and 5
2	7 and 8
3	1 and 2

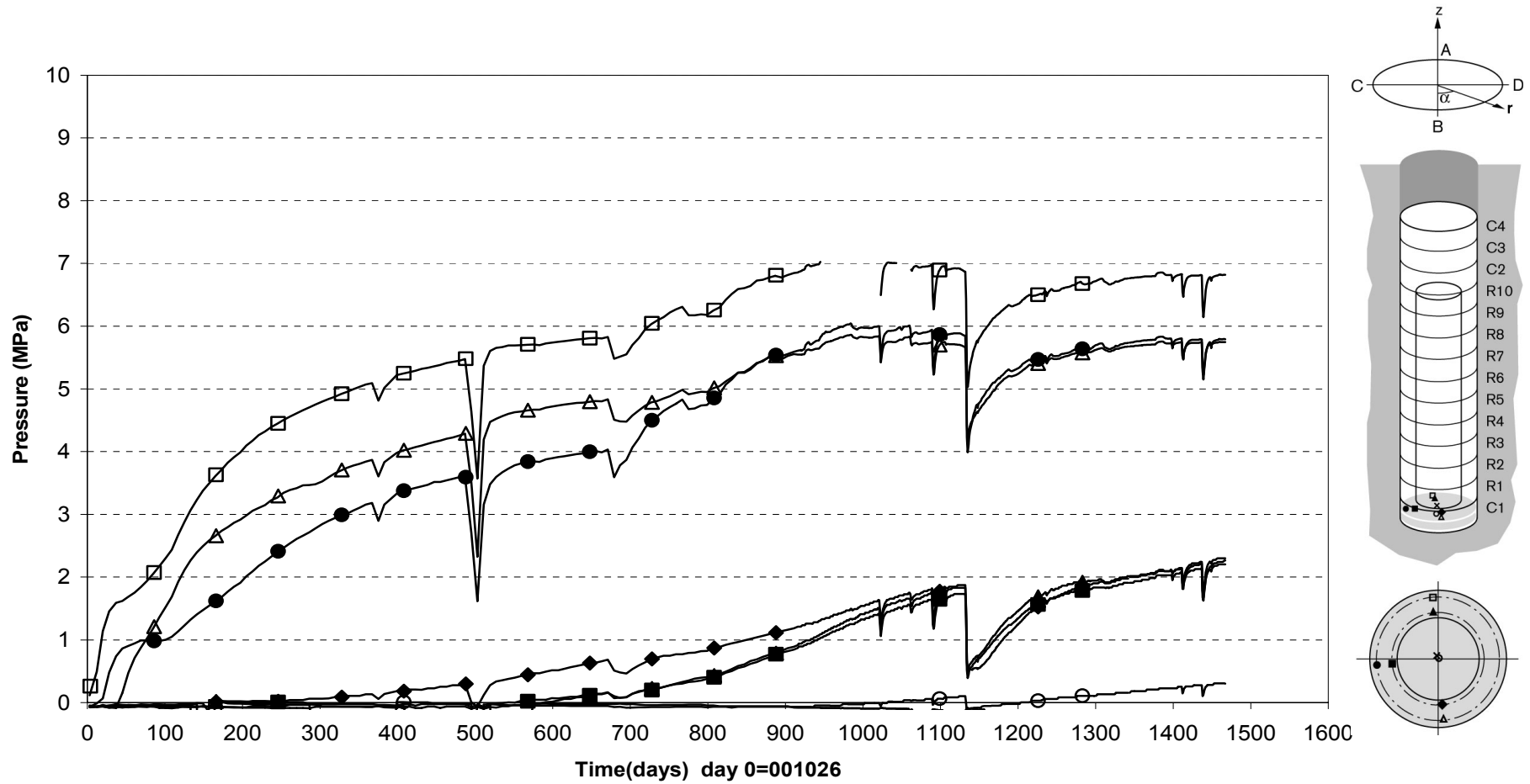
References

/1-1/ **Sanden T, Börgesson L.** Report on instrument positions and preparation of bentonite blocks for instruments and cables May 2000. SKB IPR-00-14

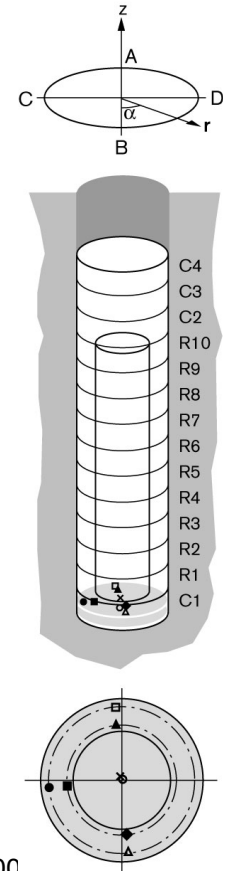
Appendix A

Measured data

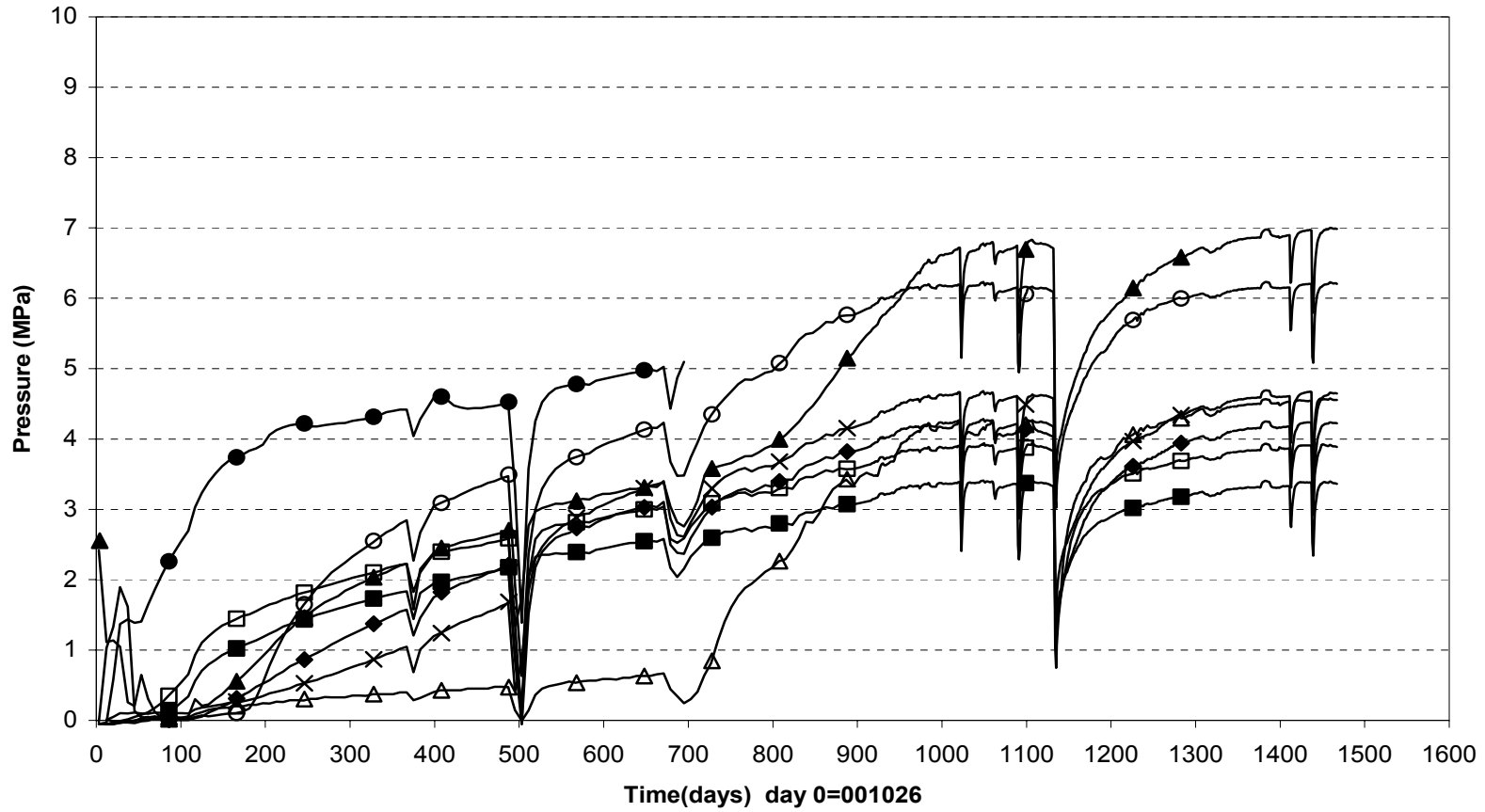
**Total pressure - Cylinder 1 (001026-041101)
Geokon**



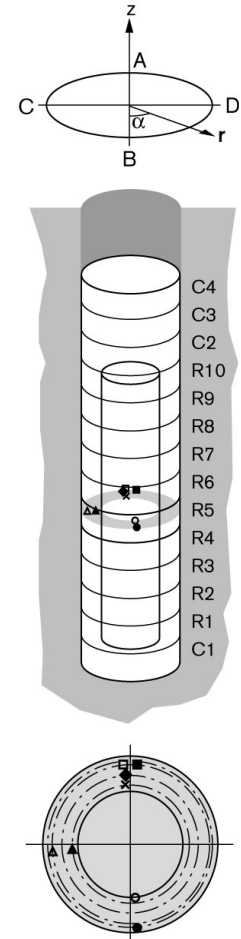
- | | | | | |
|-------------------------|-------------------------|---------------------|---------------------|---------------------|
| ○ P101(Cyl.1\center\50) | × P102(cyl.1\center\50) | ▲ P103(Cyl.1\A\585) | ◆ P106(Cyl.1\B\585) | ■ P108(Cyl.1\C\585) |
| □ P105(Cyl1\A\785) | △ P107(Cyl.1\B\785) | ● P109(Cyl1\C\785) | | |



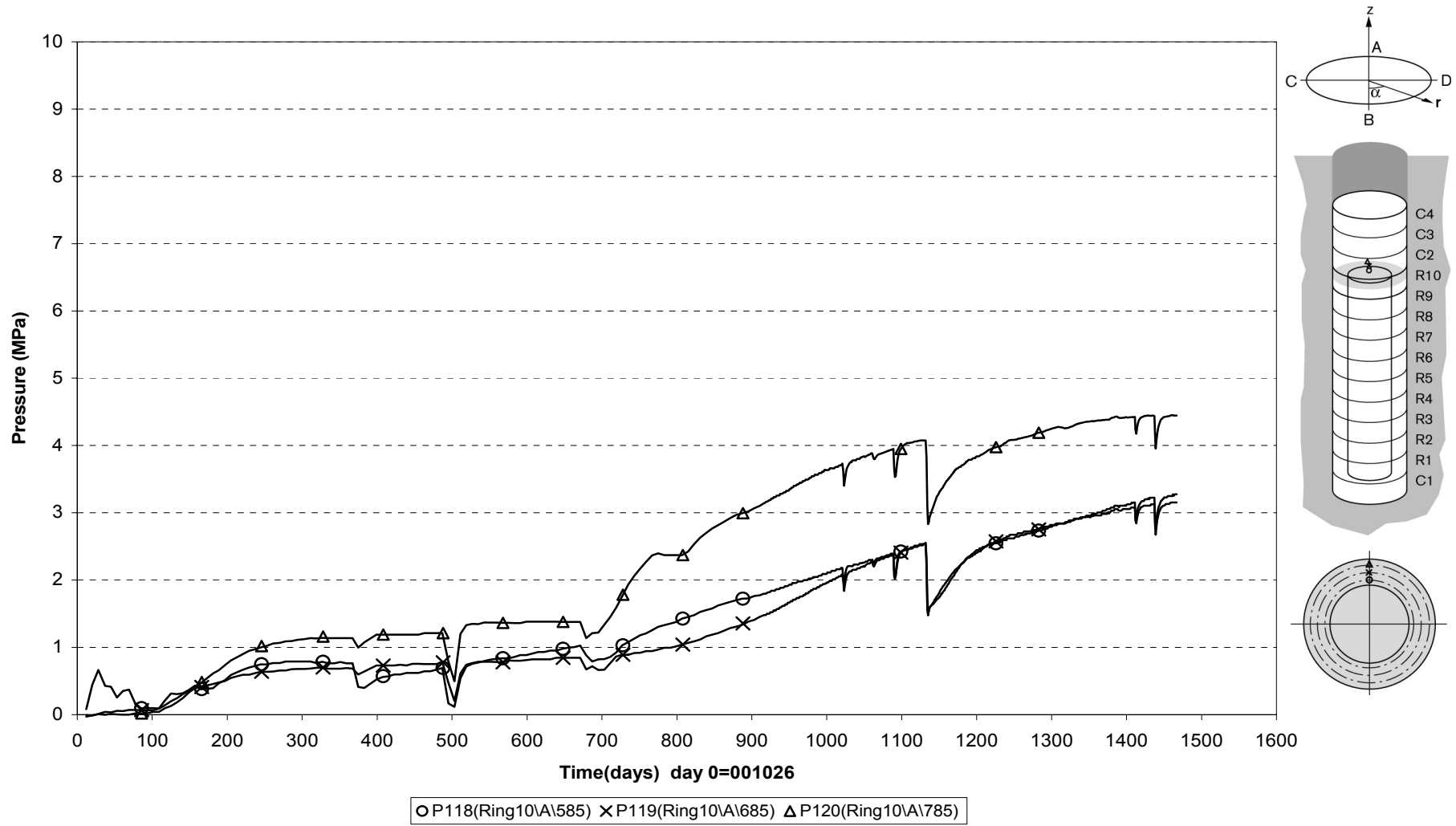
**Total pressure - Ring 5 (001026-041101)
Geokon**



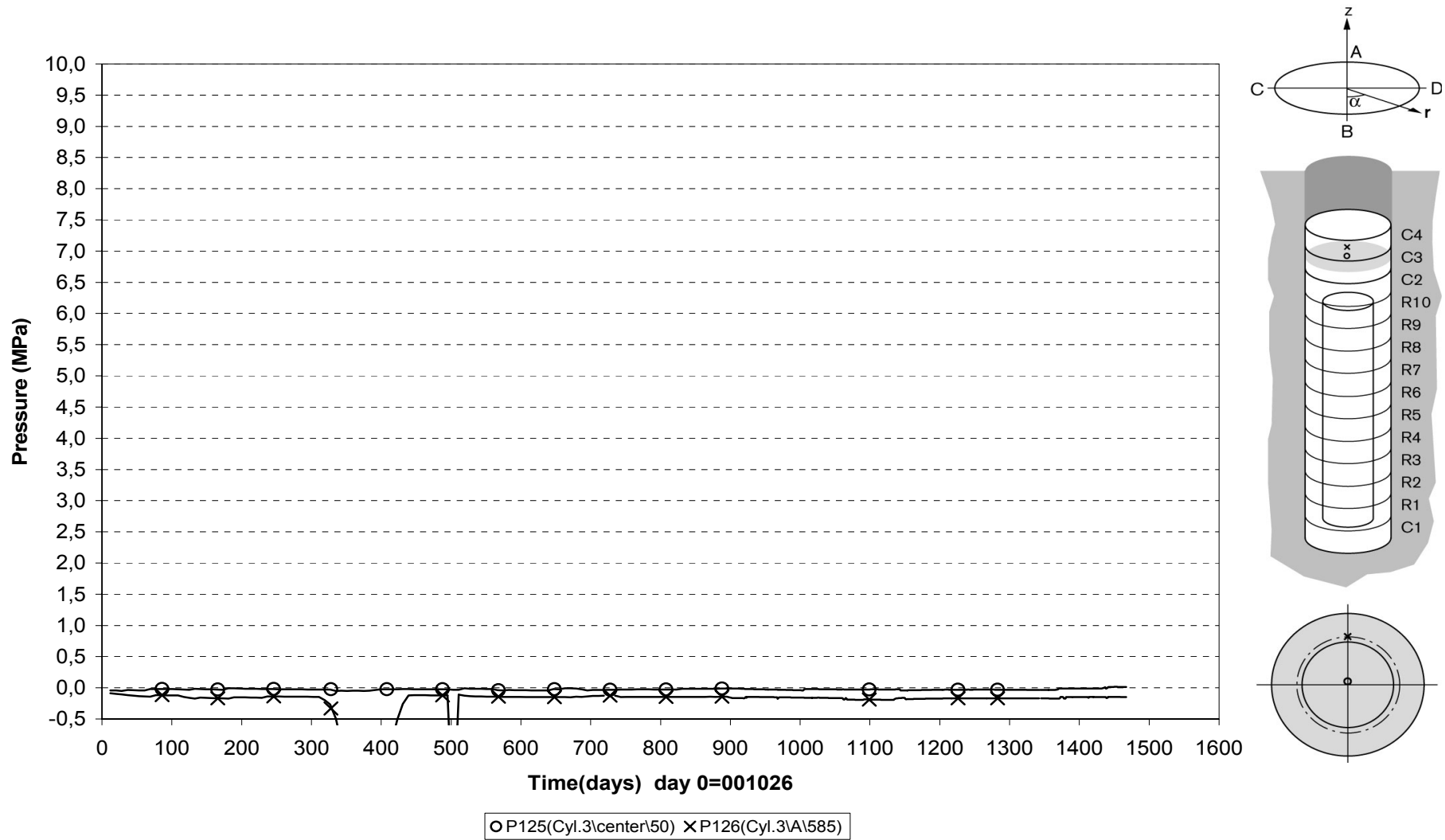
- | | | | |
|---------------------|---------------------|--------------------------|--------------------------|
| ○ P113(Ring5\B\535) | × P110(Ring5\A\585) | ▲ P115(Ring5\C\585) | ◆ P111(Ring5\A\685) |
| ■ U106(Ring5\A\785) | □ P112(Ring5\A\785) | △ P116(Ring5\C\785\slot) | ● P114(Ring5\B\815\slot) |



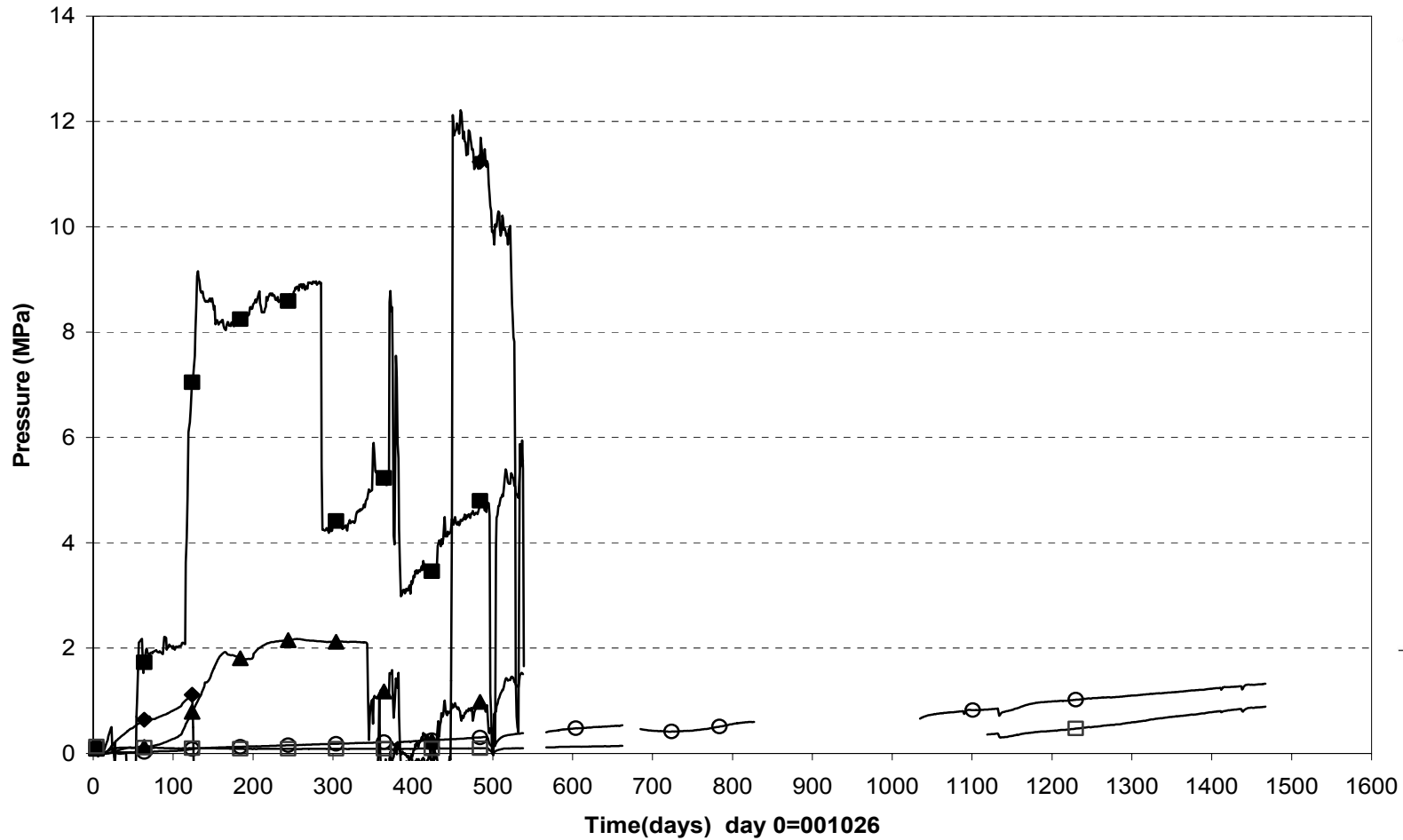
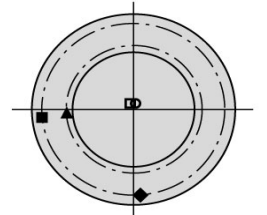
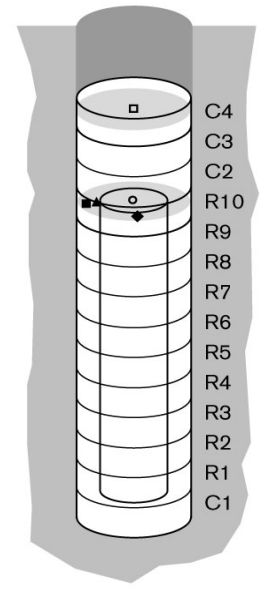
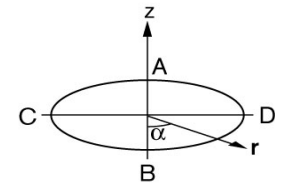
**Total pressure - Ring 10 (001026-041101)
Geokon**



**Total pressure - Cylinder 3 (001026-041101)
Geokon**

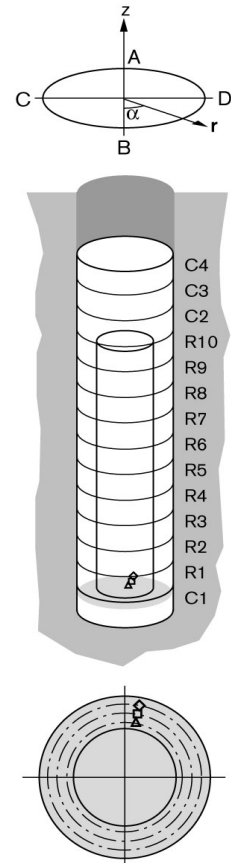
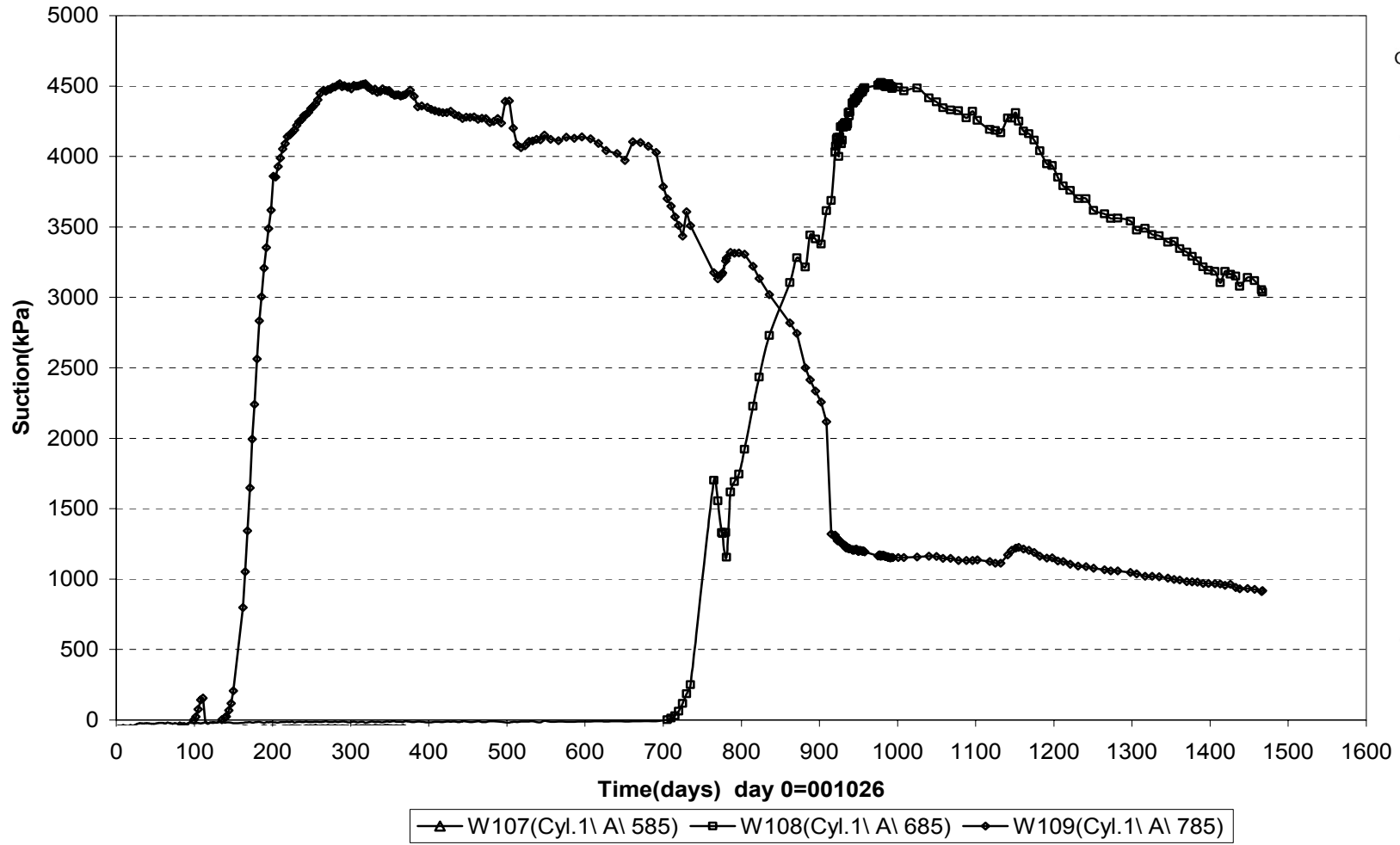


**Total pressure - Ring 10 (001026-041101)
Kulite**

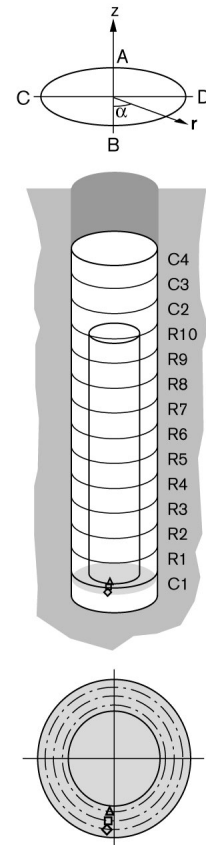
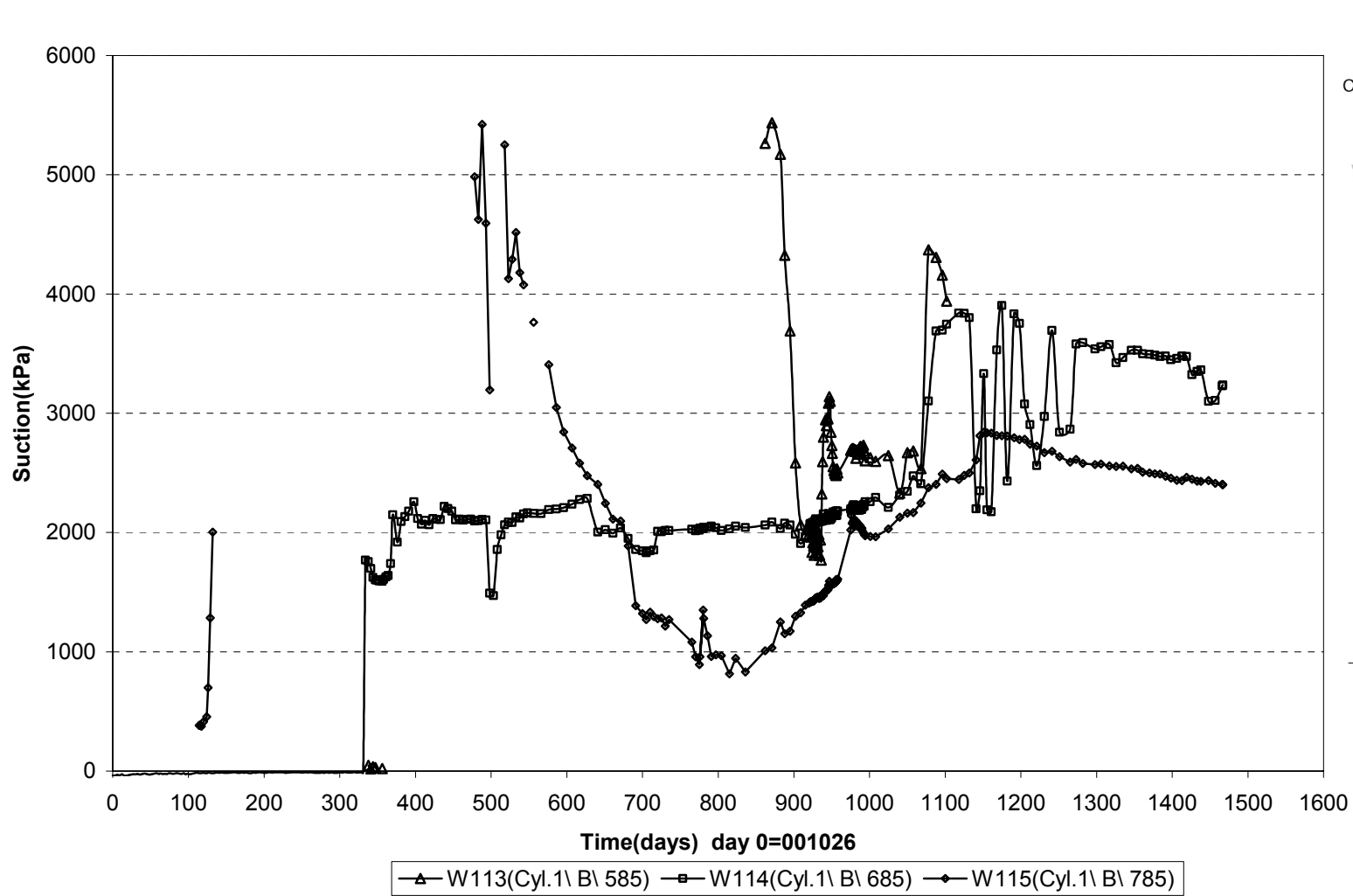


○ P217(Ring10-center-50) ▲ P223(Ring10-C-585) ◆ P222(Ring10-B-785) ■ P224(Ring10-C-785) □ P227(Cyl.4-center-50)

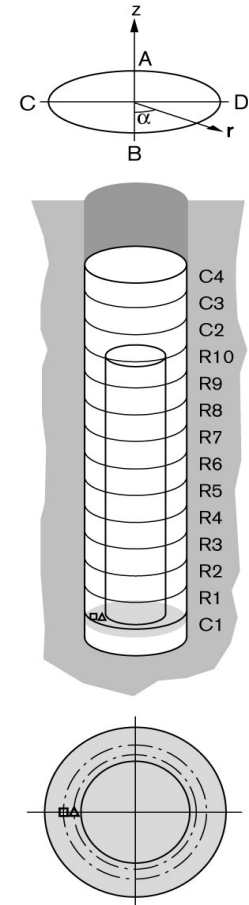
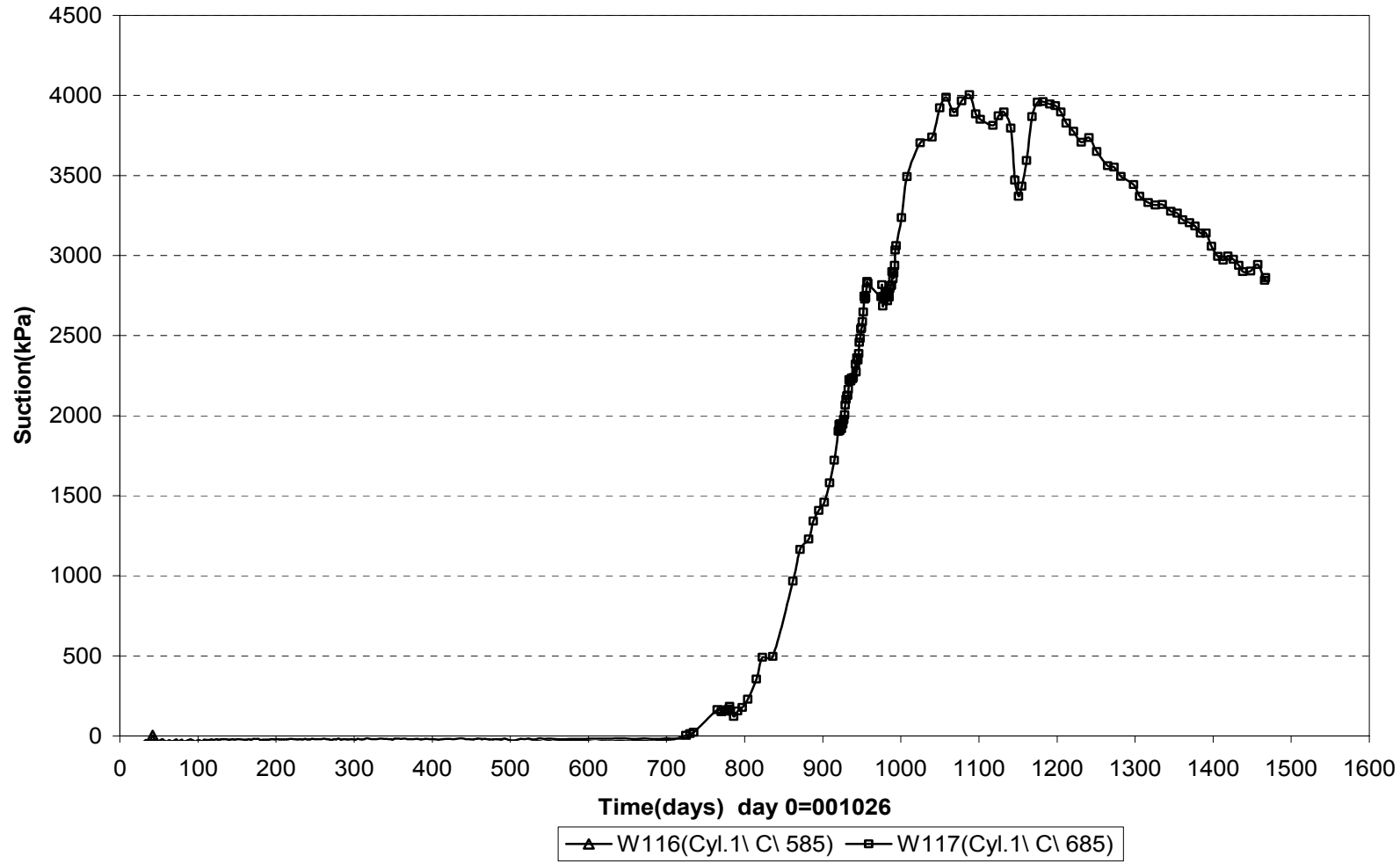
Suction in the buffer - Cyl.1 (001026-041101)
Wescor



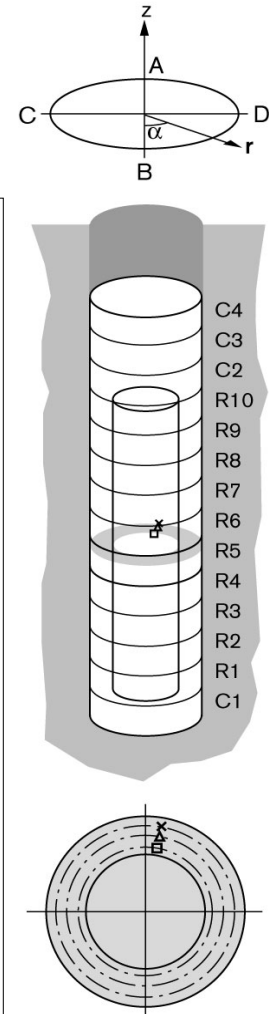
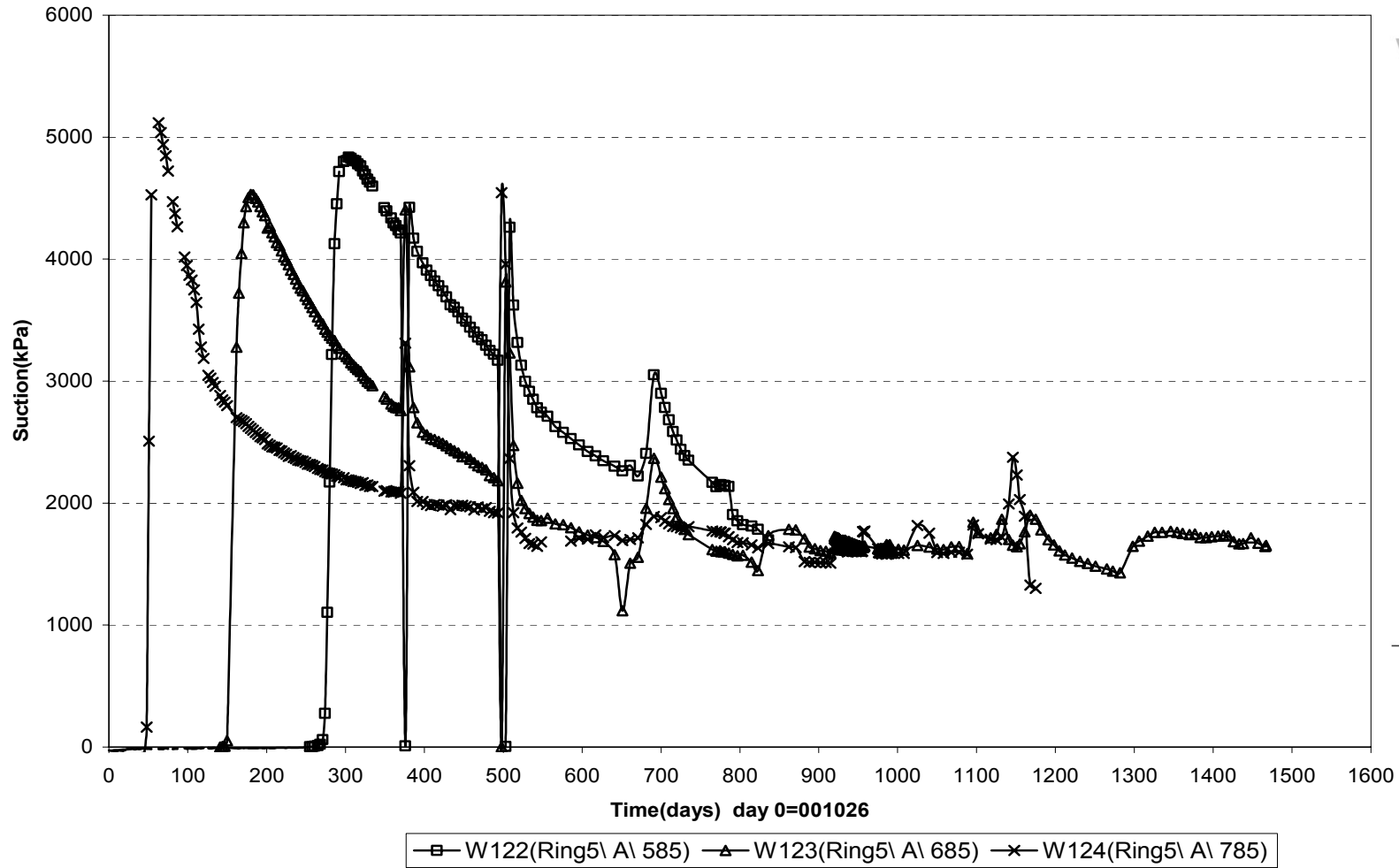
Suction in the buffer - Cyl.1 (001026-041101)
Wescor



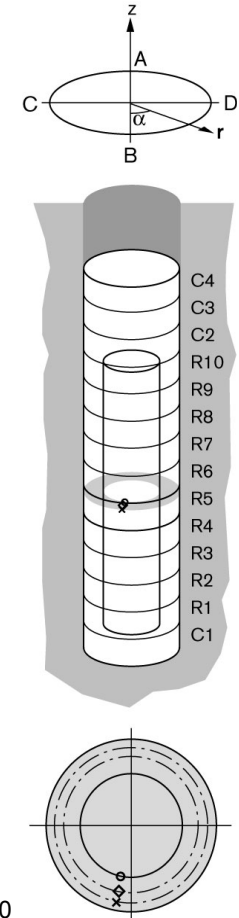
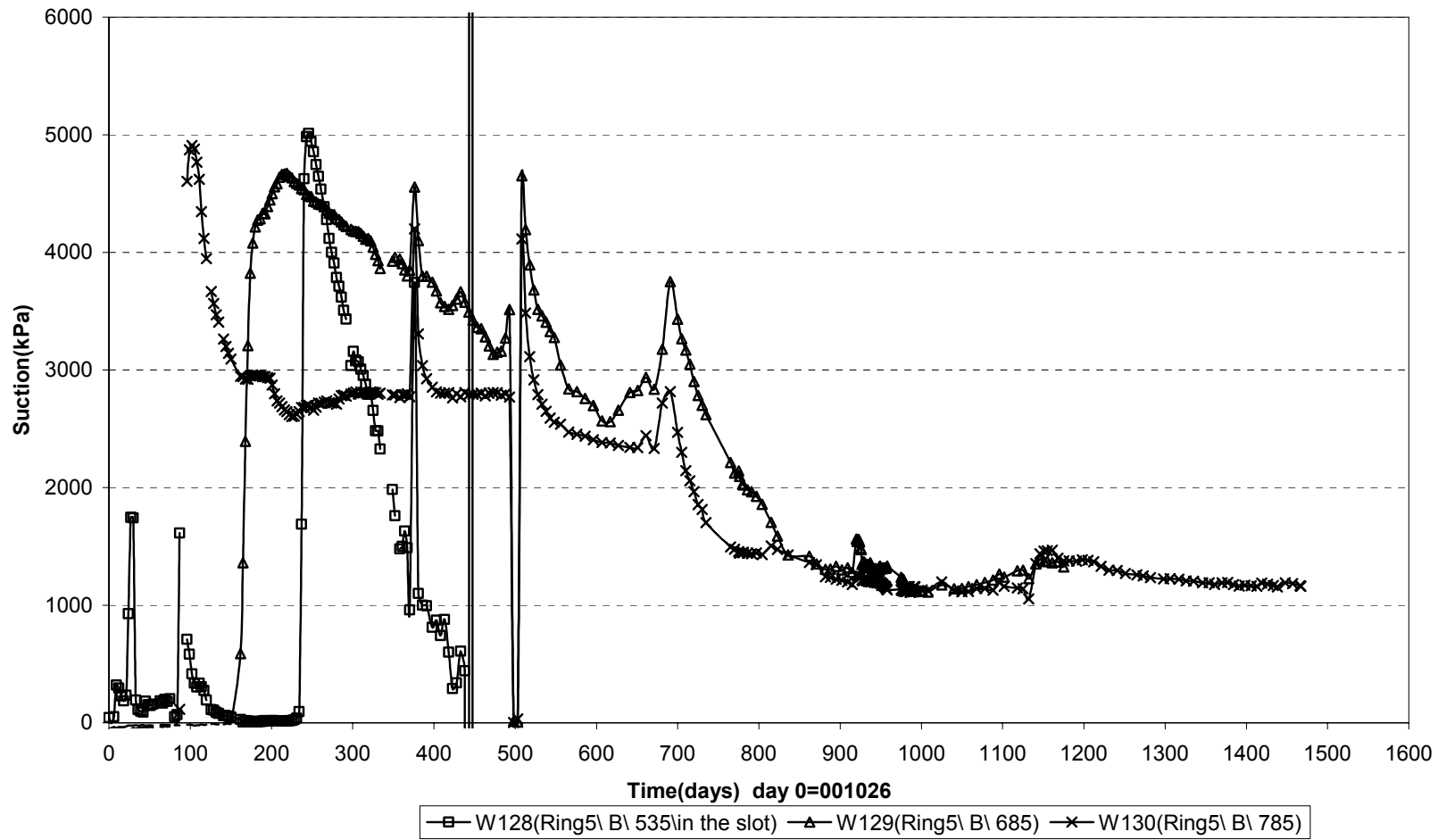
Suction in the buffer - Cyl.1 (001026-041101)
Wescor



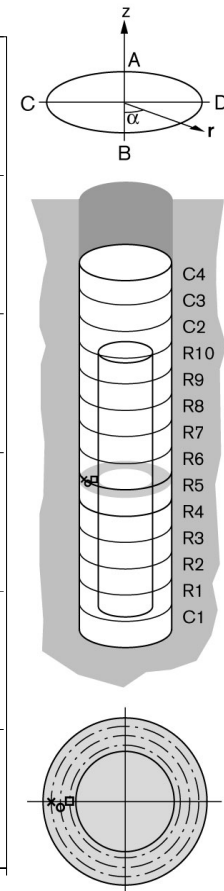
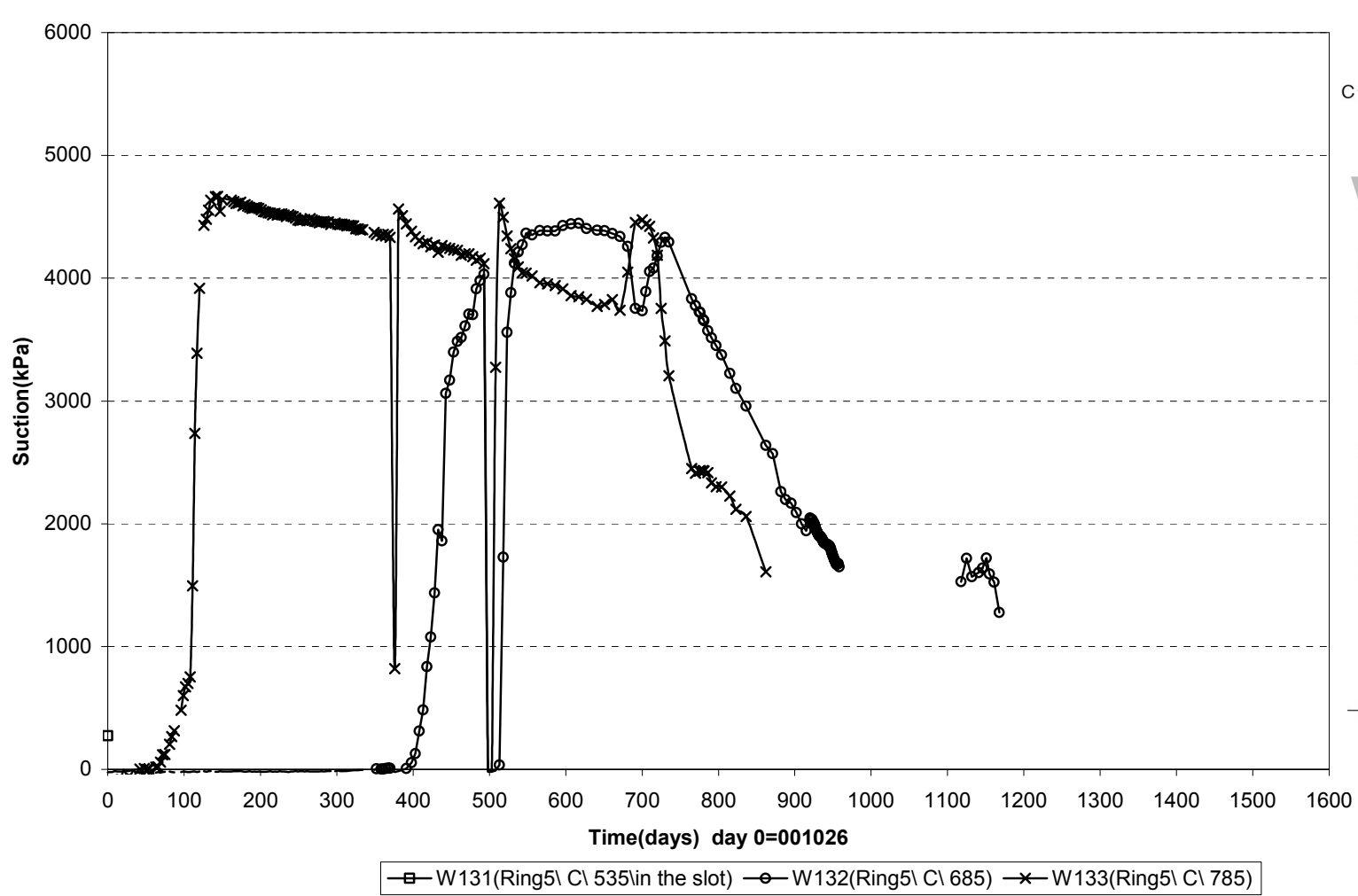
Suction in the buffer - Ring 5 (001026-041101)
Wescor



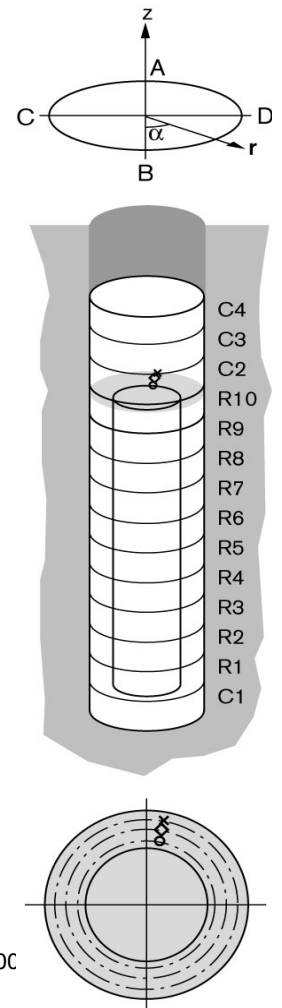
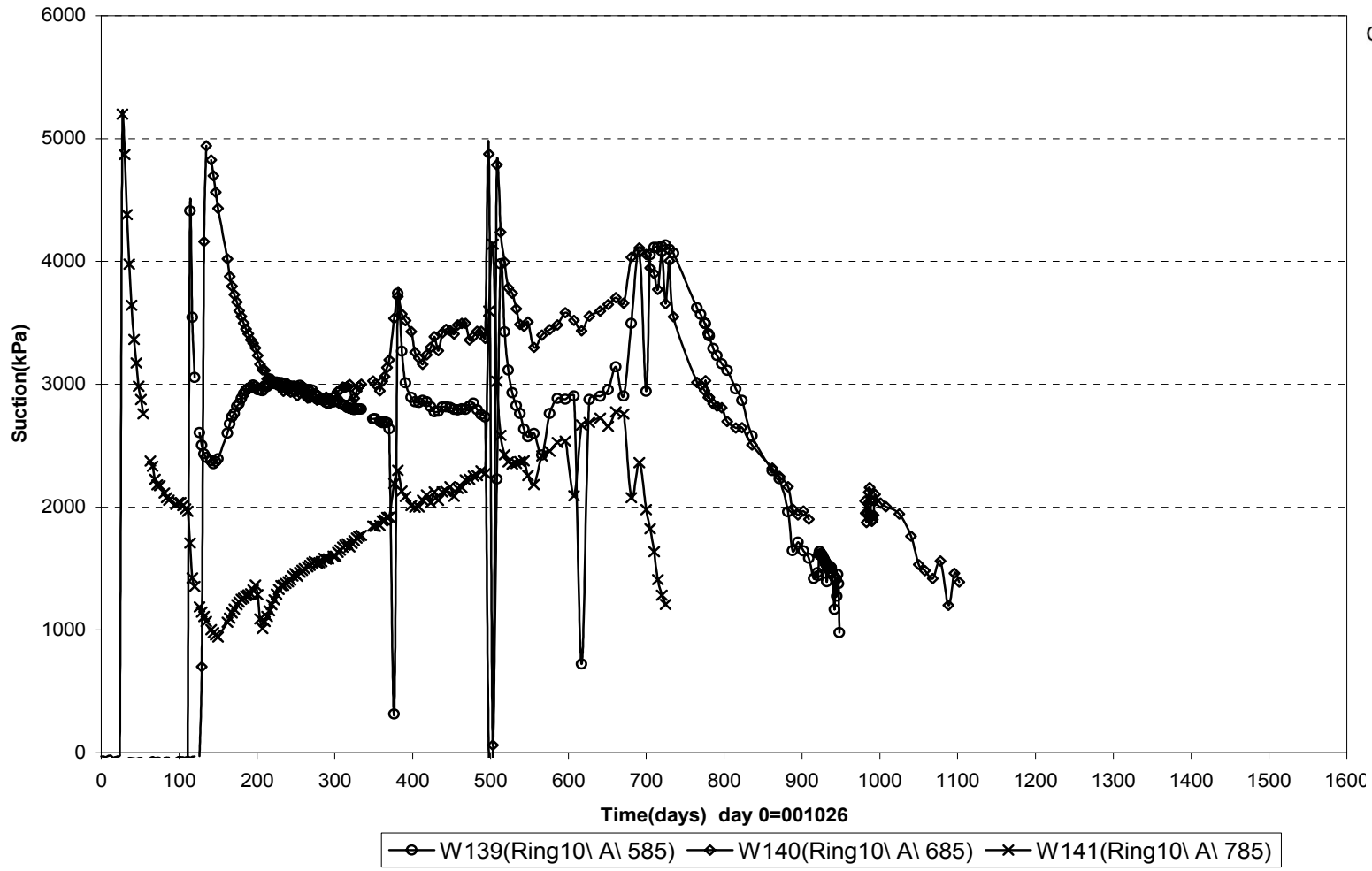
Suction in the buffer - Ring 5 (001026-041101)
Wescor



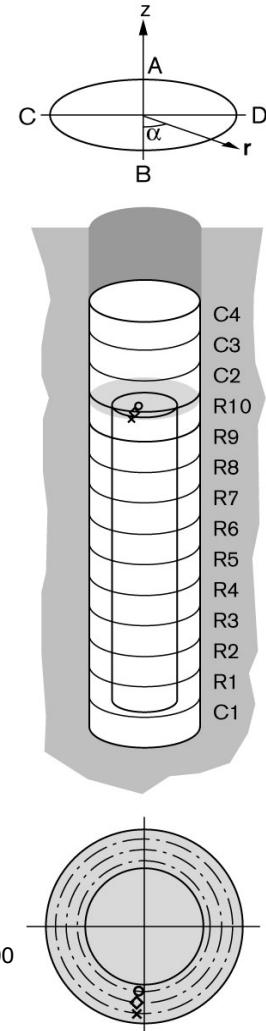
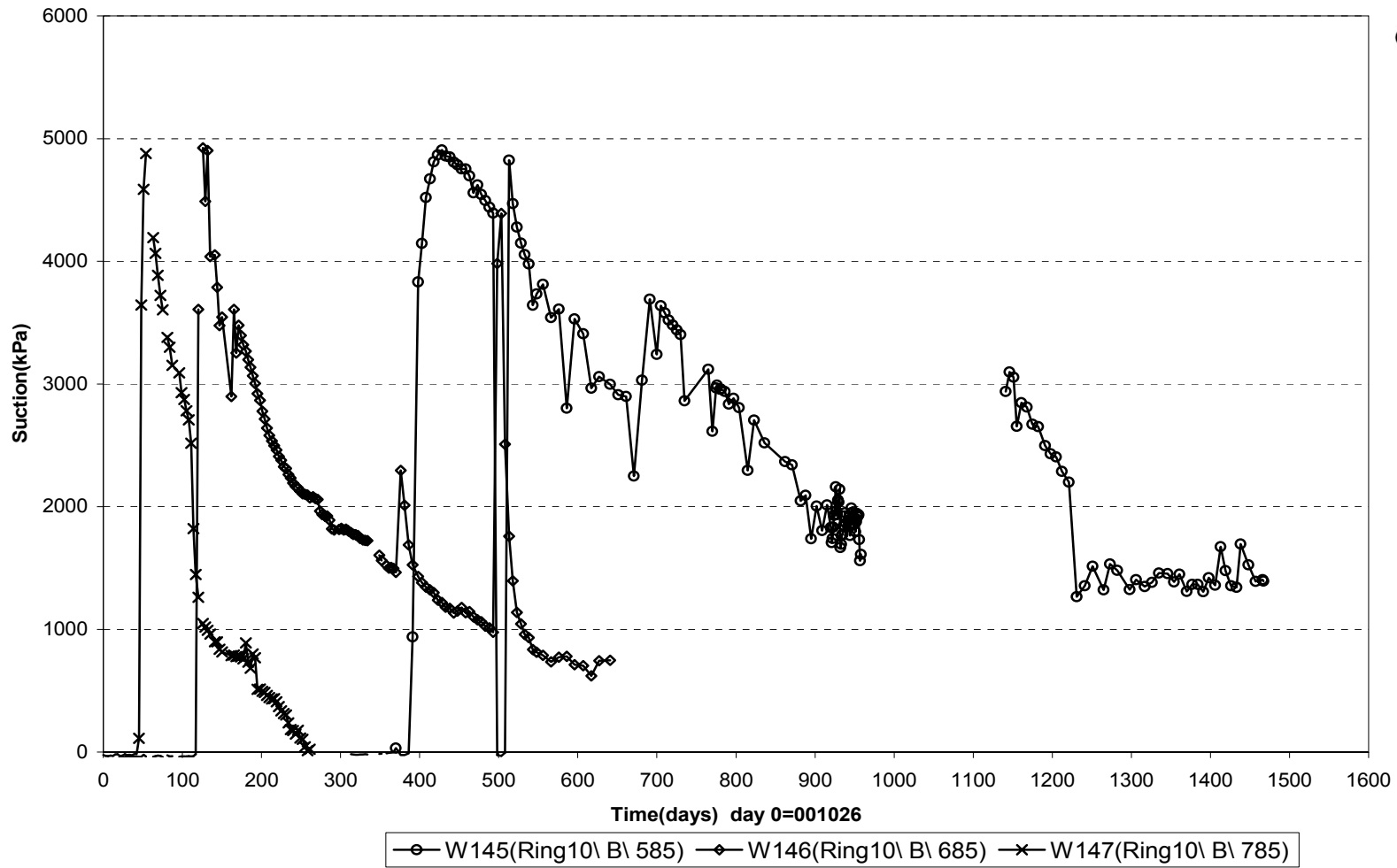
Suction in the buffer - Ring 5 (001026-041101)
Wescor



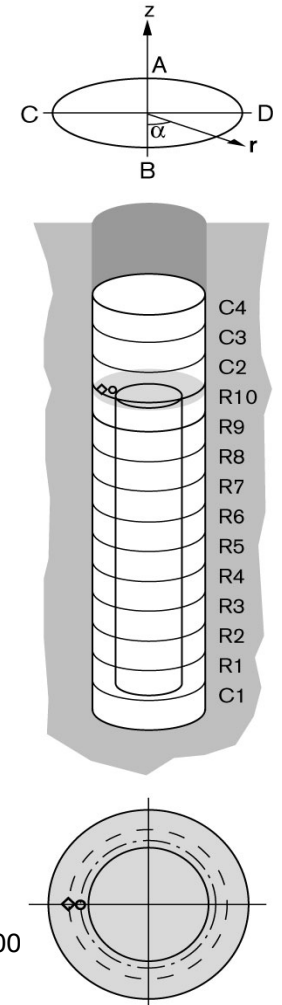
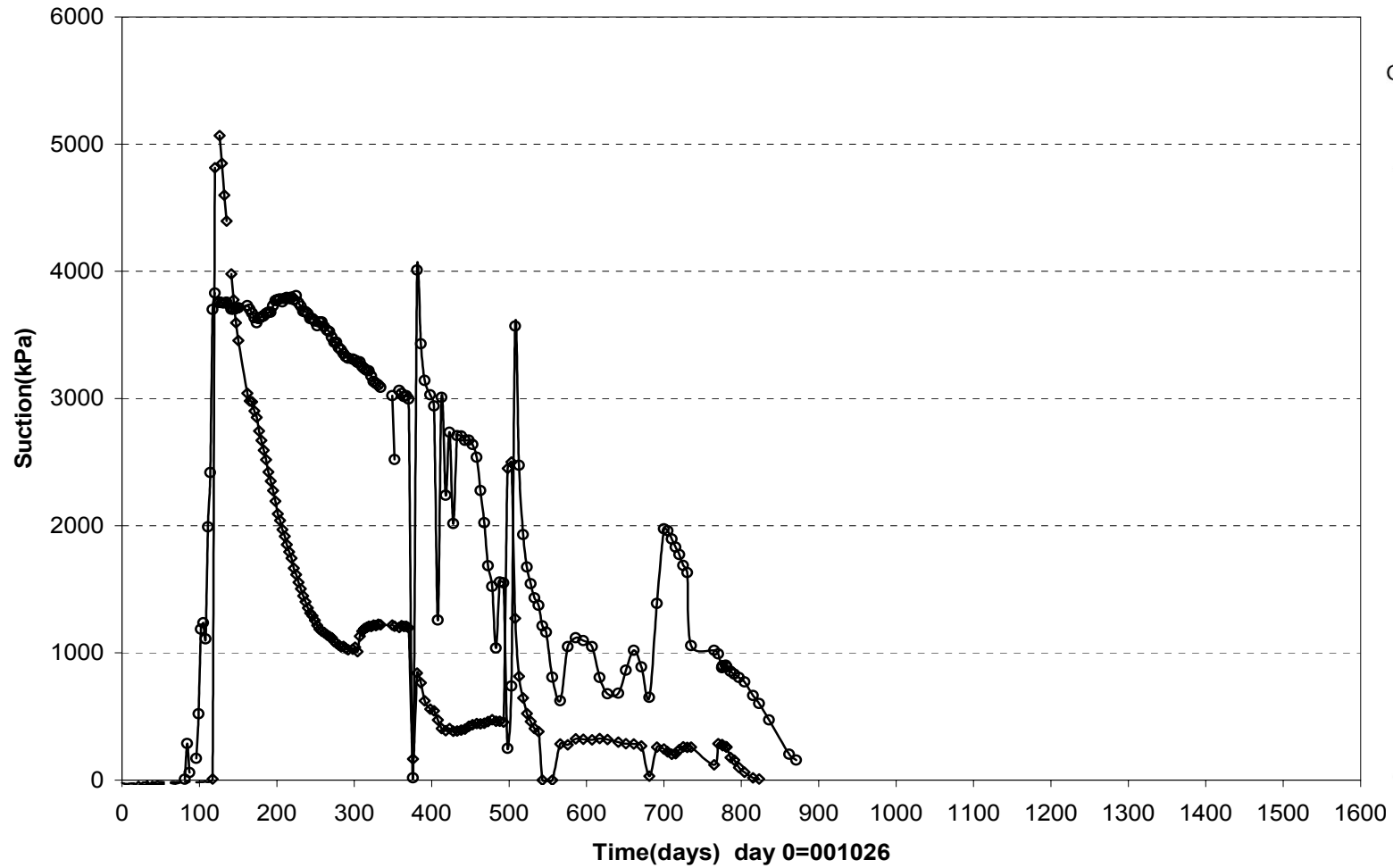
Suction in the buffer - Ring 10 (001026-041101)
Wescor



Suction in the buffer - Ring 10 (001026-041101)
Wescor

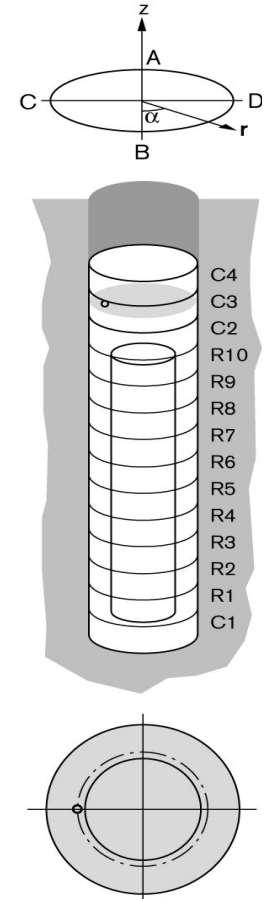
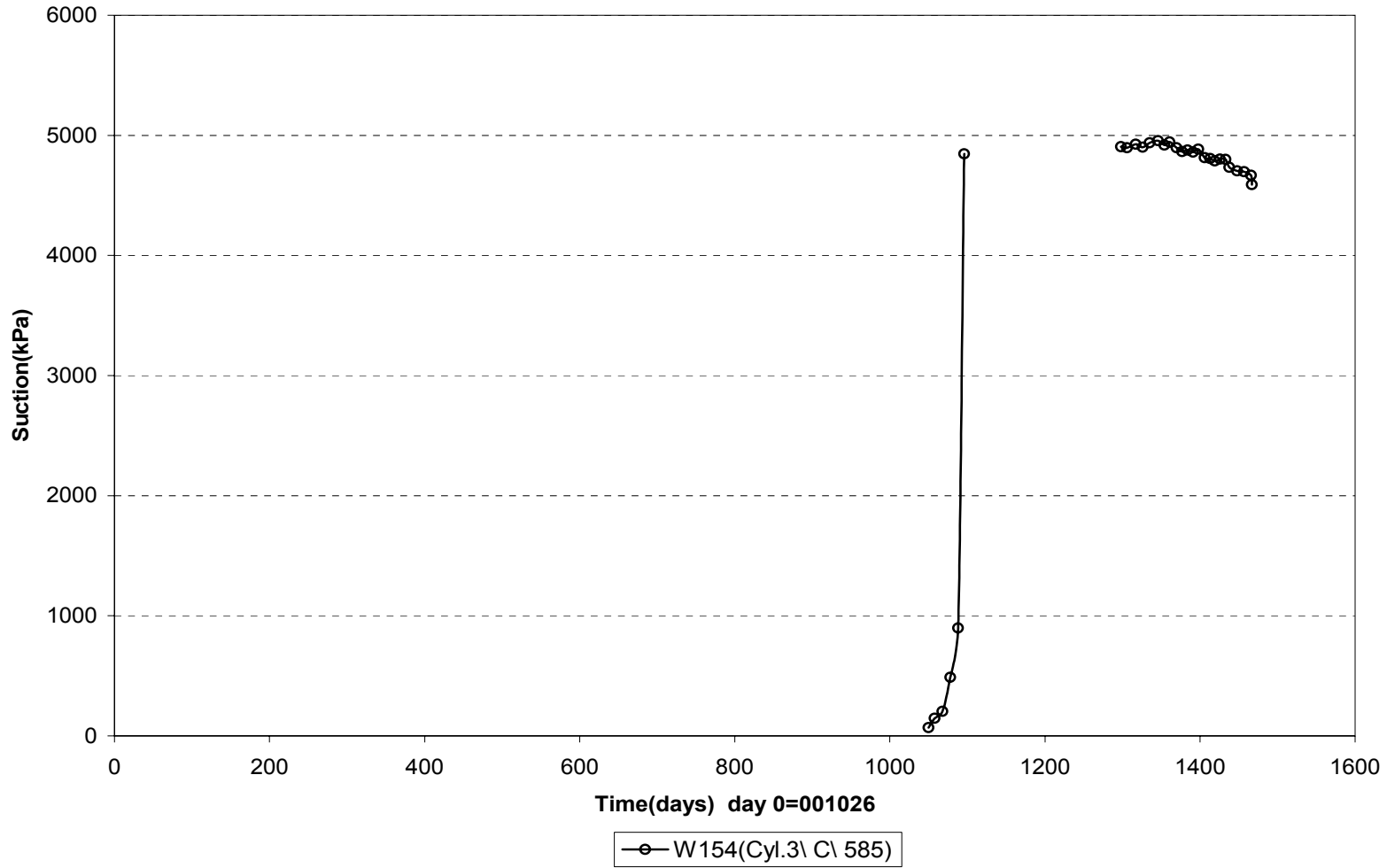


Suction in the buffer - Ring 10 (001026-041101)
Wescor

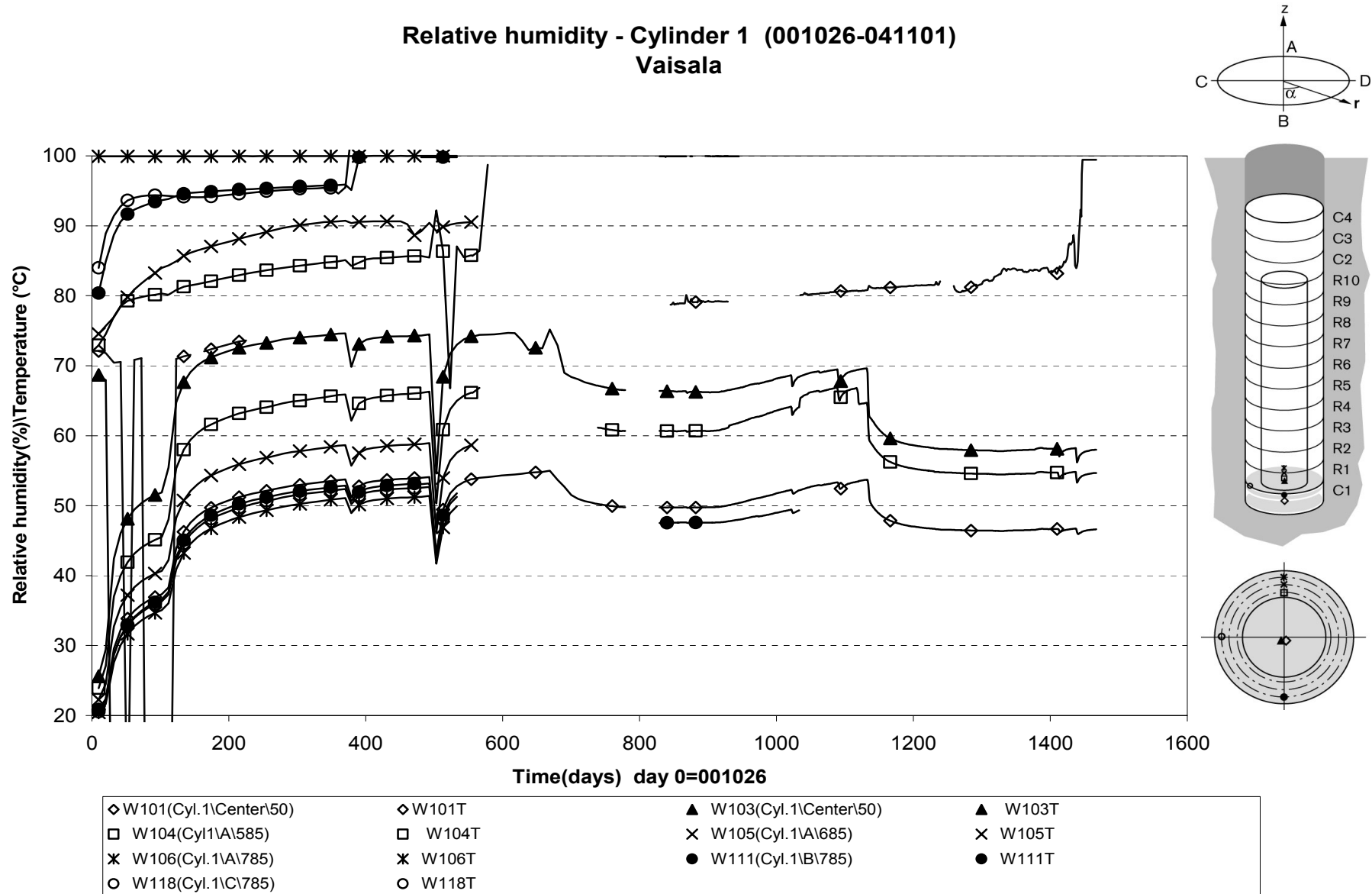


—○— W148(Ring10\ C\ 585) —◇— W149(Ring10\ C\ 685)

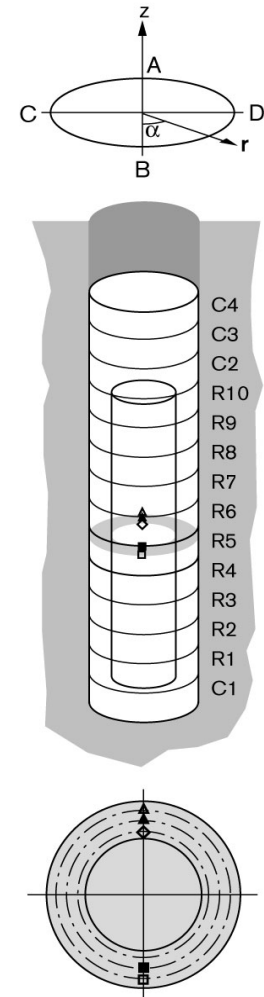
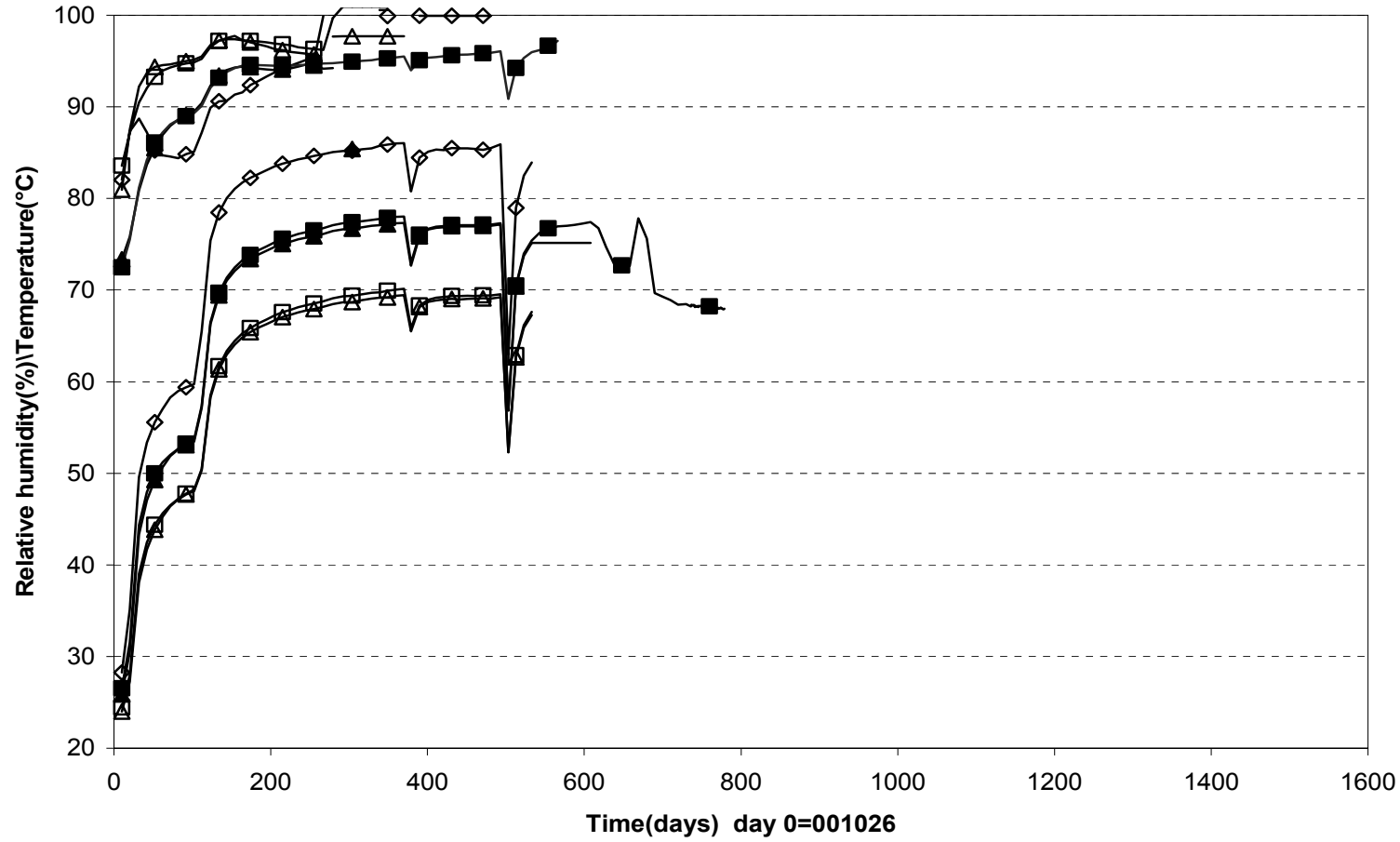
Suction in the buffer - Cyl.3 (001026-041101)
Wescor



Relative humidity - Cylinder 1 (001026-041101)
Vaisala

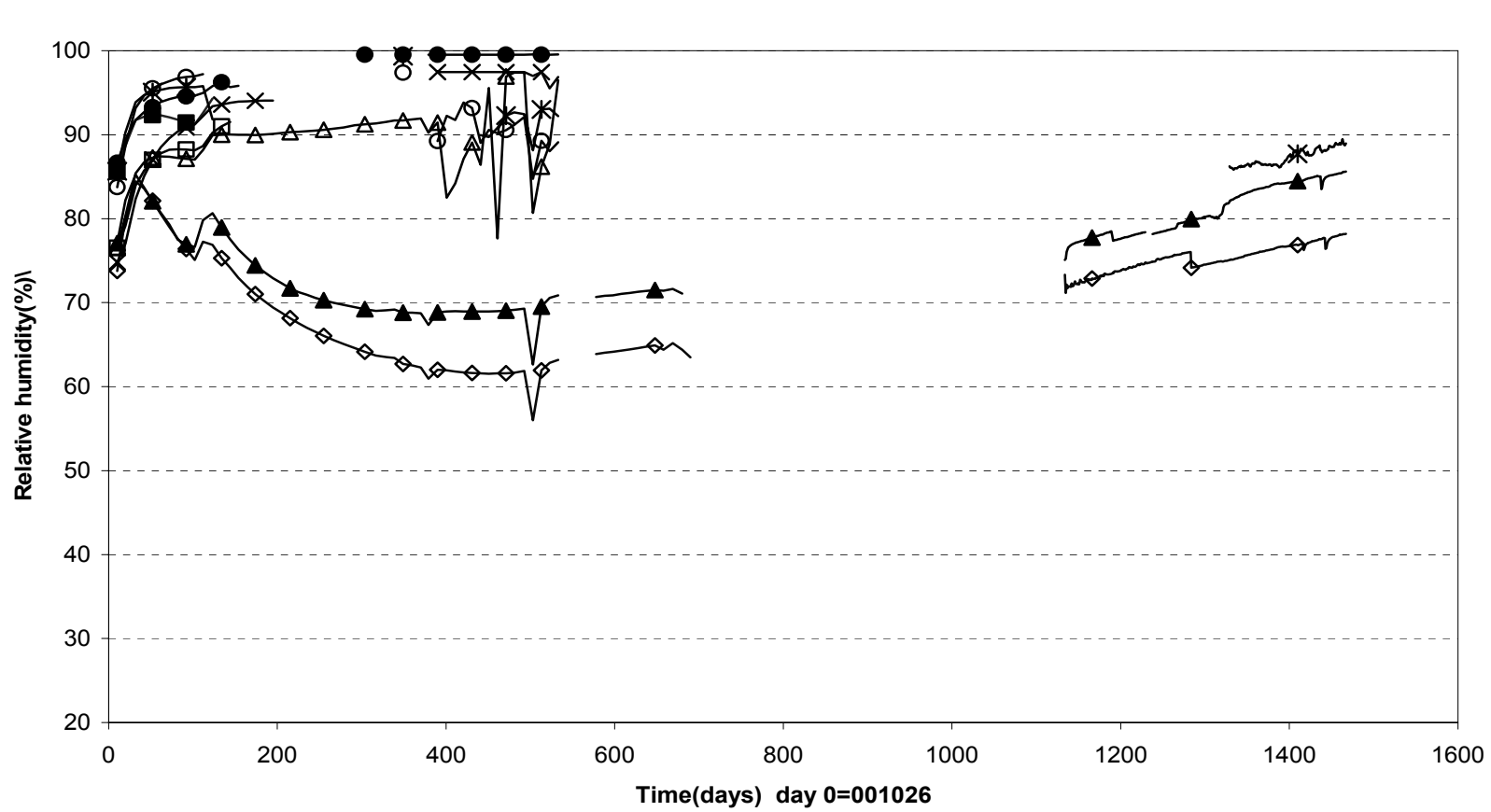


Relative humidity- Ring 5 (001026-041101) Vaisala



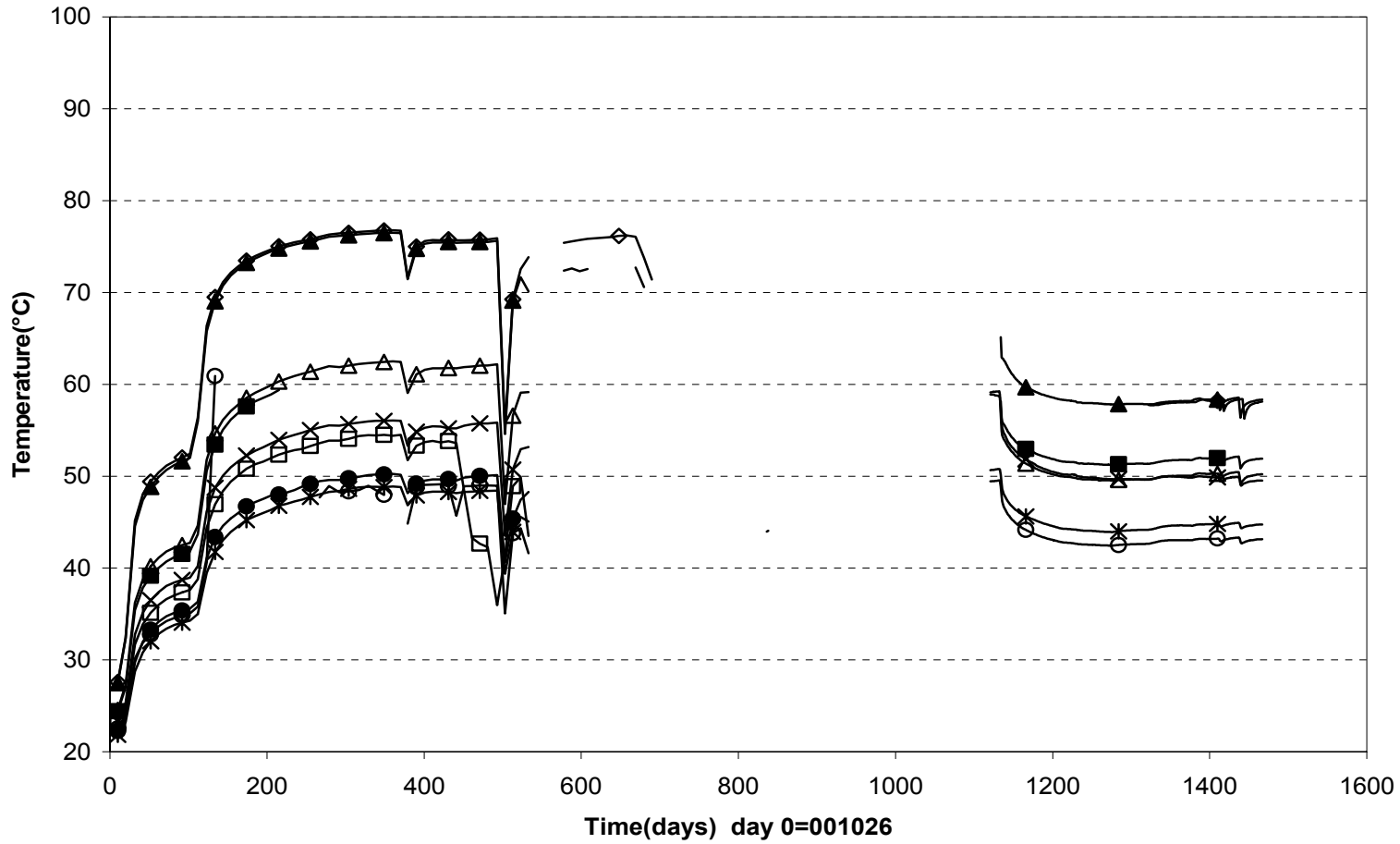
◇ W119(Ring5\A\585)	◇ W119T	▲ W120Ring5\A\685)	▲ W120T	■ W126(Ring5\B\685)
■ W126T	△ W121(Ring5\A\785)	△ W121T	□ W127(Ring5\B\785)	□ W127T

Relative humidity - Ring 10 (001026-041101) Vaisala

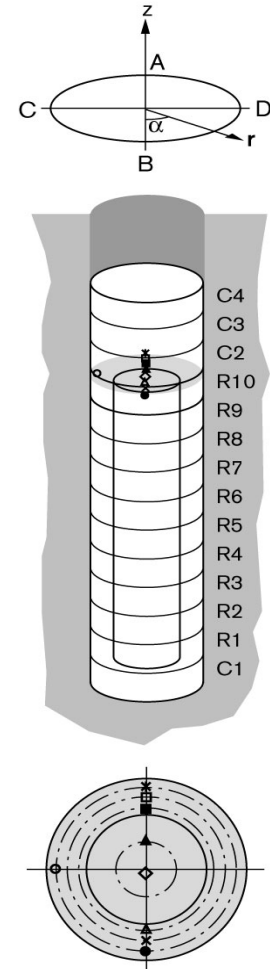


◇ W134(Ring.10\center\50)	▲ W135(Ring.10\A\262)	■ W136(Ring.10\A\585)
△ W142(Ring.10\B\585)	□ W137(Ring.10\A\685)	× W143(Ring.10\B\685)
✱ W138(Ring.10\A\785)	● W144(Ring.10\B\785)	○ W150(Ring.10\C\785)

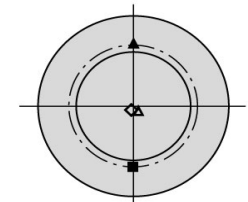
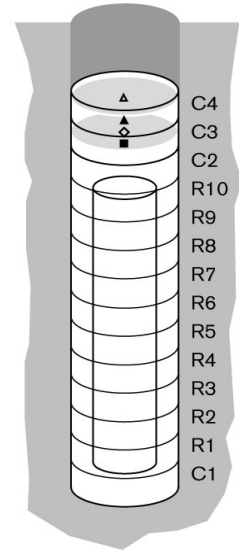
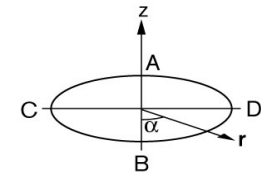
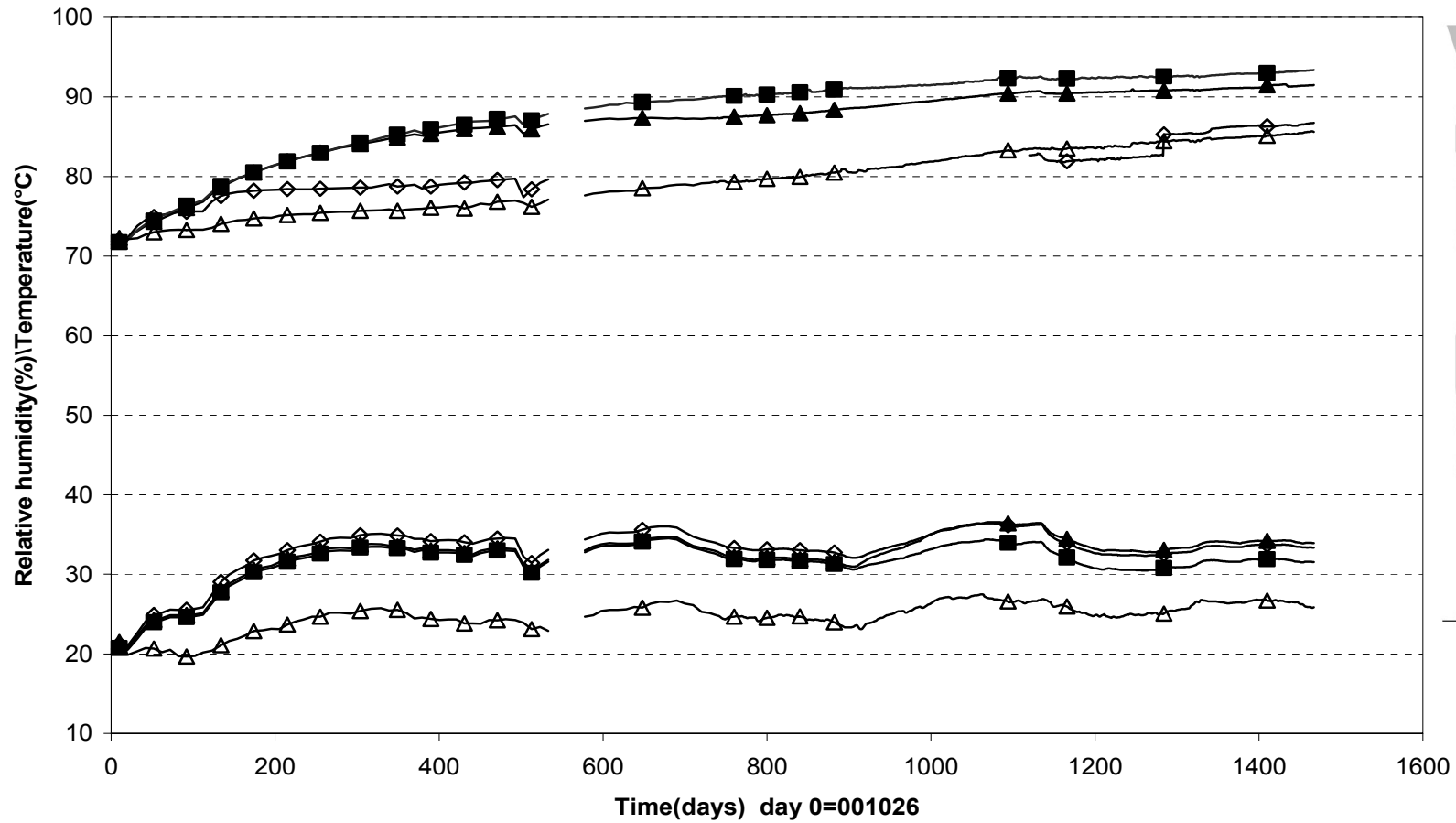
Relative humidity - Ring 10 (001026-041101)
Vaisala



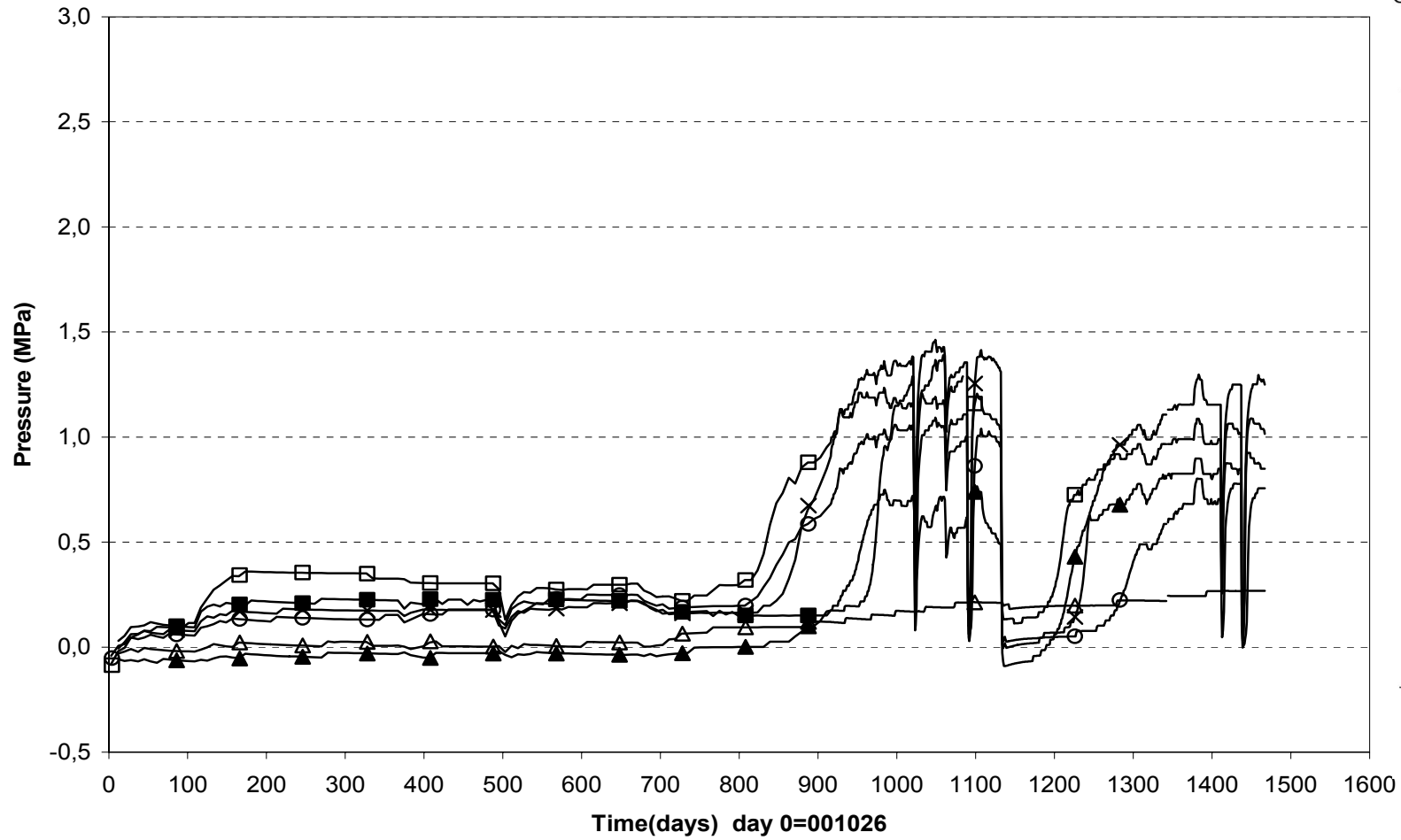
- ◇ W134T
- ▲ W135T
- W136T
- △ W142T
- W137T
- × W143T
- ✱ W138T
- W144T
- W150T



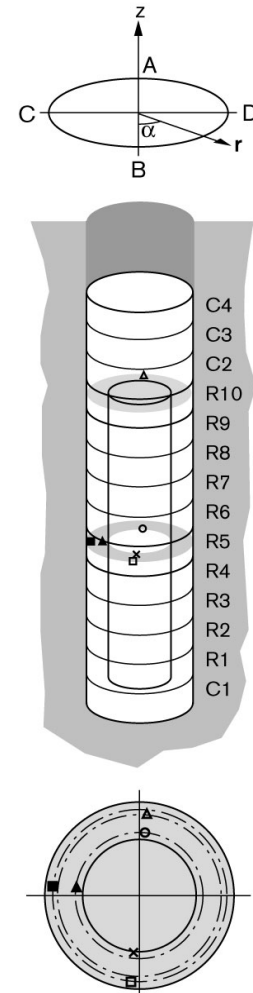
Relative humidity - Cylinder 3 and Cylinder 4 (001026-041101) Vaisala



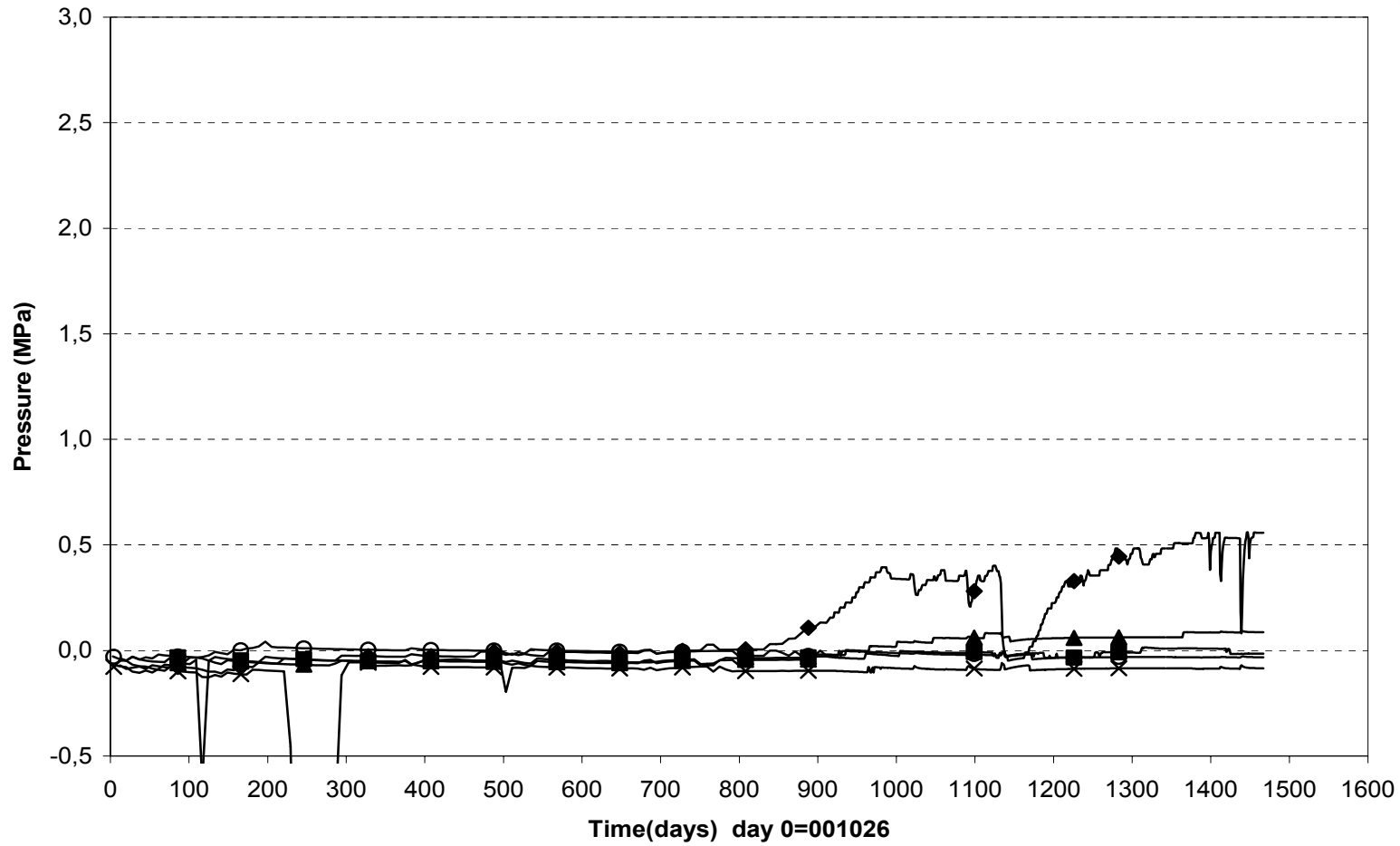
**Pore water pressure - Ring 5 and Ring 10 (001026-041101)
Geokon**



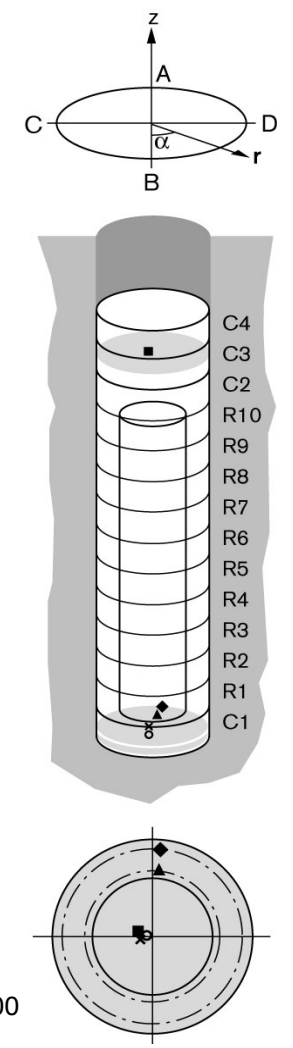
○ U105(Ring5\A\585) × U107(Ring5\B\535) ▲ U109(Ring5\C\585) ■ U110(Ring5\C\815) □ U108(Ring5\B\815\slot) ▲ U112(Ring10\A\785)



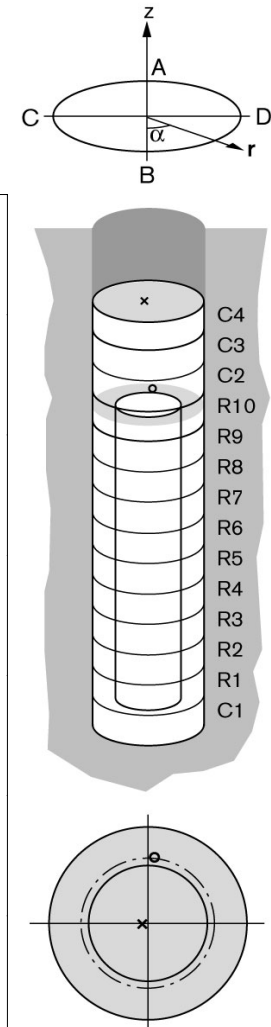
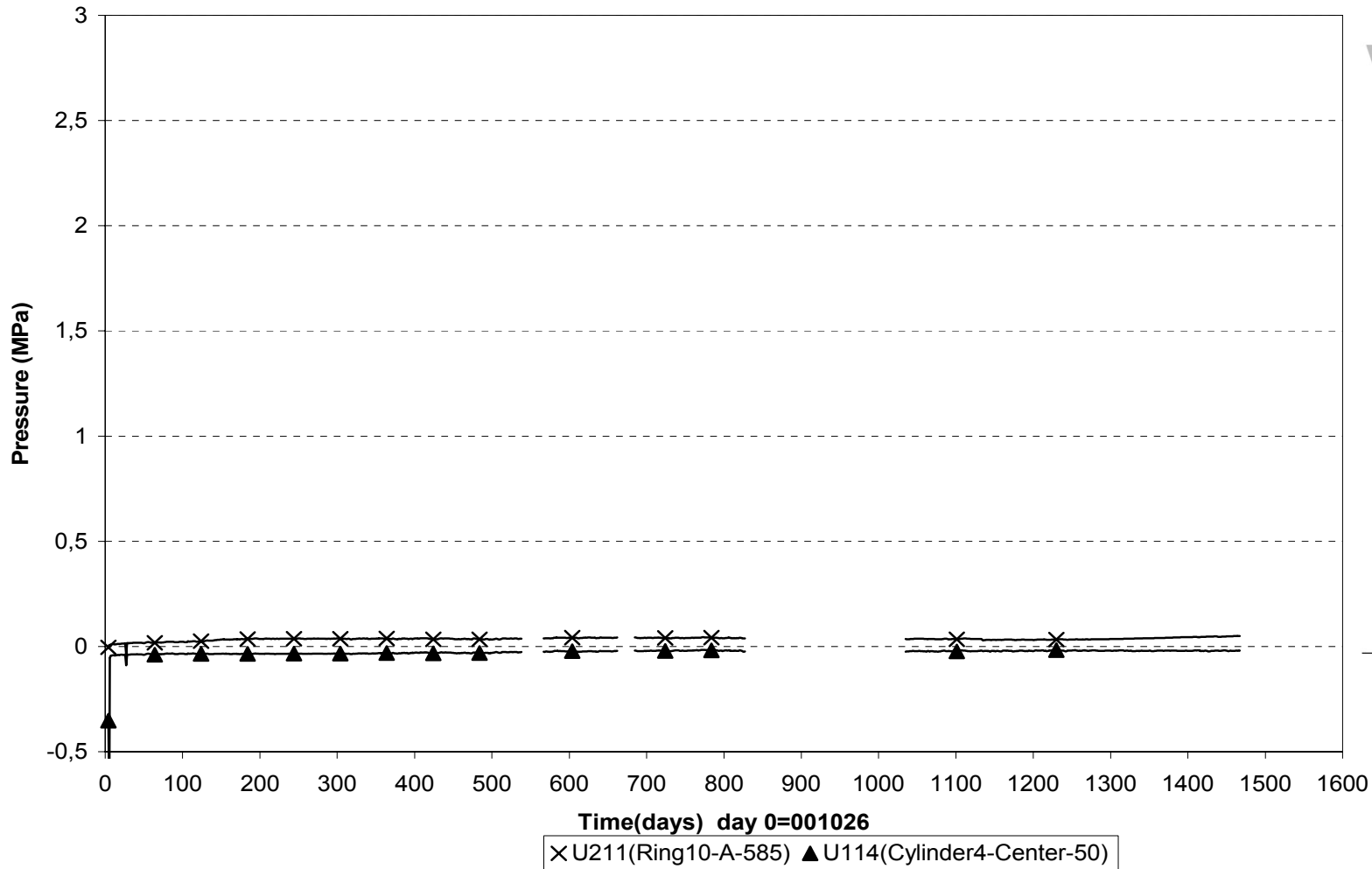
Pore water pressure - Cylinder 1 and Cylinder 3 (001026-041101)
Geokon



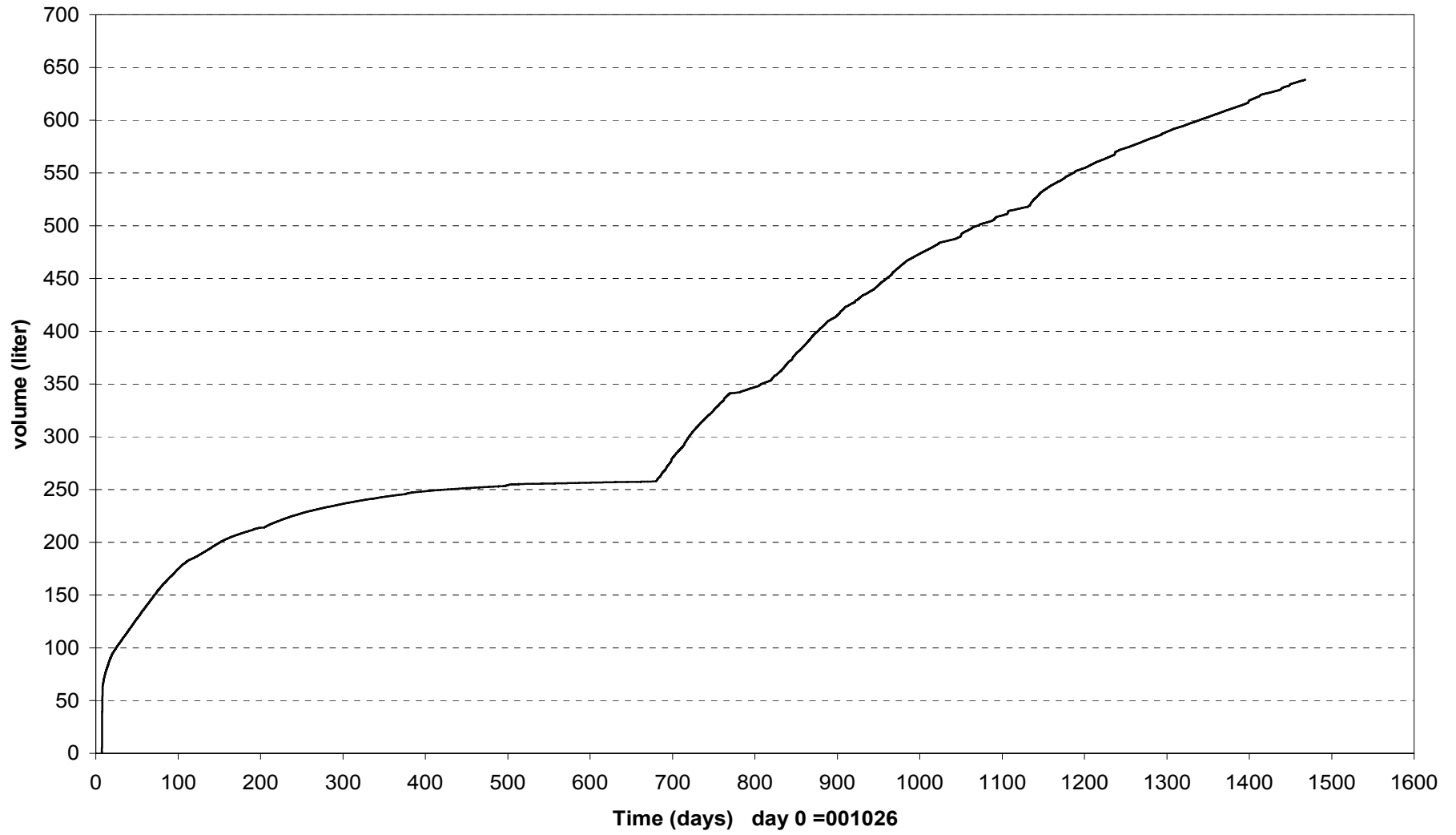
○ U101(Cyl.1\center\50) × U102(Cyl.1\center\50) ▲ U103(Cyl.1\A\585) ◆ U104(Cyl.1\A\785) ■ U113(Cyl.3\center\50)



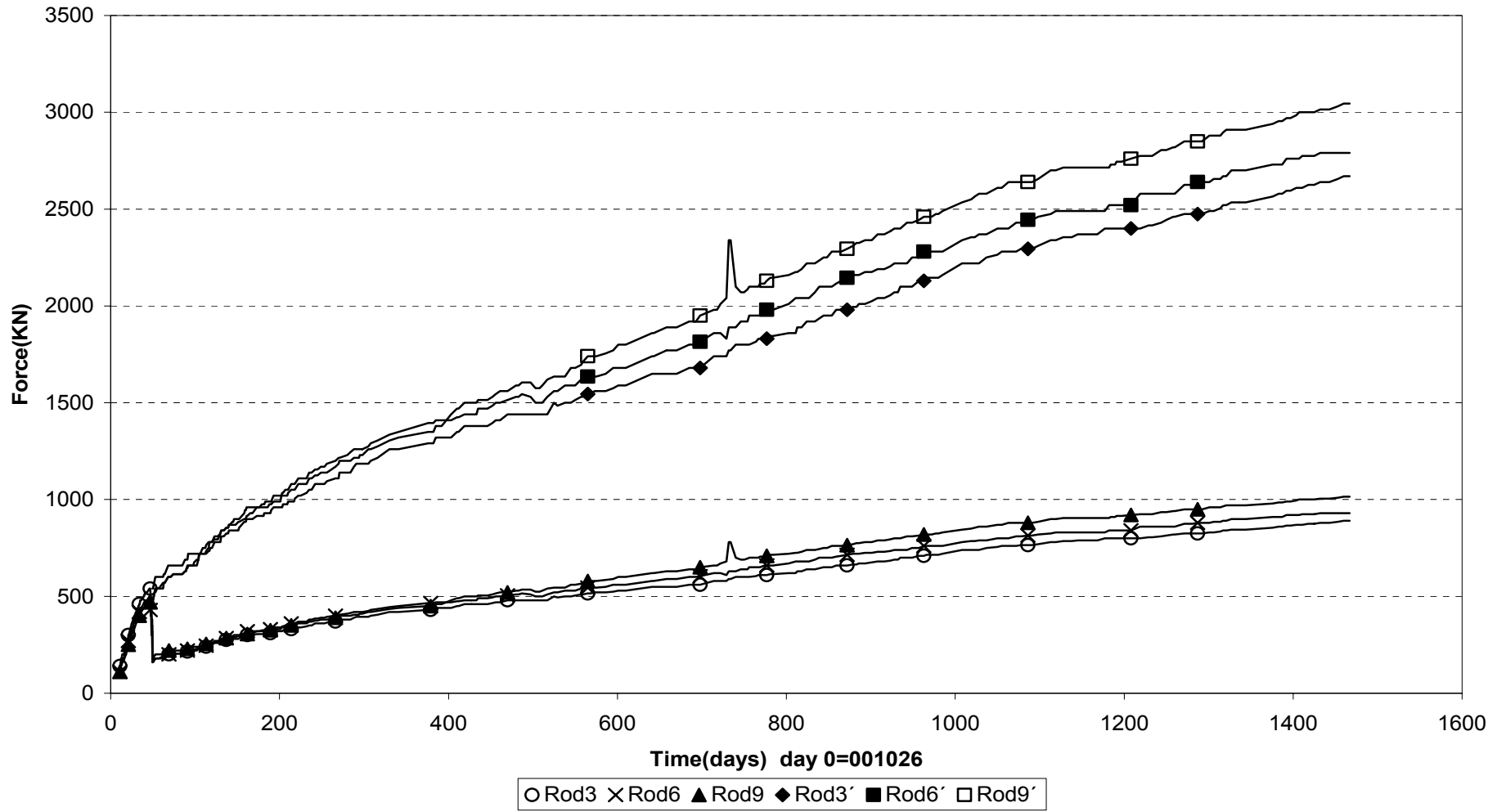
Pore water pressure - Ring 10 & Cylinder 4 (001026-041101)
Kulite



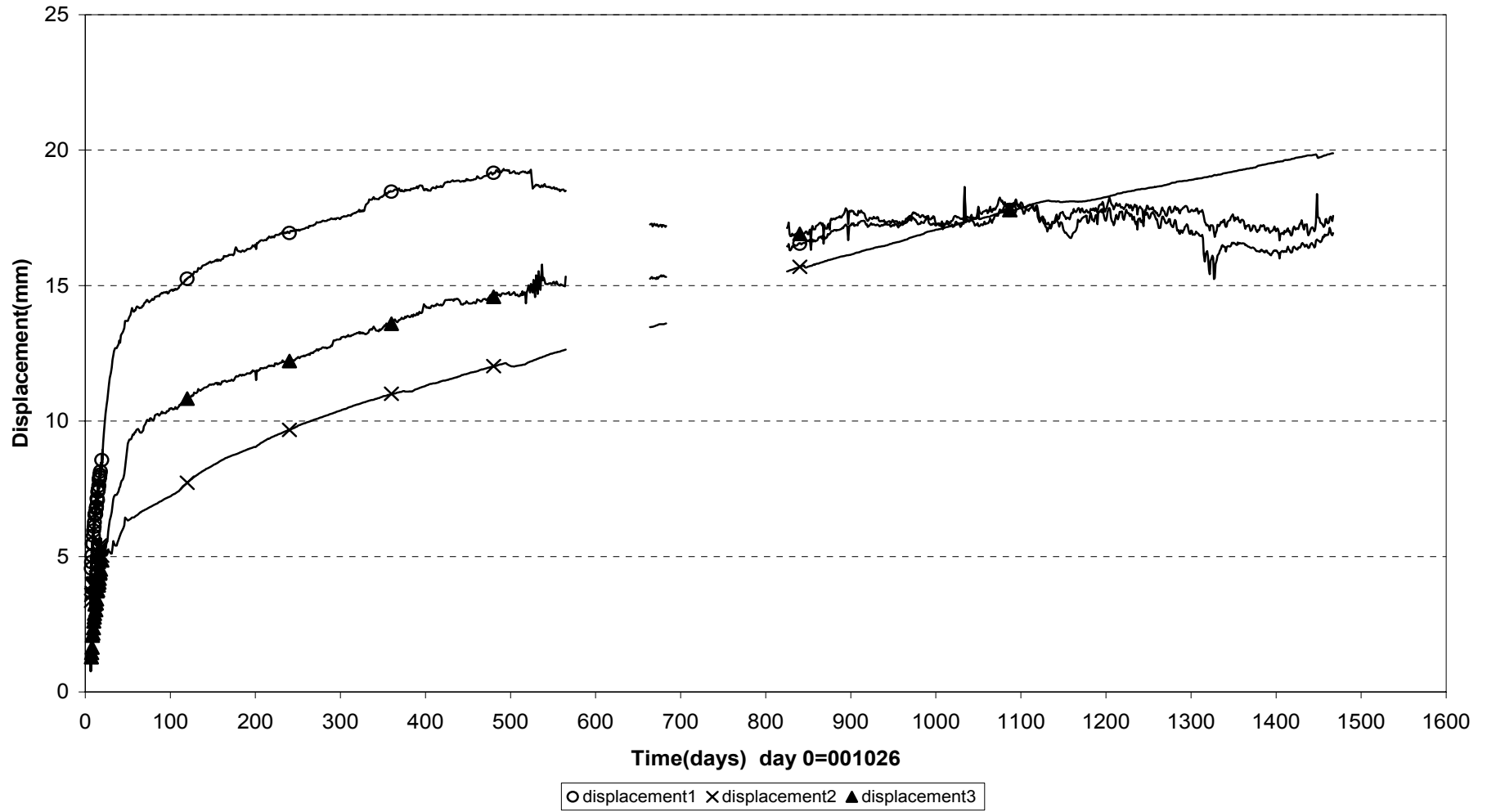
Inflow into filter (001026-041101)



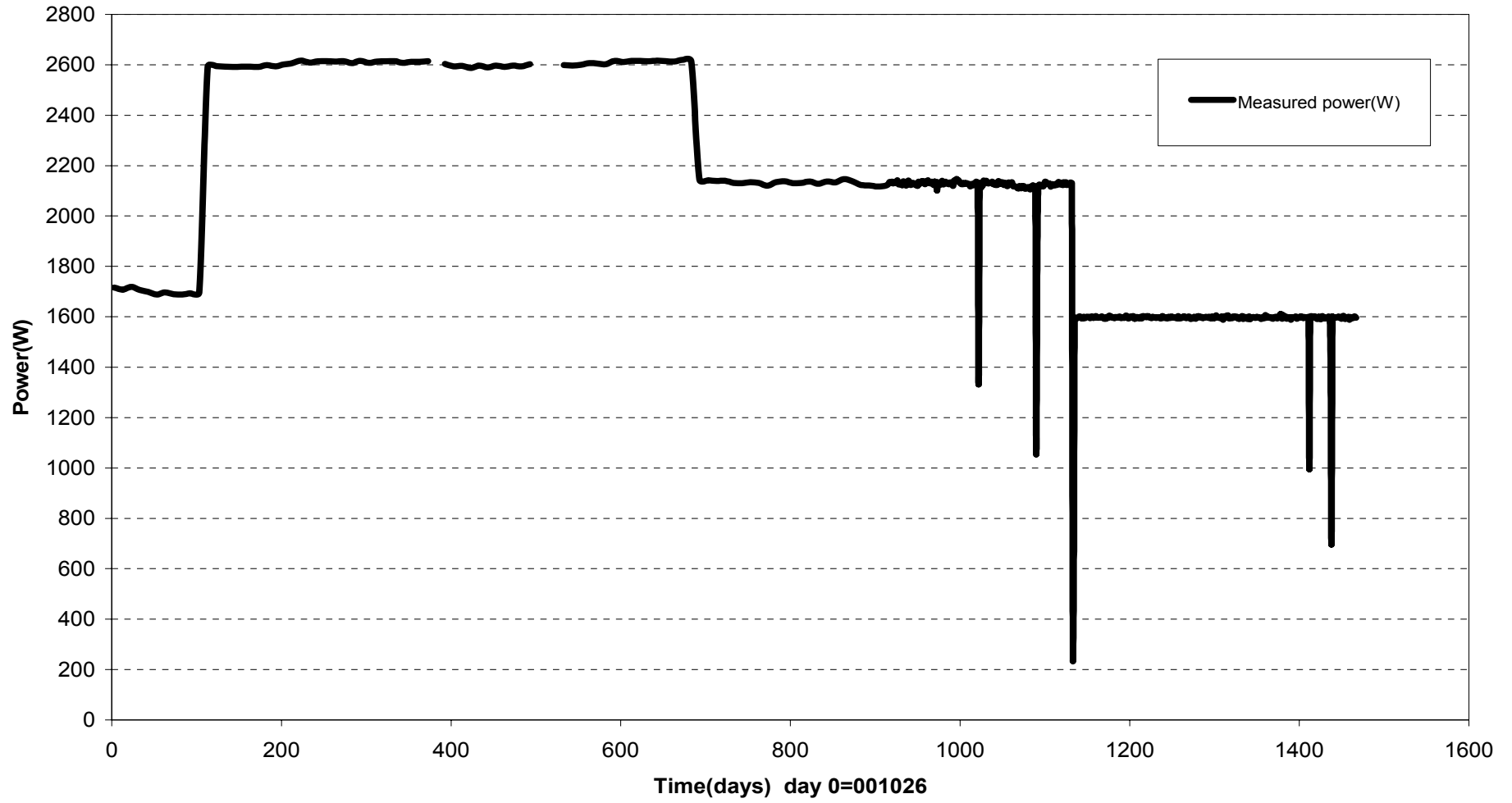
Forces on plug (001026-041101)



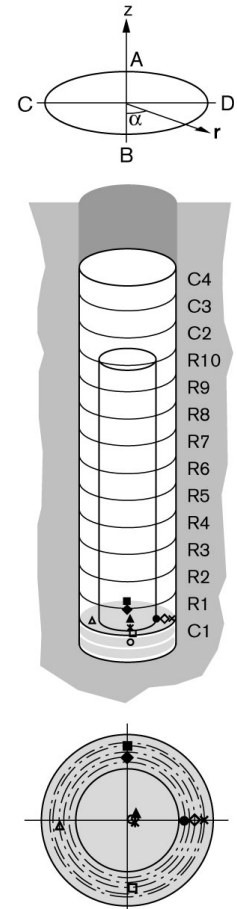
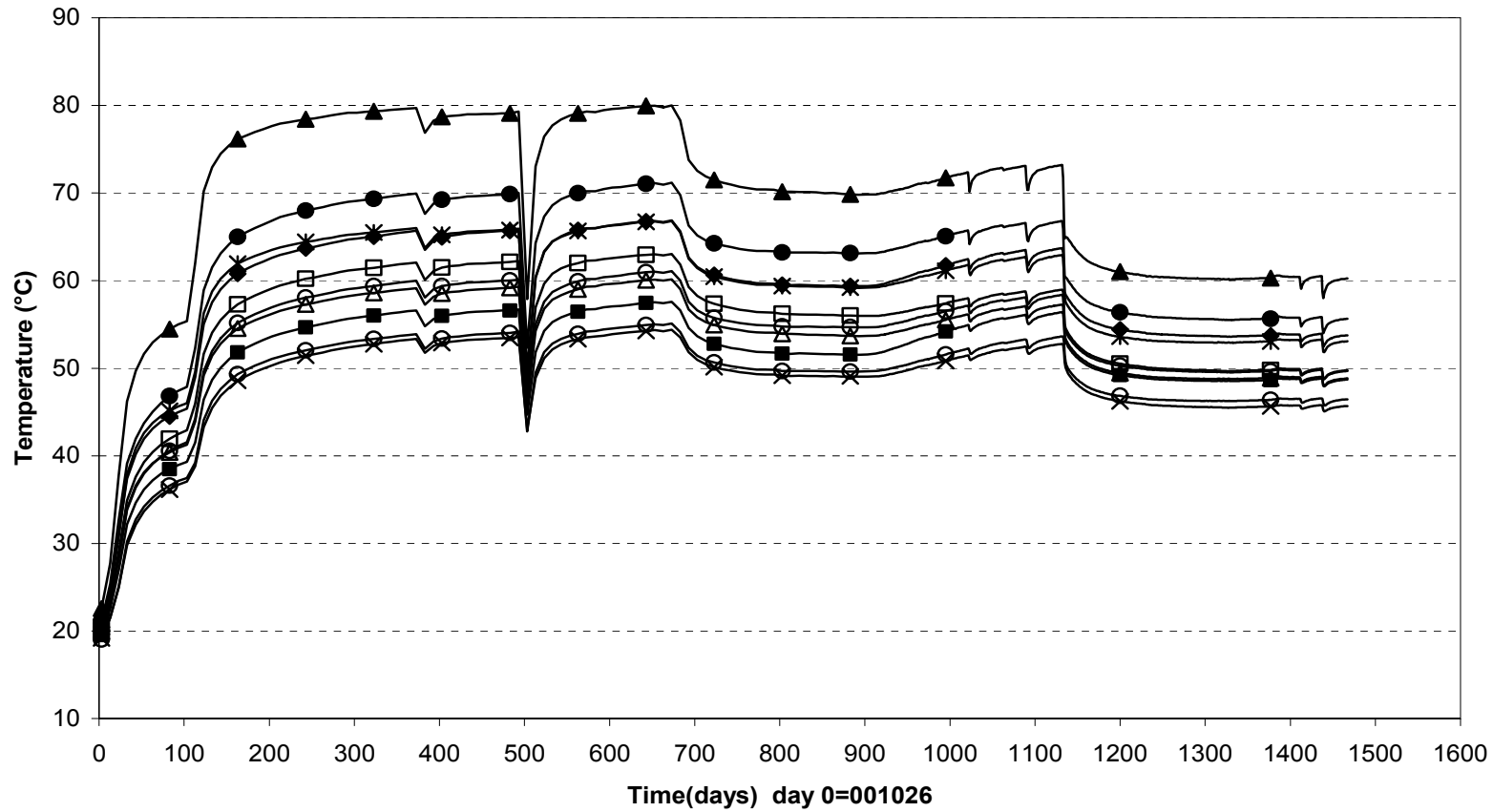
Displacement of plug (001026-041101)



Canister power (001026-041101)

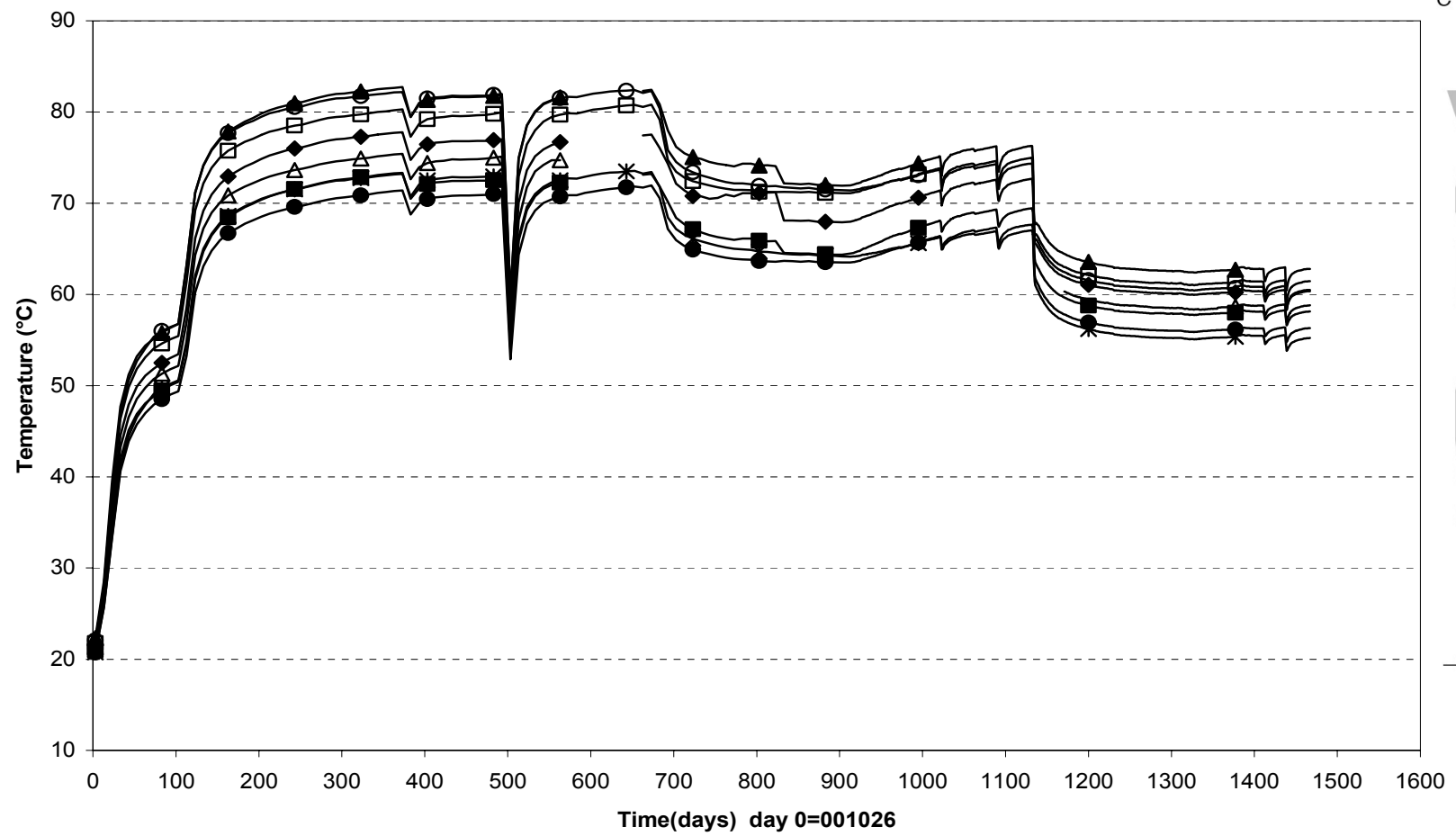


Temperature in the buffer - Cylinder 1 (001026-041101) Thermocouple

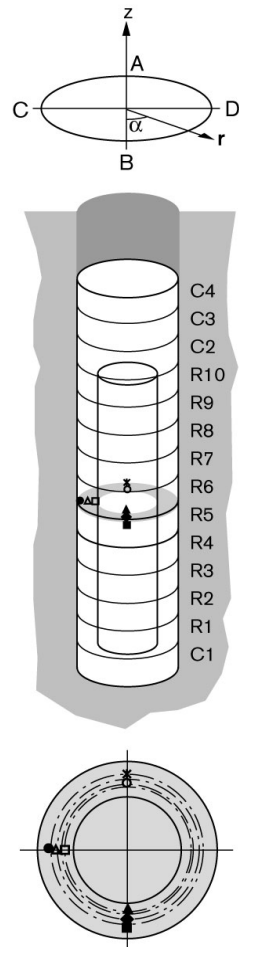


○ T101(Cyl.1\center\50)	✱ T102(Cyl.1\center\50)	▲ T103(Cyl.1\center\50)	◆ T104(Cyl.1\A\635)
■ T105(Cyl.1\A\735)	□ T106(Cyl.1\B\685)	△ T107(Cyl.1\C\685)	● T108(Cyl.1\D\585)
○ T109(Cyl.1\D\685)	✕ T110(Cyl.1\D\785)		

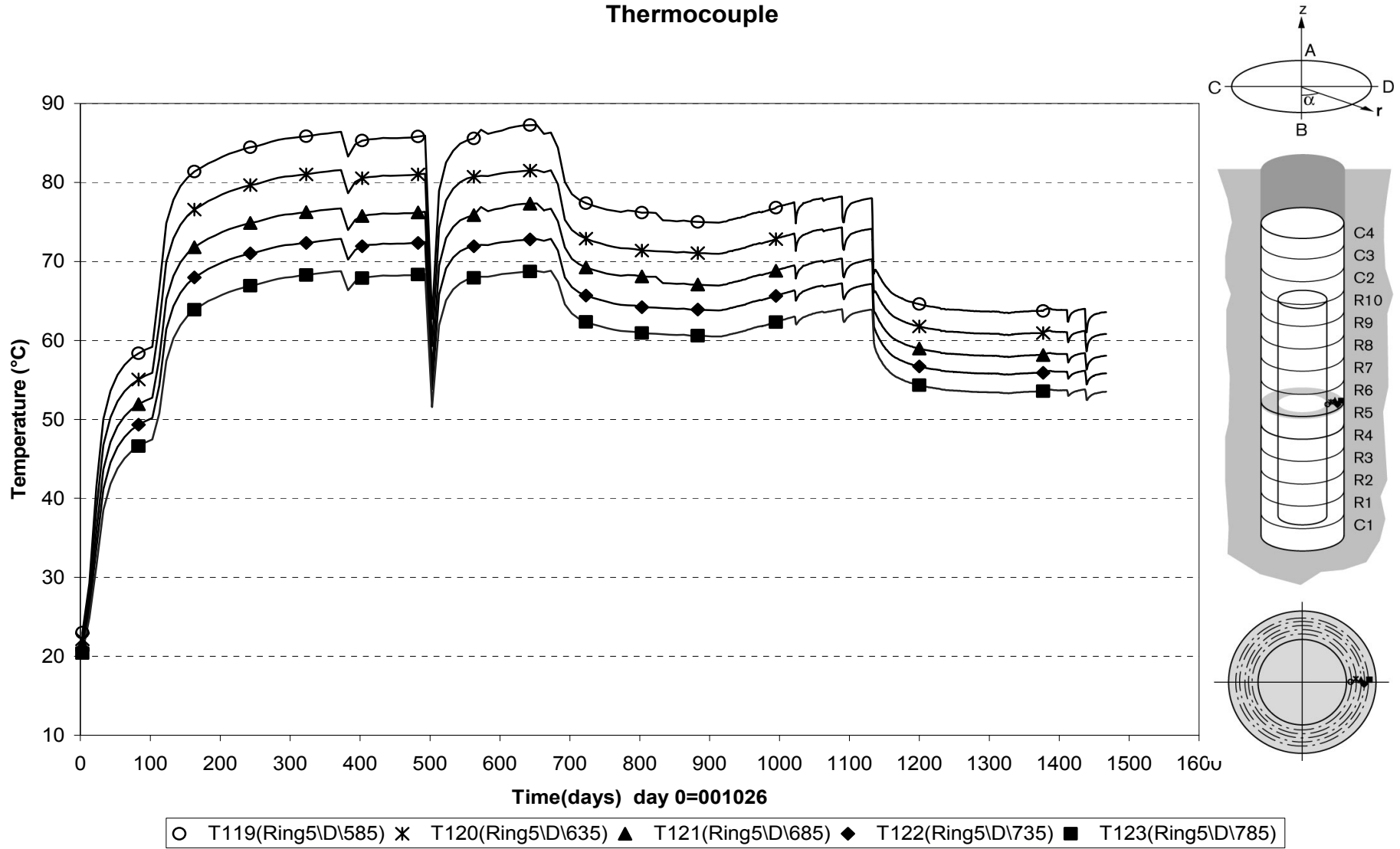
Temperature in the buffer - Ring 5 (001026-041101)
Thermocouple



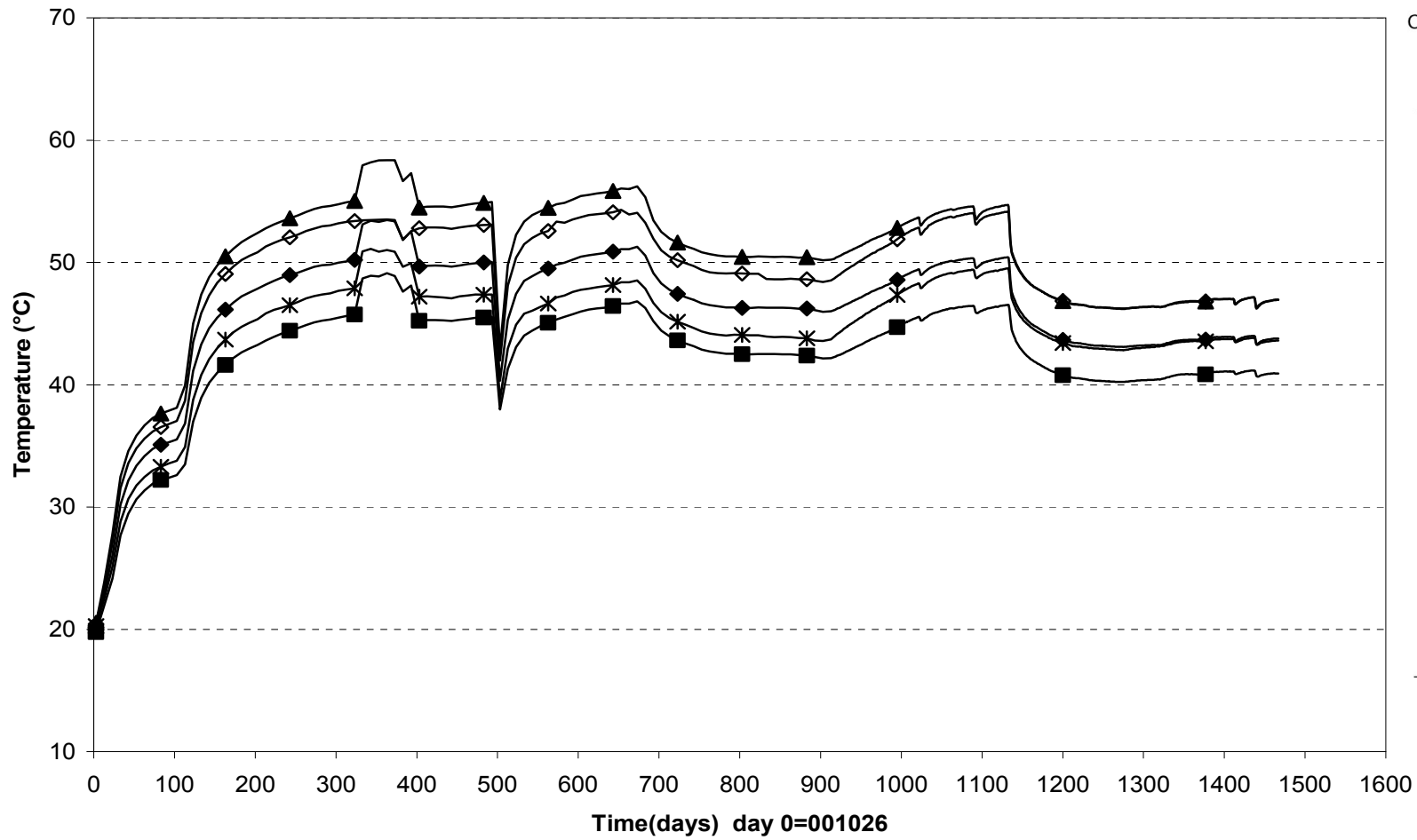
○ T111(Ring5\A\635)	✱ T112(Ring5\A\735)	▲ T113(Ring5\B\610)	◆ T114(Ring5\B\685)
■ T115(Ring5\B\735)	□ T116(Ring5\C\610)	△ T117(Ring5\C\685)	● T118(Ring5\C\735)



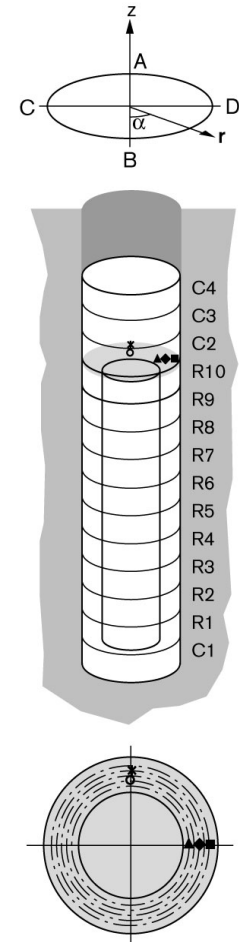
Temperature in the buffer - Ring 5 (001026-041101)
Thermocouple



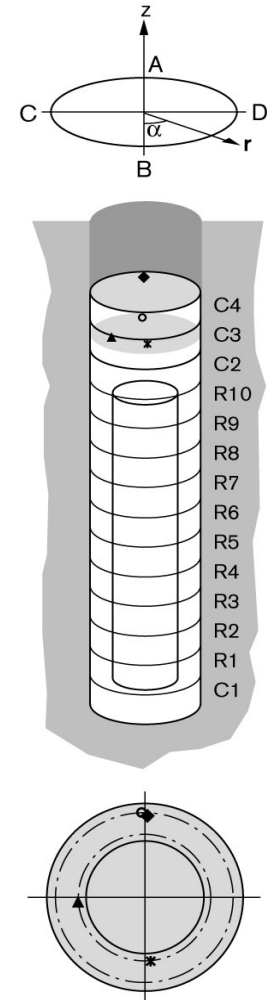
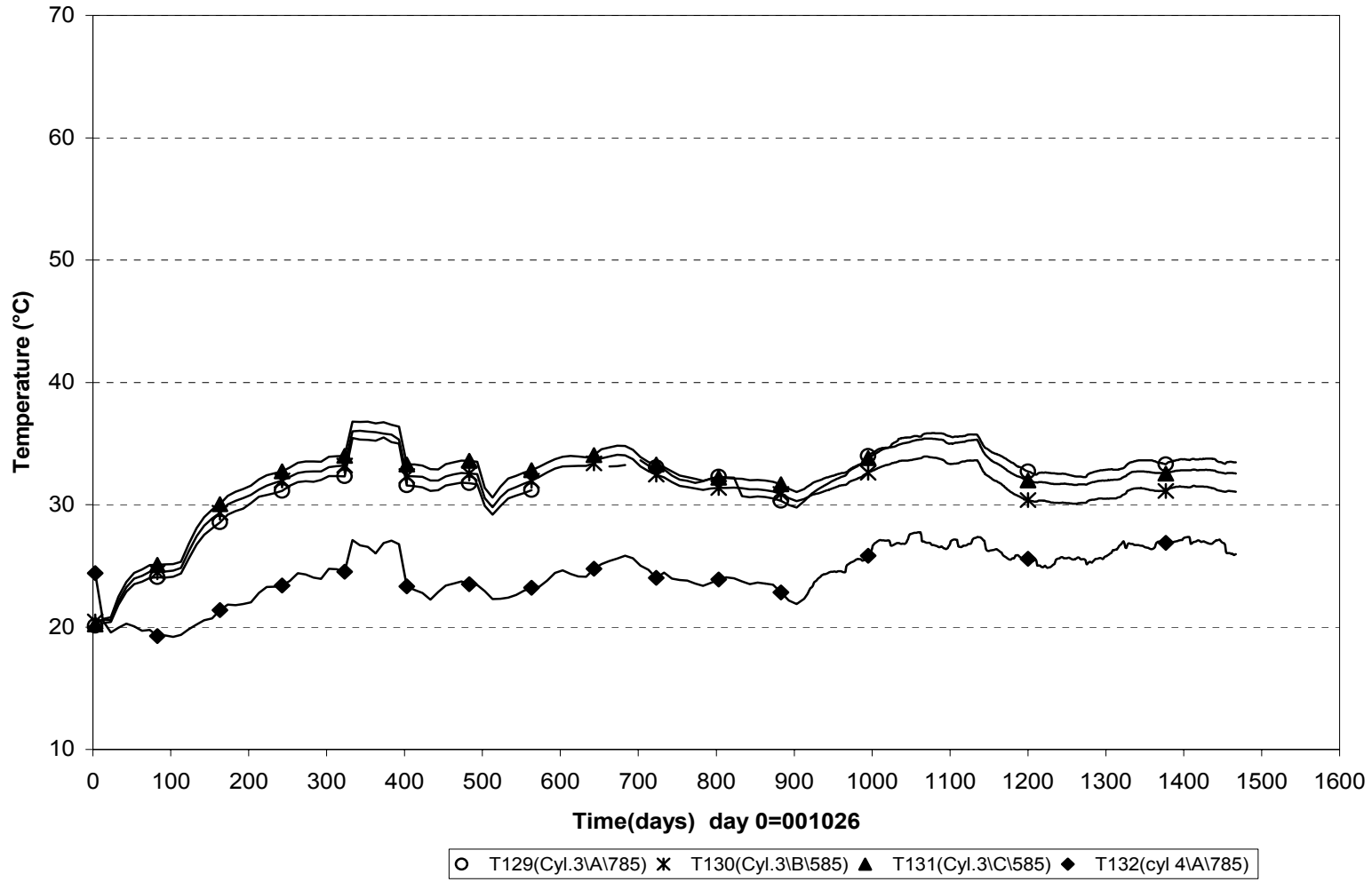
Temperature in the buffer - Ring 10 (001026-041101) Thermocouple



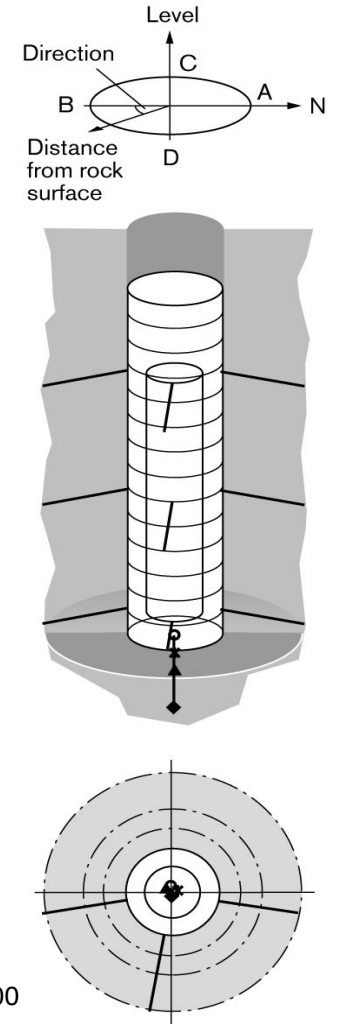
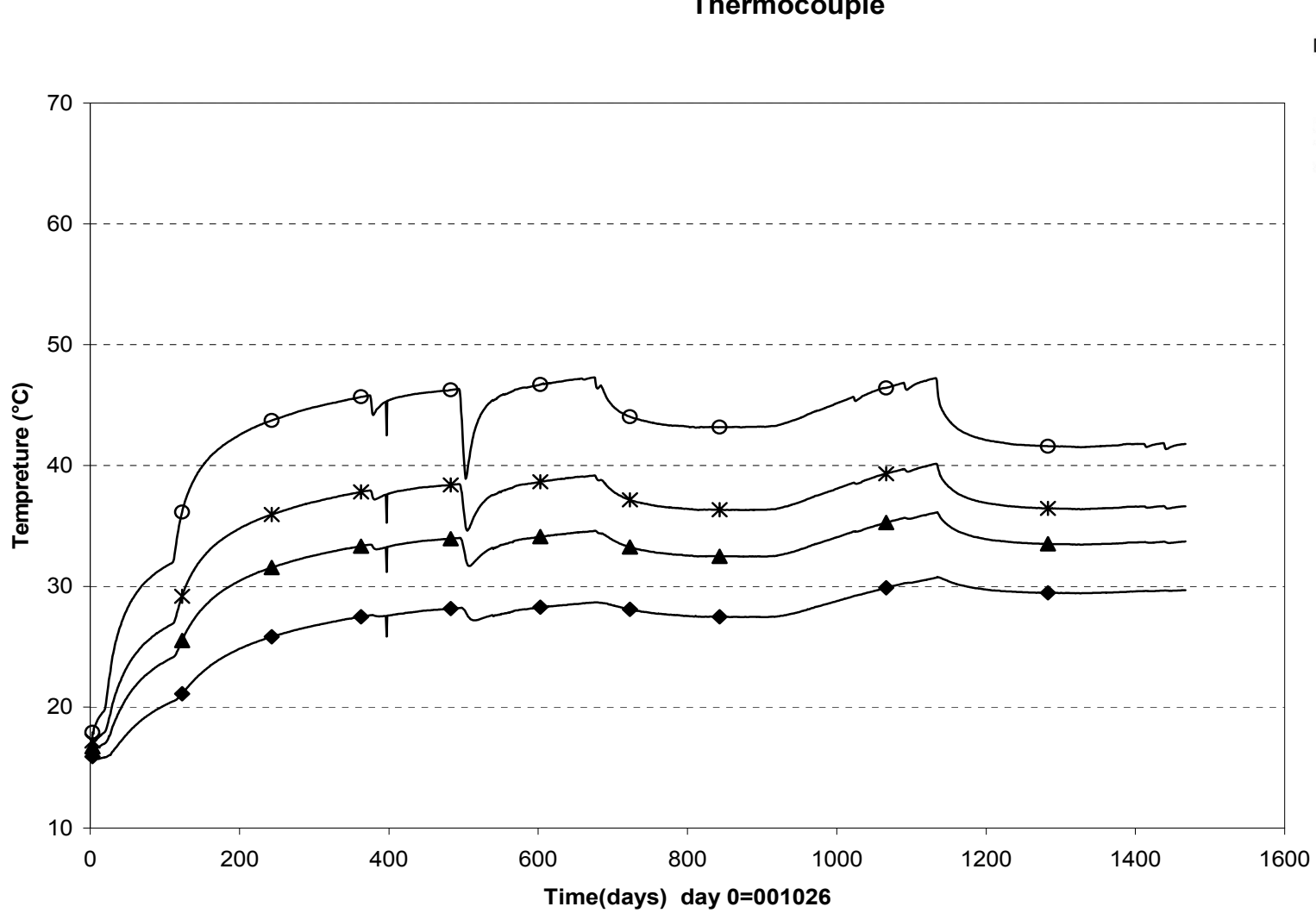
◇ T124(Ring10\A\635)
✱ T125(Ring10\A\735)
▲ T126(Ring10\D\585)
◆ T127(Ring10\D\685)
■ T128(Ring10\D\785)



Temperature in the buffer - Cylinder 3 and Cylinder 4 (001026-041101) Thermocouple

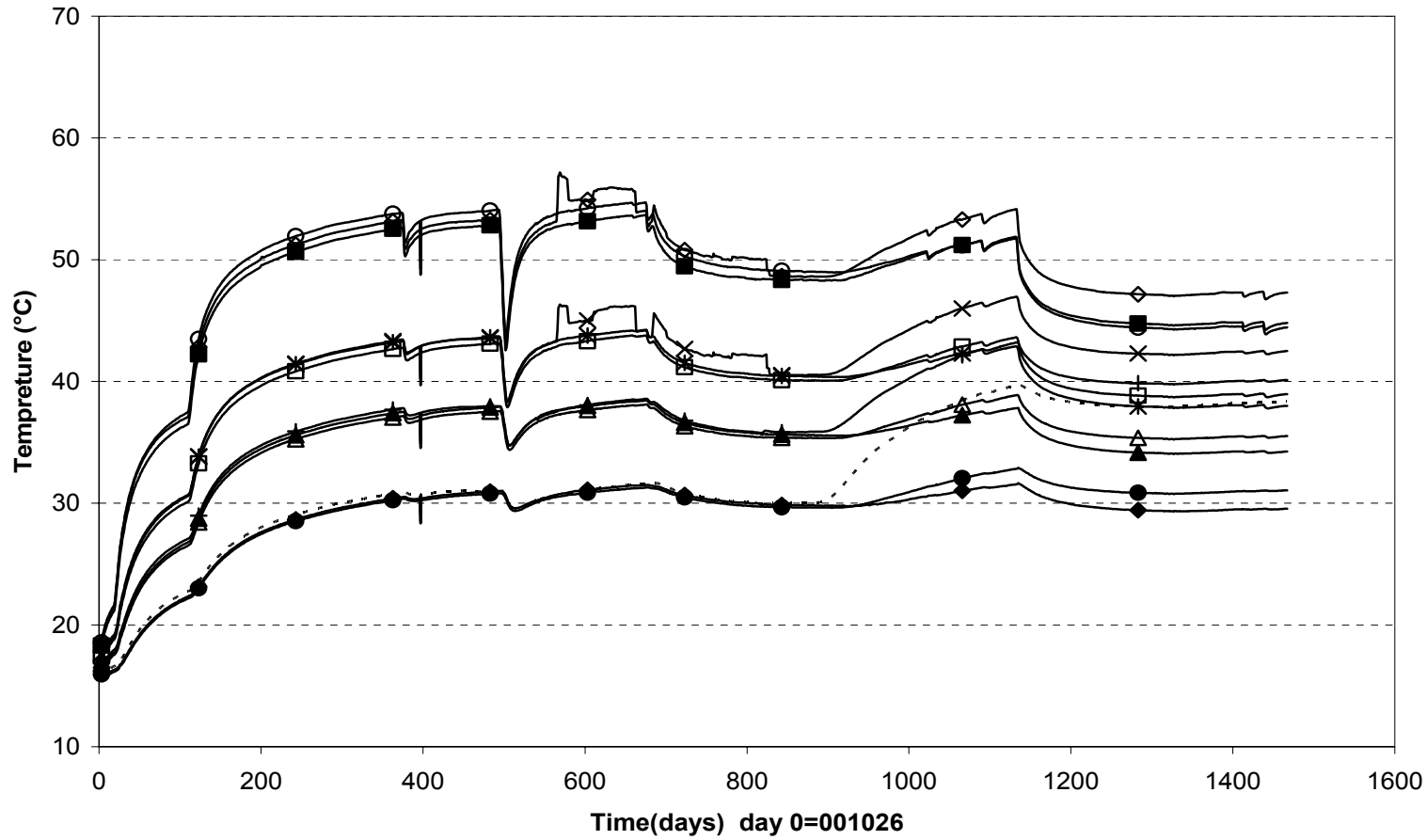


**Temperature in the rock - below the dep. hole (001026-041101)
Thermocouple**

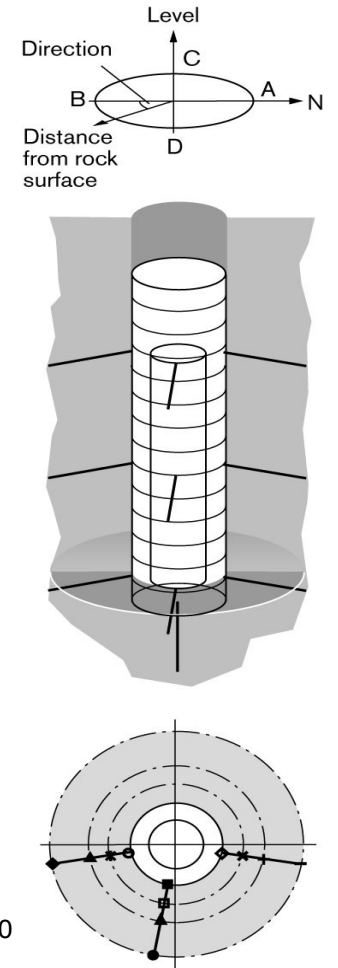


○ TR101(0\center\0,000) ✕ TR102(0\center\0,375) ▲ TR103(0\center\0,750) ◆ TR104(0\center\1,500)

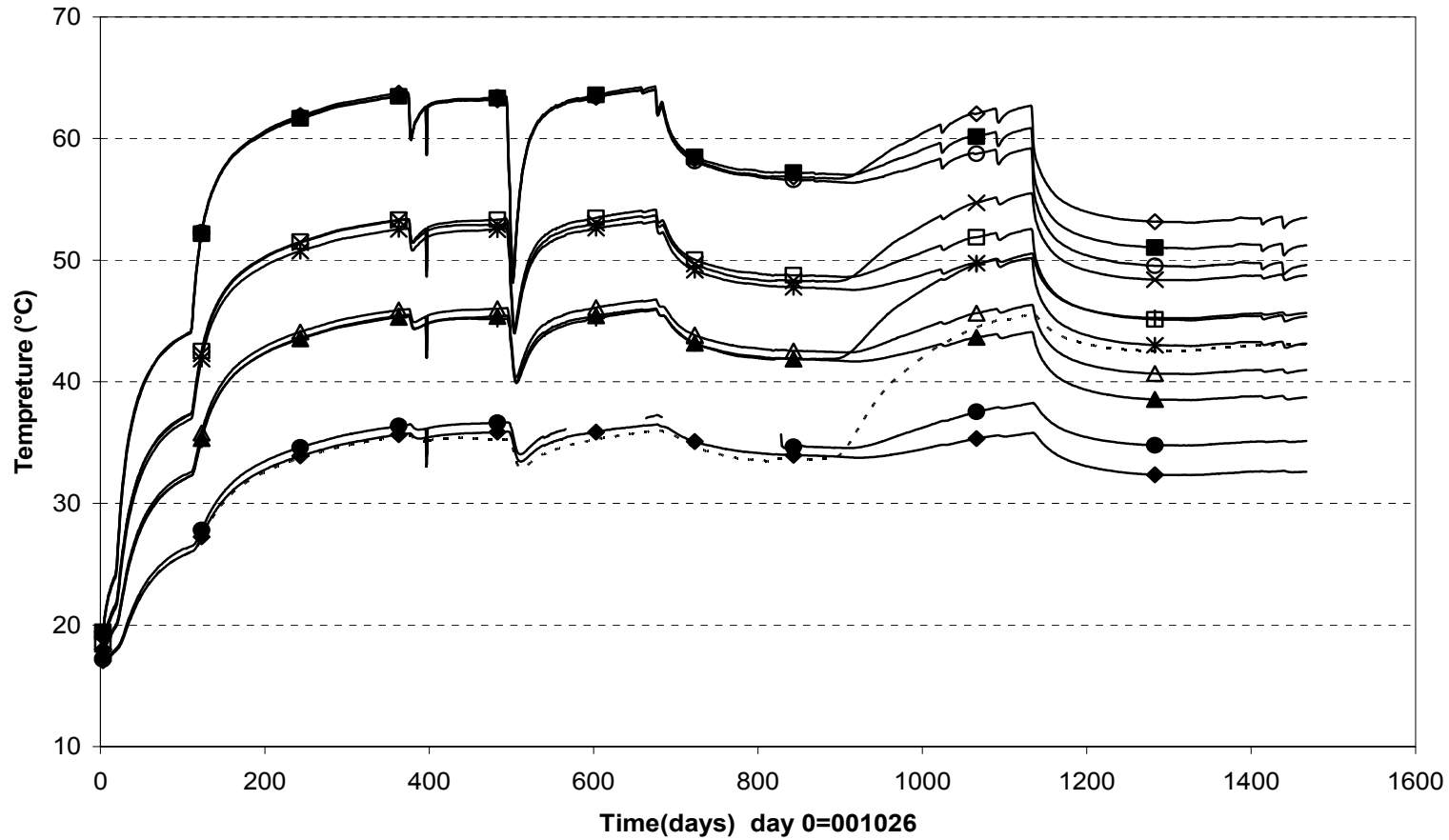
**Temperature in the rock - level 0,6 m (001026-041101)
Thermocouple**



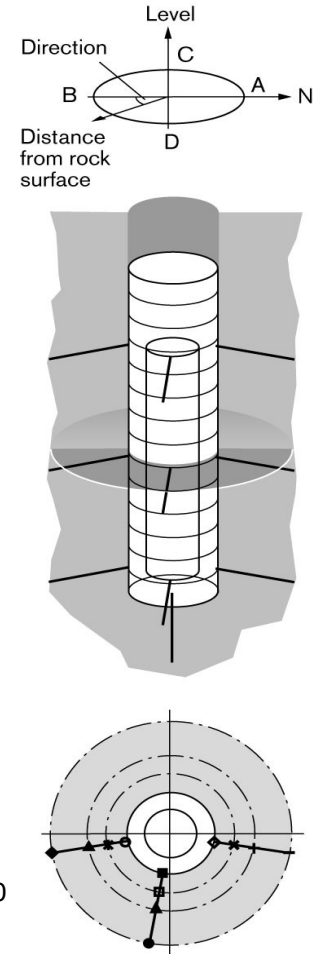
○ TR105(0,61\10°\0,000)	✱ TR106(0,61\10°\0,375)	▲ TR107(0,61\10°\0,750)	◆ TR108(0,61\10°\1,500)
■ TR109(0,61\80°\0,000)	□ TR110(0,61\80°\0,375)	△ TR111(0,61\80°\0,750)	● TR112(0,61\80°\1,750)
◇ TR113(0,61\170°\0,000)	✕ TR114(0,61\170°\0,375)	+	TR115(0,61\170°\0,750) - - - - TR116(0,61\170°\1,500)



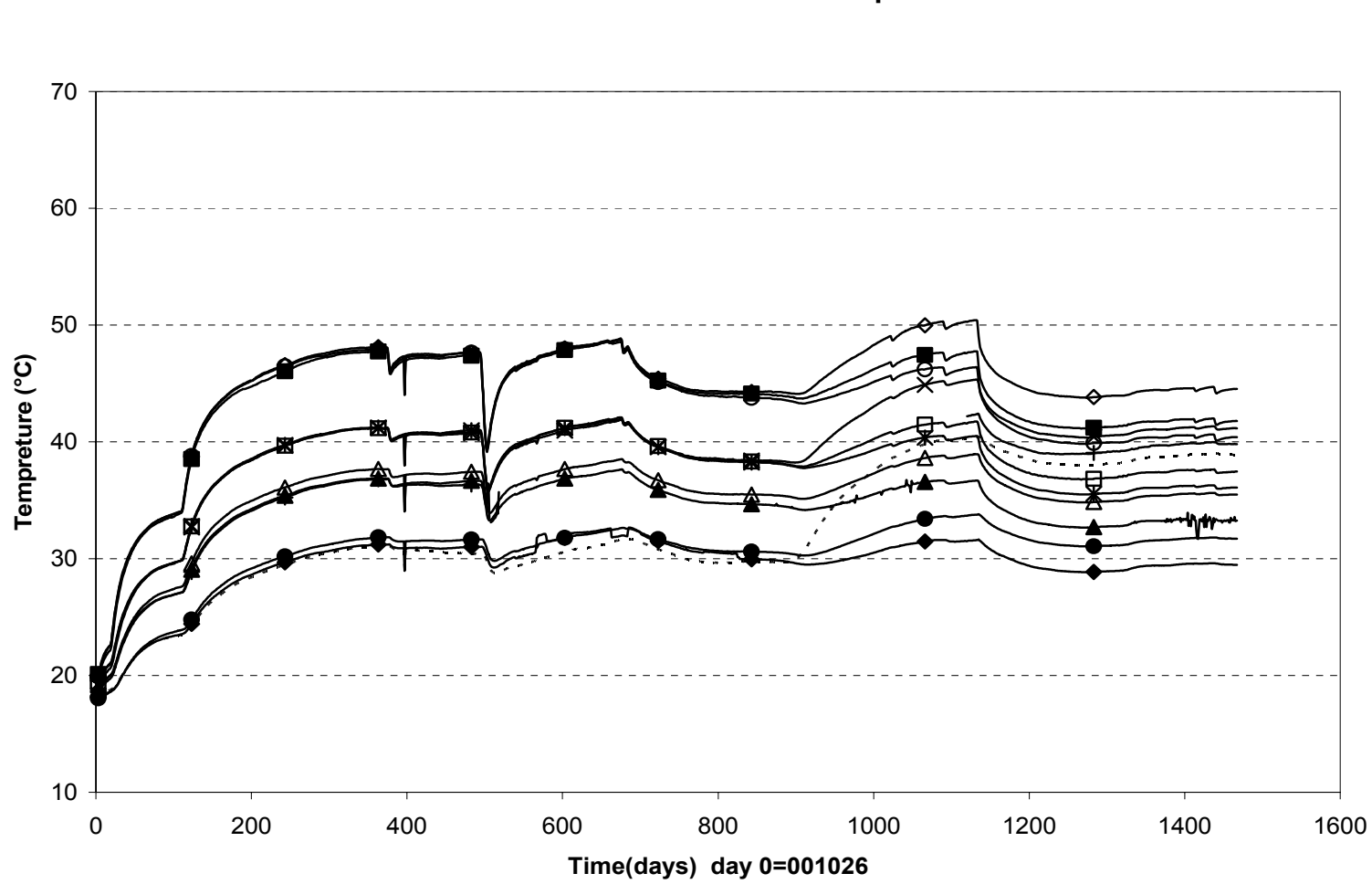
**Temperature in the rock - level 3,01 m (001026-041101)
Thermocouple**



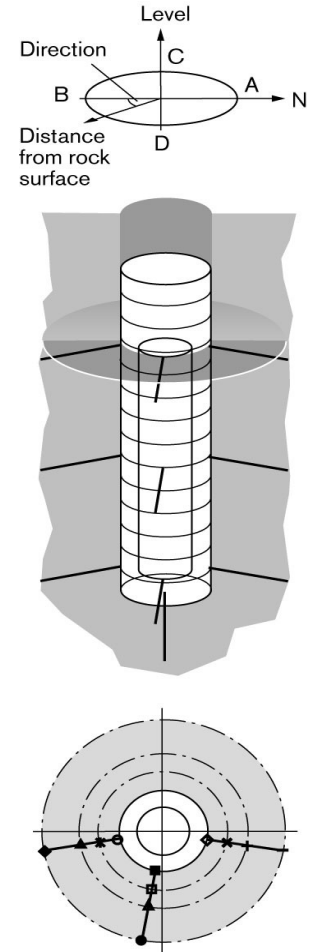
○	TR117(3,01\10°\0,000)	✱	TR118(3,01\10°\0,375)	▲	TR119(3,01\10°\0,750)	◆	TR120(3,01\10°\1,500)
■	TR121(3,01\80°\0,000)	□	TR122(3,01\80°\0,375)	△	TR123(3,01\80°\0,750)	●	TR124(3,01\80°\1,500)
◇	TR125(3,01\170°\0,000)	✕	TR126(3,01\170°\0,375)	+	TR127(3,01\170°\0,750)	- - - -	TR128(3,01\170°\1,500)



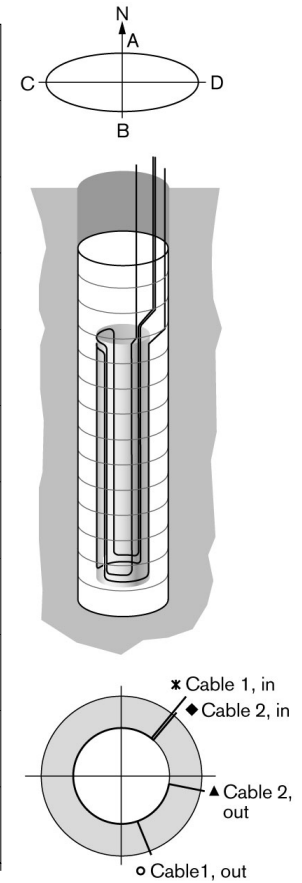
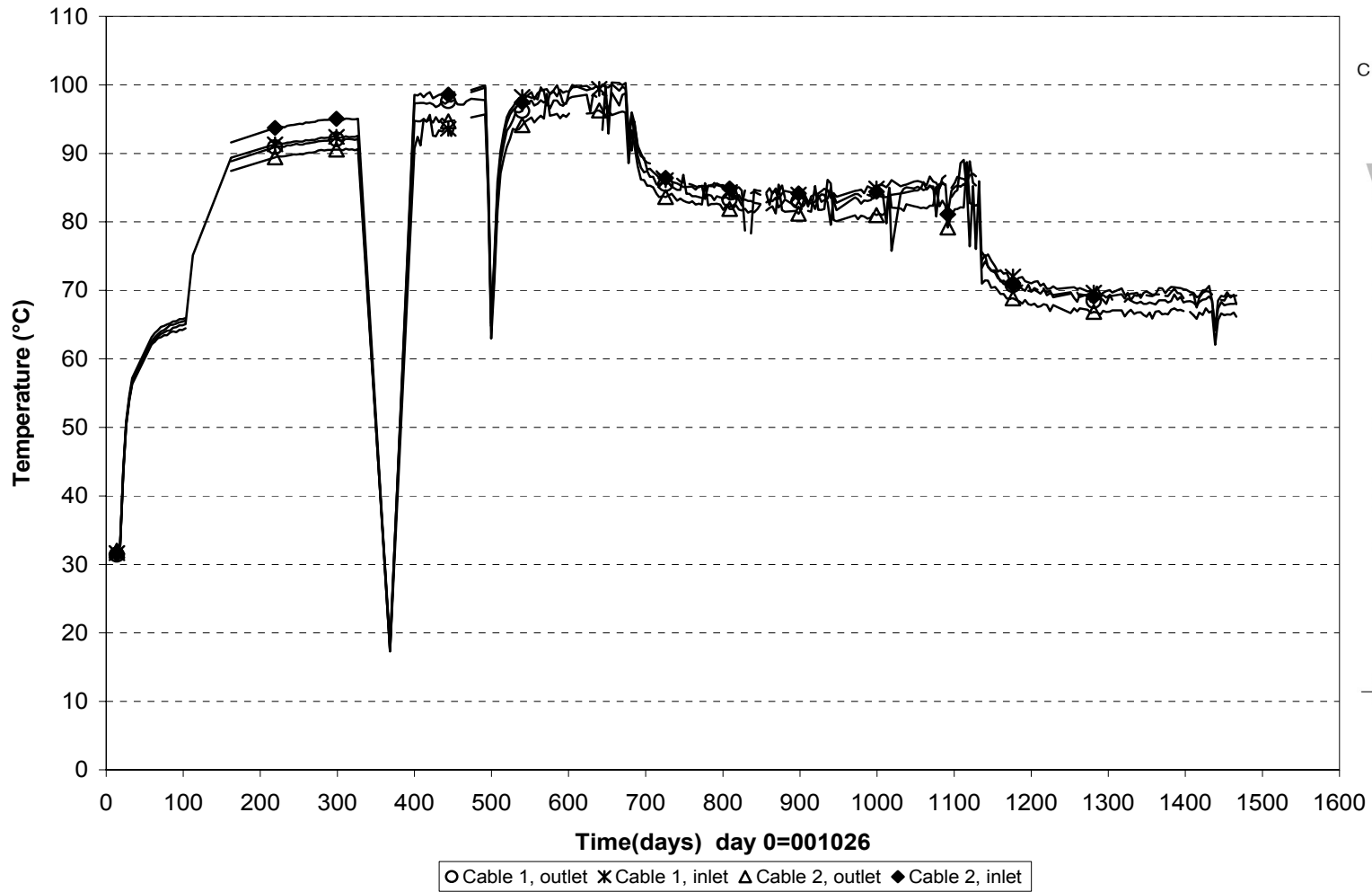
**Temperature in the rock - level 5,4 m (001026-041101)
Thermocouple**



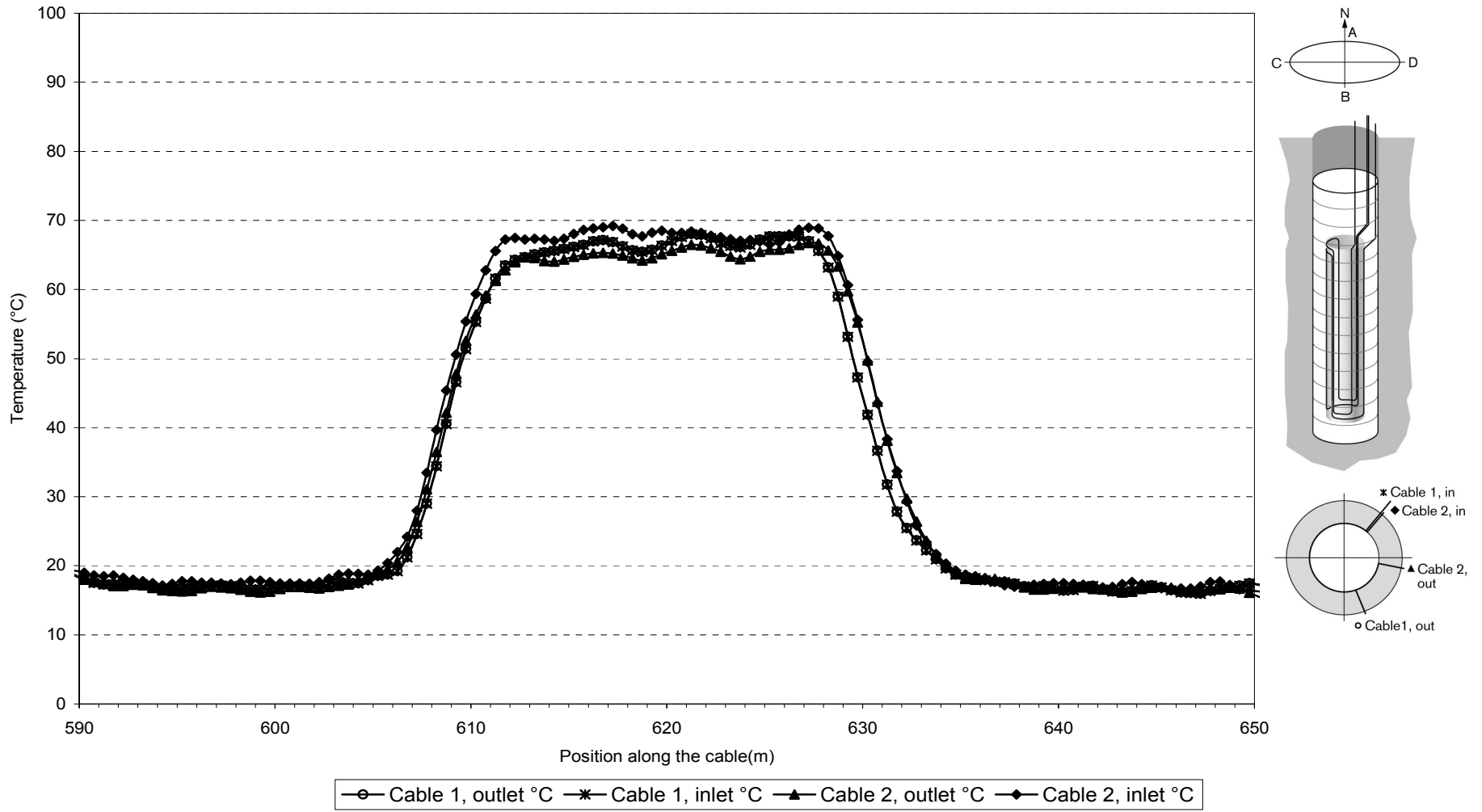
○ TR129(5,41\10°\0,000)	✱ TR130(5,41\10°\0,375)	▲ TR131(5,41\10°\0,750)	◆ TR132(5,41\10°\1,500)
■ TR133(5,41\80°\0,000)	□ TR134(5,41\80°\0,375)	△ TR135(5,41\80°\0,750)	● TR136(5,41\80°\1,500)
◇ TR137(5,41\170°\0,000)	× TR138(5,41\170°\0,375)	+ TR139(5,41\170°\0,750)	- - - - TR140(5,41\170°\1,500)



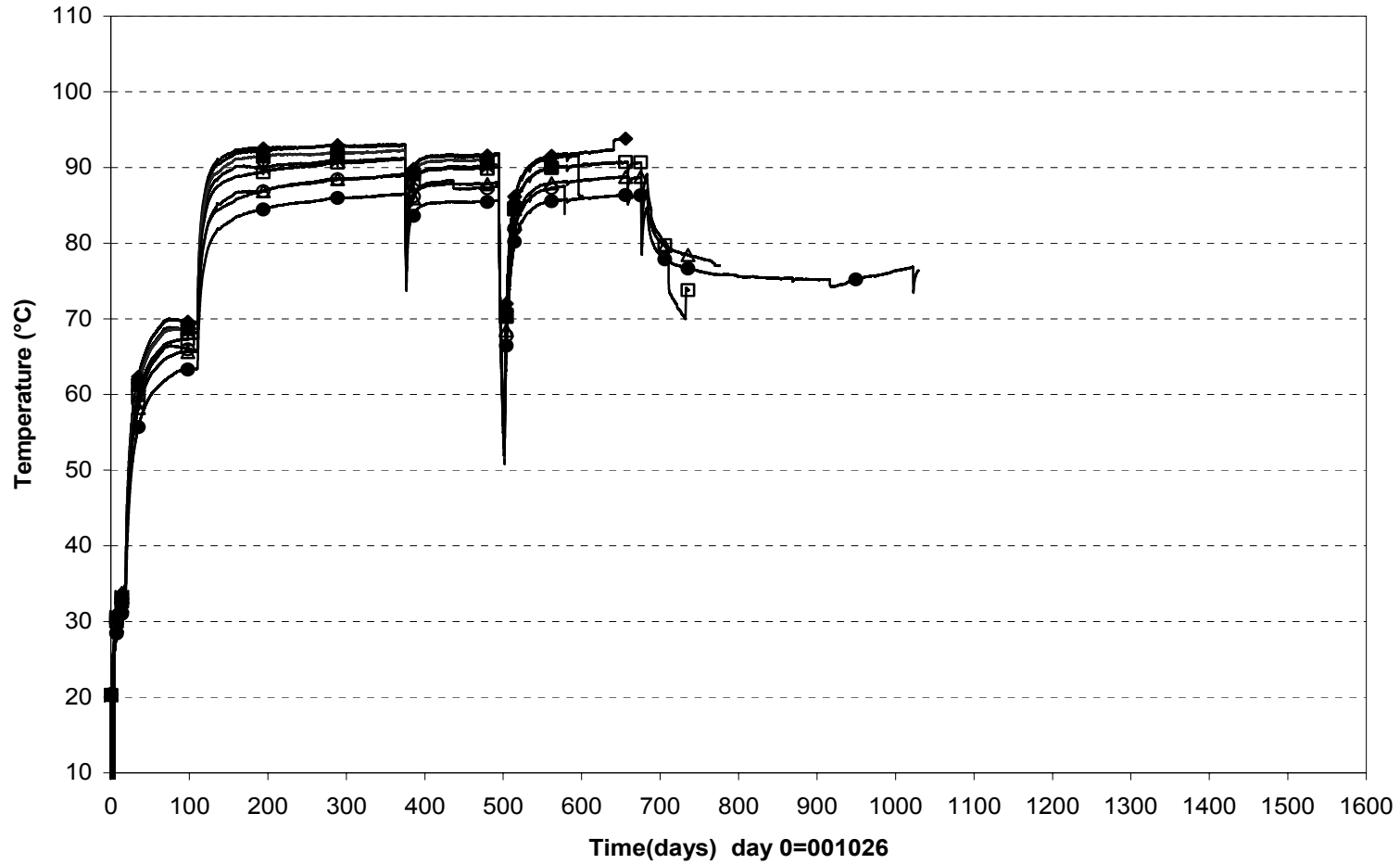
Max.temperature on the canister surface (001026-041101)
Optical fiber cables



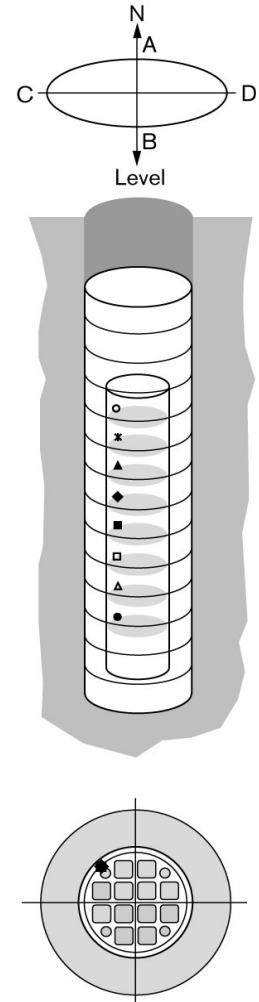
Temperature profile on the canister surface (041101)
Optical fiber cables



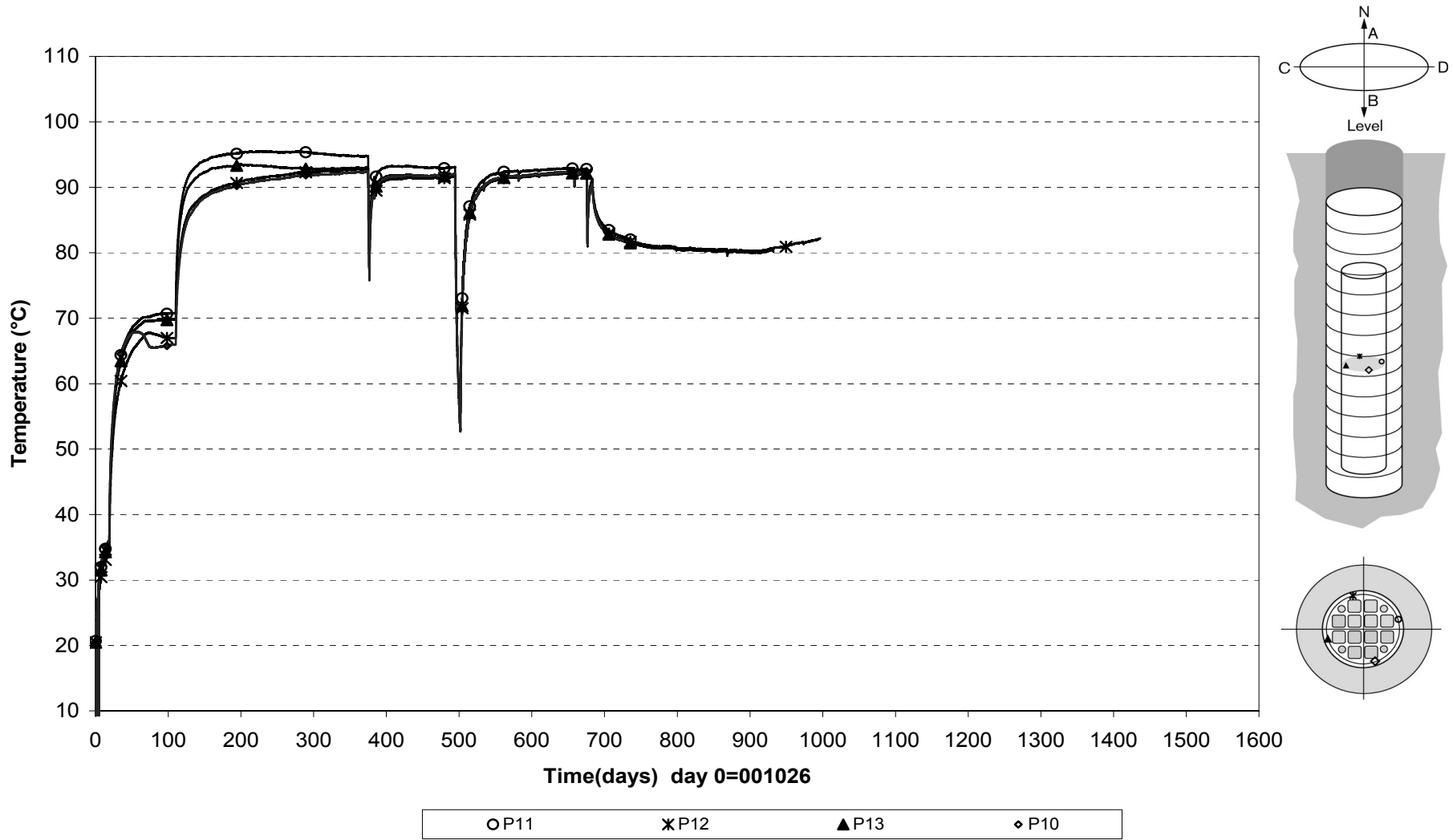
**Temperature inside the canister (001026-041101)
PT-100**



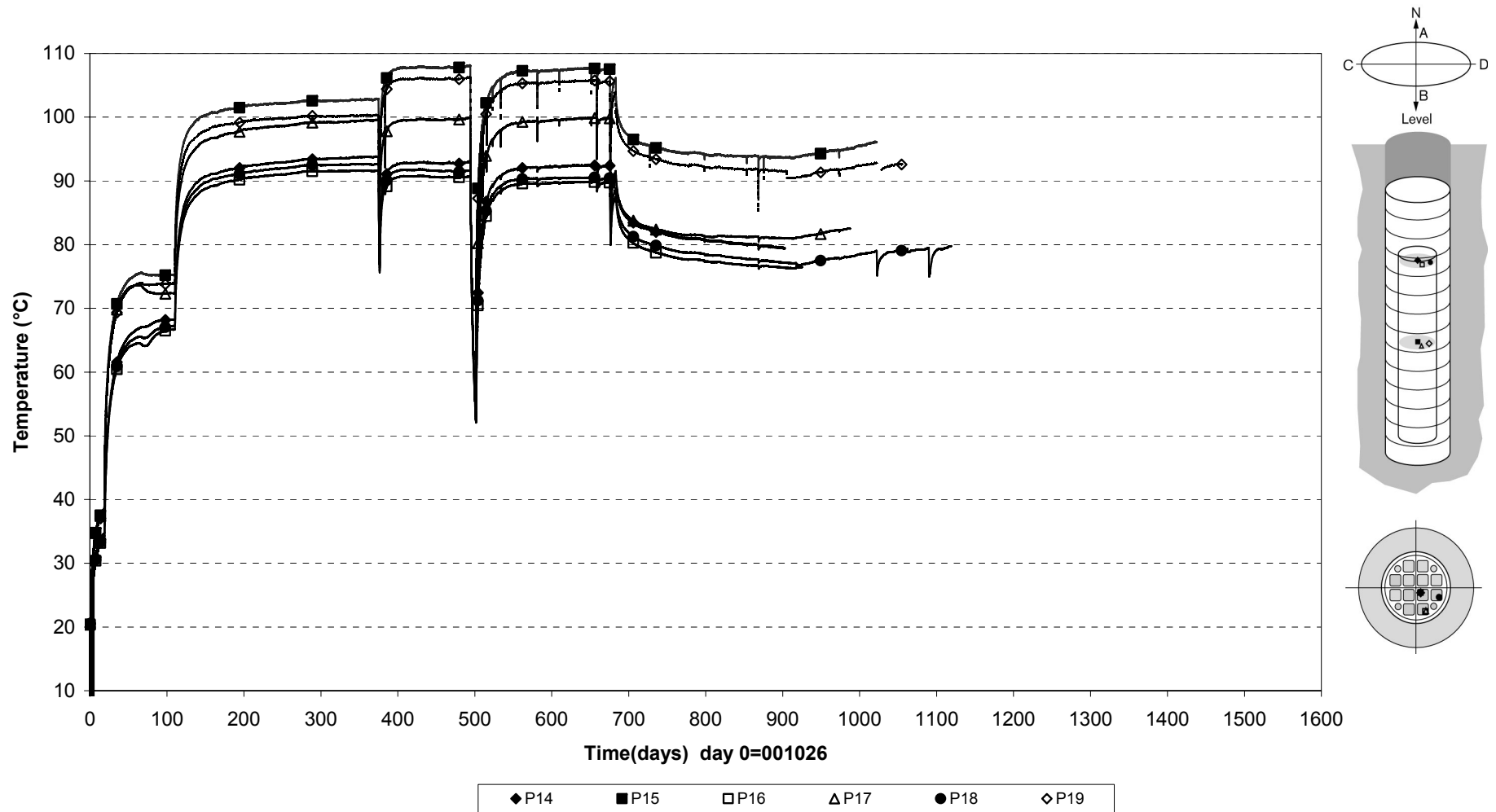
○ P2 ✕ P3 ▲ P4 ◆ P5 ■ P6 □ P7 △ P8 ● P9



**Temperature inside the canister (001026-041101)
PT-100**



Temperature inside the canister (001026-041101)
PT-100



Appendix B



**STRESS AND STRAIN MEASUREMENT OF THE ROCK MASS
RETRIEVAL TEST AT ÄSPÖ**

Measuring period
2004-05-01 – 2004-10-31

Martin Edelman

Kennert Röshoff

Alf Nilsson

2004-12-15

BergByggKonsult AB Ankdammsgatan 20 171 43, Solna, Sweden

Tel. 08-7595050 Fax 08-7595065

Contents

1	Exrent	83
2	Technical background	85
2.1	The vibrating wire embedment biaxial stressmeter	85
2.2	Embedded strain meters	85
2.3	Cement	85
3	Field measurement	87
3.1	Installation work	87
3.2	Location of instruments	87
3.3	Registration	87
4	Computer processing of field data	91
4.1	Evaluation of stresses	91
4.1.1	Radial deformations	91
4.1.2	Calculation of deformation to stresses	92
4.2	Evaluation of strain	92
4.2.1	Calculation of strain	92
4.3	Material parameters	92
4.4	Processing	93
5	Results	95
5.1	Results of canister hole 1	98
5.1.1	Stress change for each biaxial stressmeter	98
	Stressmeter A1	98
	Stressmeter B1	99
	Stressmeter C1	100
	Stressmeter D1	101
5.1.2	Strainmeter A1:1, B1:1, C1:1, D1:1, D1:2	102
5.1.3	Strainmeter C1:2	102
	Results of canister hole 2	103
5.1.4	Stress change for each biaxial stressmeter	103
	Stressmeter A2	103
	Stressmeter B2	104
	Stressmeter C2	105
	Stressmeter D2	106
5.1.5	Strainmeter B2:1, C2:1, C2:2	107

1 Extent

BBK AB and NCC Teknik have, on commission of SKB, Äspö hard rock laboratory, performed rock mechanical measurements in the CRT (Återtaget) tunnel at Äspö. The measurement program comprises of registration of the stress and the strain response around the two canister holes during drilling and heating of the rock mass.

In the first phase, the response of the rock mass was monitored during the drilling of the two canister holes (QPTD F69-00-21). This second phase includes the response registered during a heating phase. The heating experiment started on 2000-10-27 and will continue for about five years.

The aim of the instrumentation is to monitor the stress changes due to heating of the rock mass in a canister hole. The strain meter is used to monitor the relative changes of strain of the intact rock and across fractures.

The commission extends over field measurement and evaluation.

BBK AB is responsible for measuring equipment, the mobilization, field measurement, the computer processing. BBK AB and NCC Teknik are responsible for the interpretation and report of the measurements.

This report presents the measurement results during the period of the heating phase from 2004-05-01 to 2004-10-31.

2 Technical background

2.1 Vibrating wire embedment biaxial stressmeters

The biaxial stressmeter, Geokon model 4350, is designed to measure compressive stress changes in rock, salt, concrete or ice. Principal stress changes are measured in the plane perpendicular to the borehole axes. The stressmeter consists of a high-strength steel cylinder that is grouted into a 60 mm borehole. Stress changes in the host material cause the cylinder to deform.

The radial deformation of the cylinder is measured by means of three pairs of vibrating wire sensors spaced at 60° intervals. Changes of stress produce corresponding changes in the resonant frequency of the sensors. These changes of frequency can be related to stress changes using factory-supplied calibrations. Longitudinal strain sensors and temperature sensors are also included in the stressmeter.

2.2 Embedded strain meters

The vibrating wire strain gages are designed for direct embedment in concrete. The strainmeter is 15 cm long and commonly used for strain measurement in foundations, piles, bridges, dams, tunnel liners etc.

The strain is measured using the vibrating wire principle. A length of a steel wire is tensioned between two end blocks that are embedded directly in concrete. Deformation (i.e. strain changes) of the concrete mass will cause the two end blocks to move relative to one another, thus altering the tension in the steel wire. The tension is measured by excitation of the wire and measuring its resonant frequency of vibration using an electro magnetic coil.

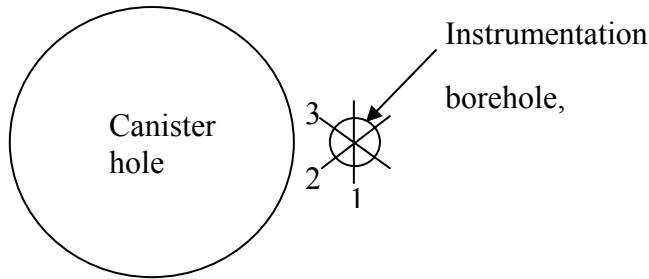
2.3 Cement

Special expansive grout was used to insure that the gage is in complete contact with the surrounding rock. The instruments are grouted in special cement from Denmark named Densitop T2. This cement is chosen to have as similar properties as the rock as possible. The compression strength is 150 MPa. The coefficient of expansion is approximate 8.5 microstrain/C° that is similar to hard rock as granite and as 85 % of common concrete.

3 Field measurement

3.1 Installation work

Installation of the stressmeter gage is accomplished by inserting the gage into a grout-filled borehole using a setting tool and self-aligning setting rod.



The stress cell is orientated so that the first vibrating wire is orientated tangentially to the canister hole. The second string is orientated 60° from tangential direction and the third string is orientated 120° from tangential direction.

The strainmeters were fixed to a 6 mm glasfiber rod and pushed into the grout after the stress cell was installed.

3.2 Location of instruments

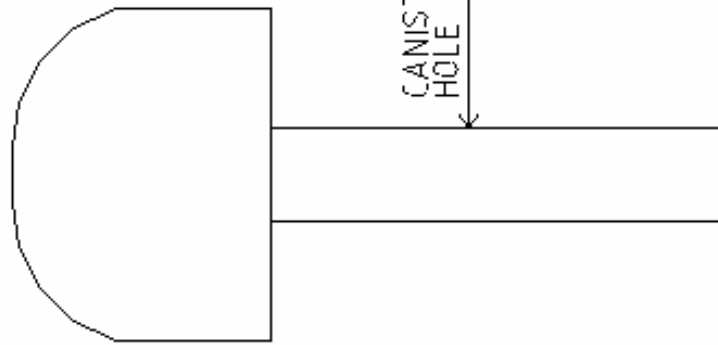
See figure 3.1 and figure 3.2.

3.3 Registration

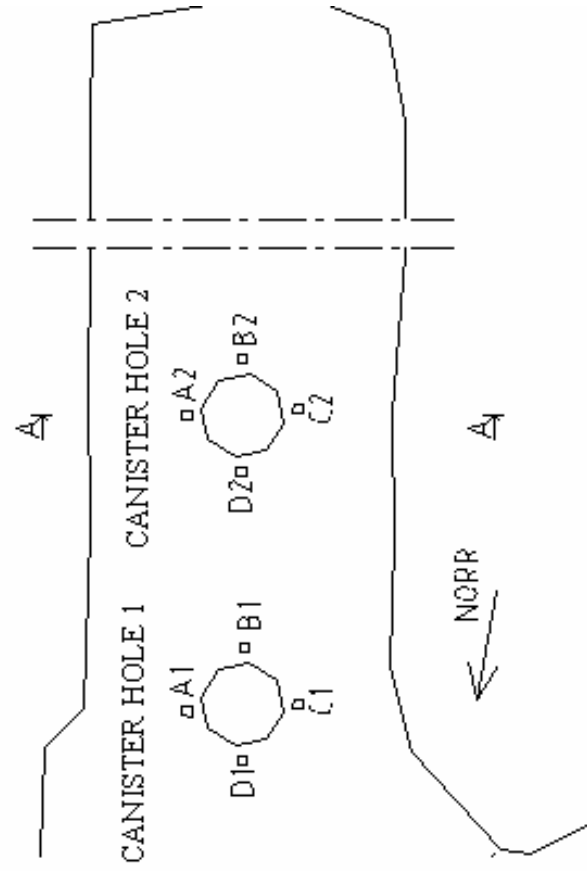
A datalogger type Campbell CR10X has captured the measurements, which have been recorded once every hour during the period 2000-10-01 to 2001-01-01, and once every six hours during the period 2001-01-03 to 2004-10-31.

MEASUREMENT LAYOUT

SECTION A-A



PLAN



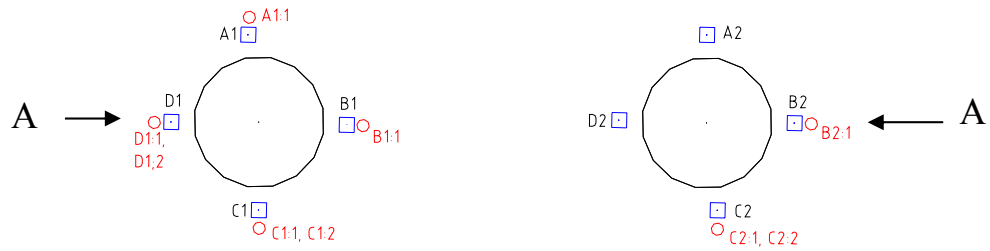
□ BOREHOLE LAYOUT

Figure 3.1 Measurement Layout

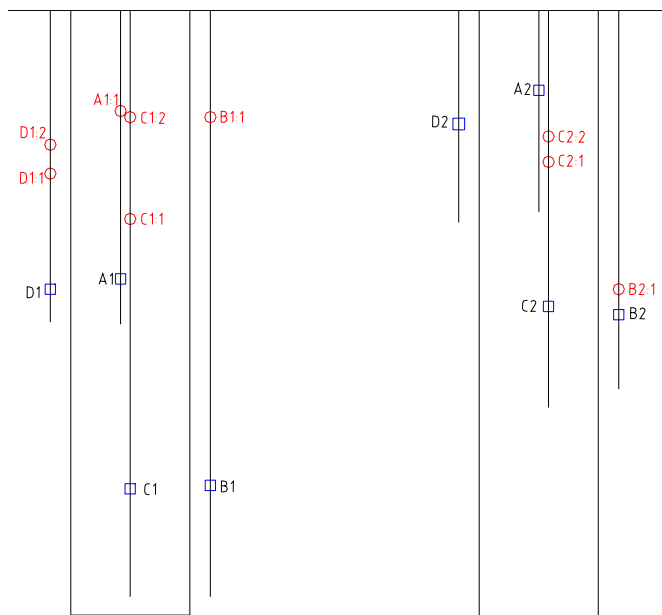
Canister Hole 1

Canister Hole 2

PLAN



SECTION A-A



□ Biaxial stressmeter

○ Deformationmeter

Figure 3.2 Location of instruments

4 Computer processing of field data

4.1 Evaluation of stresses

The stress changes are evaluated from the measured deformations registered by the vibrating wires.

4.1.1 Radial deformations

Radial deformation for each of the strings are calculated with the equation:

$$V_r = (R_1 - R_0) * \text{Gagefactor} \quad (\text{in. or mm})$$

V_r = Radial deformation for each of the strings

R_1 = Deformation reading in digits (= frequency² / 1000)

R_0 = Deformation zero reading in digits (= frequency² / 1000)

4.1.2 Calculation of deformation to stresses

The magnitude and the direction of the stress changes are determined from the measured radial deformation of the sensor in three directions.

The equations below give the magnitude and the direction of the maximum stress increase and reduction in a plane perpendicular to the borehole axes:

Maximal stress increase

$$p = \frac{1}{2} \left[\frac{1}{3B} \left((2V_{r_1} - V_{r_2} - V_{r_3})^2 + 3(V_{r_2} - V_{r_3})^2 \right)^{1/2} + \frac{1}{3A} (V_{r_1} + V_{r_2} + V_{r_3}) \right]$$

V_{r_1} = Radial deformation for string 1

V_{r_2} = Radial deformation for string 2

V_{r_3} = Radial deformation for string 3

A, B = Coefficients depending on the sensor geometry and the material properties

Maximal stress reduction

$$q = \left[\frac{1}{3A} (V_{r_1} + V_{r_2} + V_{r_3}) - p \right]$$

The angle of the maximal stress increase

The angle in the plane perpendicular to the borehole axes is measured clockwise from the tangential direction of the canister hole.

$$\theta = \frac{1}{2} \cos^{-1} \left[\frac{V_{r_1} - A(p+q)}{B(p-q)} \right]$$

4.2 Evaluation of strain

Nine strain gages were installed in the same boreholes as the biaxial stressmeters.

4.2.1 Calculation of strain

Strain measurement were calculated as temperature compensated load related strain with the following equation:

$$\mu_{true} = (R_1 - R_0) * B + (T_1 - T_0)(C_1 - C_2)$$

μ_{true} = temperature compensated microstrain

R_1 and R_0 = Digits reading

B = batch calibration factor

C_1 and C_2 are the coefficients of expansion of steel and concrete, 12.2 microstrain/ C° and 8.5 microstrain/ C° .

4.3 Material parameters

Material parameters used in the calculations are as the following:

- Young's modulus of intact rock 69 Gpa
- Poisson's ratio of intact rock 0.25
- Coefficients of expansion of steel 12.2 microstrain/ C°
- Coefficients of expansion of concrete 8.5 microstrain/ C°

4.4 Processing

The raw data registered have been processed in Microsoft Excel software. The calculation and evaluation gathered from the deformations in the plane perpendicular to the borehole axes are presented as:

Temperature

Radial deformation of the three pairs of wires in plane perpendicular to borehole axes

Maximal stress increases and stress reduction in plane perpendicular to borehole axes

Orientation of maximal stress increase in plane perpendicular to borehole axes

Strain measurement

5 Results

A summary of the results of the stress changes is presented in Table 1. These values represent total changes in stress magnitude and stress orientation during each reporting period during phase 2 (heating) together with maximum changes in stress magnitude and orientation recorded during phase 1 (drilling). Figure 5.1 presents graphically the maximum typical changes in stress magnitude and orientation during this reporting period from 2004-05-01 to 2004-10-31. These results are not compensated for temperature changes, nor are they compensated for longitudinal stress changes.

Although the measurements of stress meters are affected by temperature, the temperature compensated results of stress meters are not presented in this report because a further detailed study of the relationship between temperature and stress meter measurements will be required in order to quantify these effects. In addition, the longitudinal stress changes are affected by temperature changes and for this reason these longitudinal measurements are not currently used for determination of radial stresses. Results of the biaxial stress meters without temperature or longitudinal stress compensation, and the strain meters with temperature compensation from each borehole for the period 2004-05-01 to 2004-10-31 are summarized on the diagrams in section 5.1 and 5.2. There is a stop in the readings for all sensors from mid September to beginning of October.

The diagrams in section 5.1 and 5.2 for each borehole display:

- Maximum stress increases and stress reductions in plane perpendicular to borehole axes.
- Orientation of maximum stress increase in plane perpendicular to borehole axes.
- Strain measurements presented in the diagrams are temperature-compensated with the unit of micro strain. Positive values represent elongation.

The data during this reporting period indicate that:

- The temperature is inhomogeneous around these two canister holes.

Hole 1

Around canister hole 1, the temperature varies with values from 60 to 74°C.

Stressmeter A1 stopped temporarily measuring one set of vibrating wires (4-6) by the beginning of September and (1-3) by the end of October noise disturbed the readings. Stressmeter B1 registered no measurement throughout the whole period. Stressmeter C1 stopped measuring one set of vibrating wires (4-6) by the end of August. Stressmeter D1 stopped measuring in the mid of September and noise disturbed the readings rest of the period.

Maximum stress increase at A1 and C1 have risen by 3-5MPa to values from 47 to 52MPa. Maximum stress increase at D1 has risen by 1-3MPa to values from 84 to 86MPa.

Maximum stress reduction at A1 and C1 have risen by 4-9MPa to values from -3 to 18MPa. Maximum stress reduction at D1 has risen by 5MPa to values from 30 to 37MPa.

Readings for A1 and D1 are presented before they stopped to take readings.

The orientation for the maximum stresses for C1 and D1 shows to be steady.

At A1 the orientation has changed from 4 to 2°.

Measurements taken at the strain gauge locations display steady values in micro strain as well as temperature. At C1:2 the value has increased from 800 to 790 micro strain, still showing steady temperature at 41°C. Strainmeter D1:2 reduced the value from -176 to -276 micro strain during the period.

Hole 2

Around canister hole 2 small changes in temperature can be seen for at A2, B2, C2 and D2. All sensors display steady values towards the end of the period. Instruments located at greater depths (B2, C2 and B2:1) show temperatures on average 20°C higher than at the more shallow instruments.

The stress meters around canister hole 2 show small variations in stresses (0 to 1 MPa). At C2 the set of vibrating wires (1-3) stopped giving values in March.

The orientation of the stress field around stress meter A2 are still steady at about -7°. The orientation of the stresses around the other stress meters changed less than 1 degree.

During an earlier period of time the vibrating wire Vr5 stopped giving values at stress meter B2. There are still no values from this vibrating wire, and as for stress meter B1, the calculated stresses and orientation still don't give meaningful values.

The strain meters display steady values with small changes.

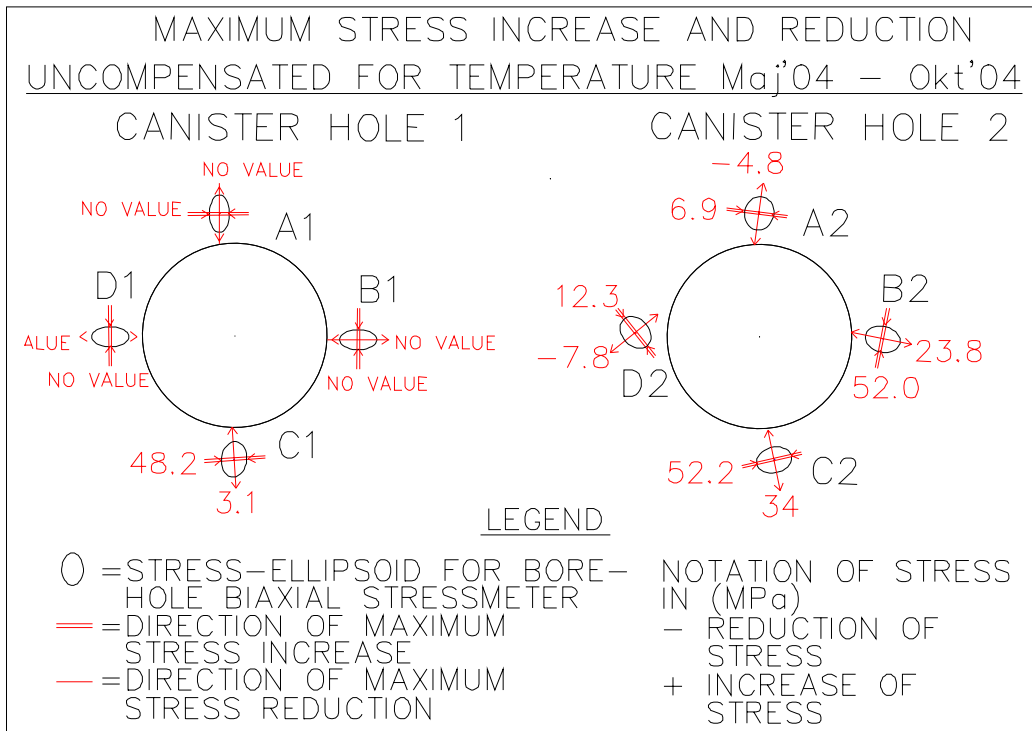


Figure 5.1 Maximum stress changes uncompensated for temperature

Table 1. Summary of results for stress measurements

Stress-meter	Measuring period								
	Phase 1: Drilling phase			Phase 2: Heating phase					
				Period: 2000-10-01 to 2001-11-30			Period: 2000-10-01 to 2001-11-30		
	Typical max. stress increase (Mpa)	Typical max. stress reduction (Mpa)	Orientation of max. Stress increase (degree)	Typical max. stress increase (Mpa)	Typical max. stress reduction (Mpa)	Orientation of max. Stress increase (degree)	Typical max. stress increase (Mpa)	Typical max. stress reduction (Mpa)	Orientation of max. Stress increase (degree)
A1	17.0	-10.0	11.5	22.7	-10.9	10.3	22.6	-10.8	10.3
B1	15.0	-11.0	17.0	21.1	-10.3	16.8	26.9	-10.5	16.8
C1	12.0	-7.4	0	21.9	-9.9	5.4	21.9	-9.8	5.4
D1	22.0	-11.0	0	25.8	-9.1	0	26.3	-9.4	0
A2	5.0	-4.0	-11.0	4.4	-3.3	-18.3	3.7	-3.3	-17.7
B2	11.0	-7.3	-7.5	31.1	-4.6	-14.1	57.9 (*)	-4.6	-21.3
C2	11.0	-7.7	29.5	29.1	-6.6	31.2	33.7 (*)	-7.6	30.2
D2	9.3	-7.2	38.5	16.5	-9.9	38.7	16.2	-9.9	38.3

Stress-meter	Measuring period			Measuring period			Measuring period		
	Phase 2: Heating phase con't (see Note 5)			Phase 2: Heating phase con't			Phase 2: Heating phase con't		
	Period: 2002-05-01 to 2002-10-31			Period: 2002-11-01 to 2003-04-30			Period: 2003-05-01 to 2003-10-31		
	Typical max. stress increase (Mpa)	Typical max. stress reduction (Mpa)	Orientation of max. Stress increase (degree)	Typical max. stress increase (Mpa)	Typical max. stress reduction (Mpa)	Orientation of max. Stress increase (degree)	Typical max. stress increase (Mpa)	Typical max. stress reduction (Mpa)	Orientation of max. Stress increase (degree)
A1	23.3	-11.0	10.4	34.7(*)	-17	5.7	38.7	-13.7	6.1
B1	21.1	-10.6	15.9	34(*)	-9.6	17.1	51 to 68	5 to 34	5 to 19
C1	22.3	-10.4	5.3	34(*)	-9.1	5.7	41.5	-5.2	5.2 to 6.6
D1	27.3	-9.7	-2.9	45(*)	-5.6	-4.3	60.3	4.8	-3.2 to -4.9
A2	4.3	-3.9	-13.9	3.5	-3.5	-9(*)	6.9	-4.3	-7.4
B2	34 to 57	4 to 21	-0.6 to -8	32 to 54	6 to 22	-1 to -10	53.2	23.2	-10.7
C2	50 to 71	5.3 to 22.7	22 to 33	48 to 70	6 to 26	19 to 33	53 to 74	8 to 31	16 to 32
D2	16.0	-10.1	38.7	15	-9	38	12.4	-8.1	38

Notes:

1. Positive values of stress indicate compression, negative values of stress indicate extension.
2. Positive values of orientation indicate anti-clockwise rotation, negative values of orientation indicate clockwise rotation.
3. Typical maximum stress increases and reductions represent maximum stabilised readings during the measuring period.
(*) indicates that the reading had not stabilised during the measuring period.
4. Orientation of maximum stress increase is the orientation that corresponds to the typical maximum stress increase.
5. Calculation and processing methods revised during this reporting period to eliminate compensation for both temperature and longitudinal strains until further studies on these effects are carried out.

Stress-meter	Measuring period			Measuring period			Measuring period	
	Phase 2: Heating phase con't			Phase 2: Heating phase con't			Phase 2: Heating phase con't	
	Period: 2003-11-01 to 2004-04-30			Period: 2004-05-01 to 2004-10-31			Period: 2004-11-01 to 2005-04-30	
	Typical max. stress increase (Mpa)	Typical max. stress reduction (Mpa)	Orientation of max. Stress increase (degree)	Typical max. stress increase (Mpa)	Typical max. stress reduction (Mpa)	Orientation of max. Stress increase (degree)	Typical max. stress increase (Mpa)	Typical max. stress reduction (Mpa)
A1	47,3	1,3	4,0 to 4,7	no value	no value	no value		
B1	no value	no value	-89,7 to 0,1	no value	no value	no value		
C1	46,0	10,0	4,3 to 9,4	48,2	3,1	3,8		
D1	82,0	31,7	-9,5 to 0,6	no value	no value	no value		
A2	6,7	-4,3	-7,0	6,9	-4,8	-7,2 to -7,7		
B2	50,8	23,0	-4,9 to -59,7	52,0	23,8	-11,2		
C2	51,5	32,7	14,1 to 59,3	52,2	34,0	13,3		
D2	12,1	-7,7	37,9	12,3	-7,8	38,8 to 38,1		

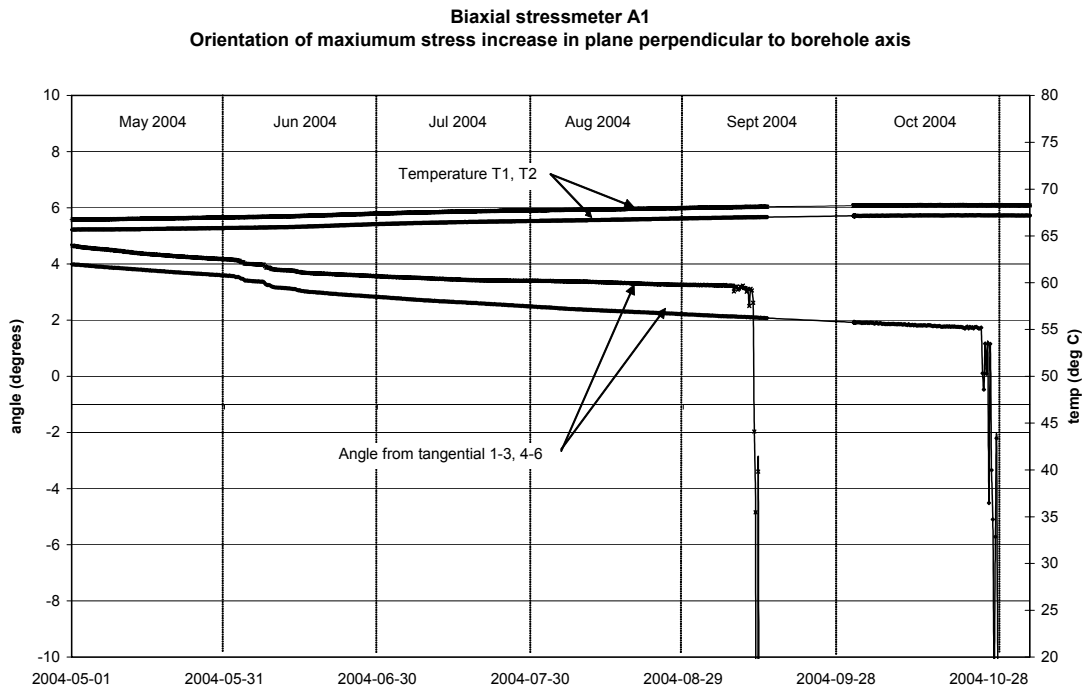
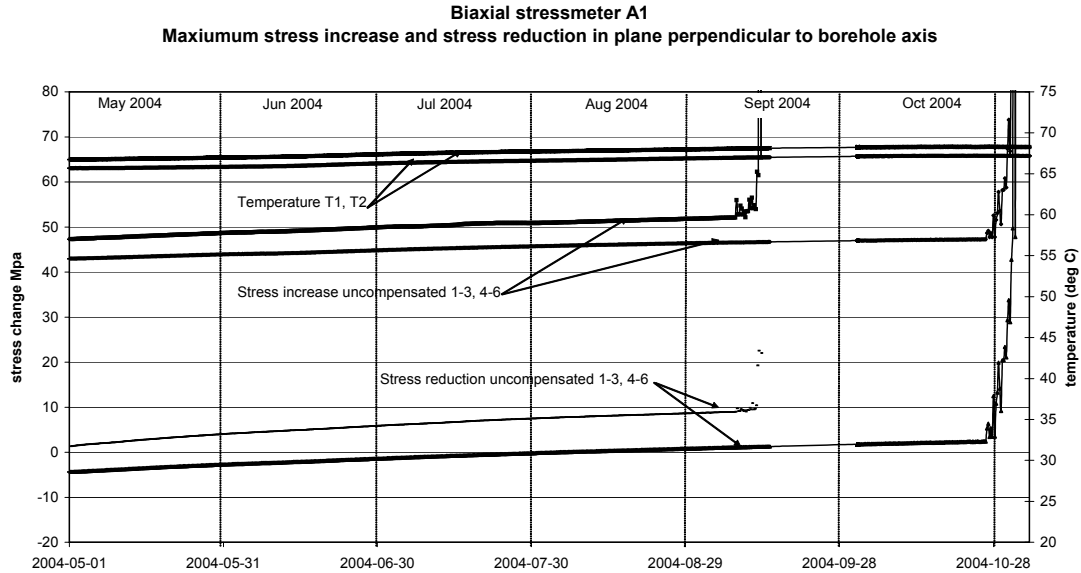
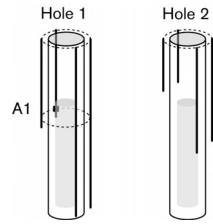
Notes:

1. Positive values of stress indicate compression, negative values of stress indicate extension.
2. Positive values of orientation indicate anti-clockwise rotation, negative values of orientation indicate clockwise rotation.
3. Typical maximum stress increases and reductions represent maximum stabilised readings during the measuring period.
(*) indicates that the reading had not stabilised during the measuring period.
4. Orientation of maximum stress increase is the orientation that corresponds to the typical maximum stress increase.
5. Calculation and processing methods revised during this reporting period to eliminate compensation for both temperature and longitudinal strains until further studies on these effects are carried out.

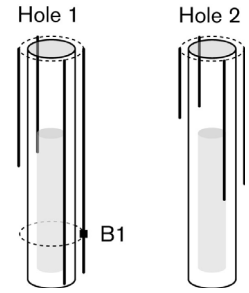
5.1 Results of canister hole 1

5.1.1 Stress change for each biaxial stressmeter

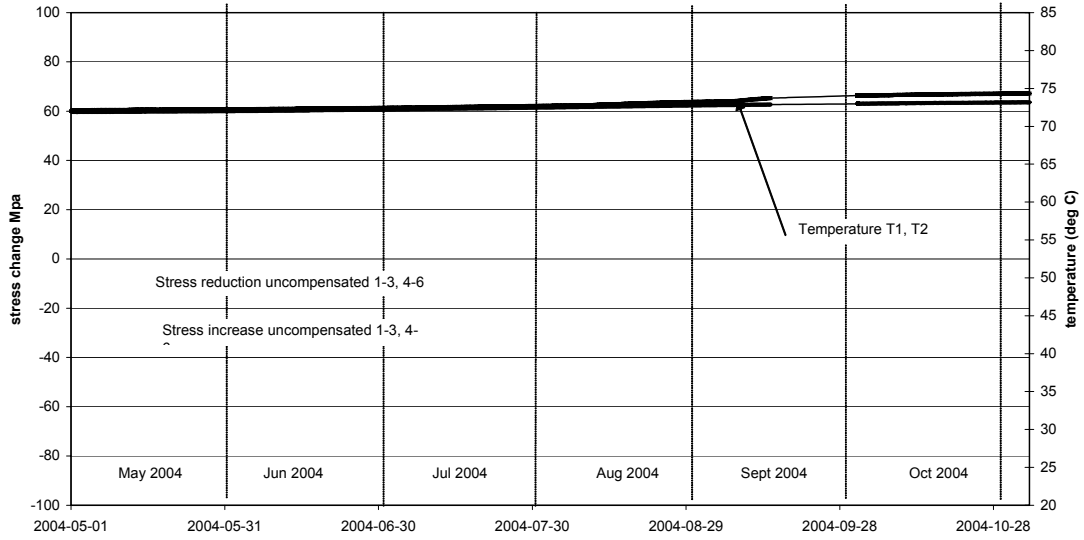
Biaxial stressmeter A1 uncompensated for temperature:



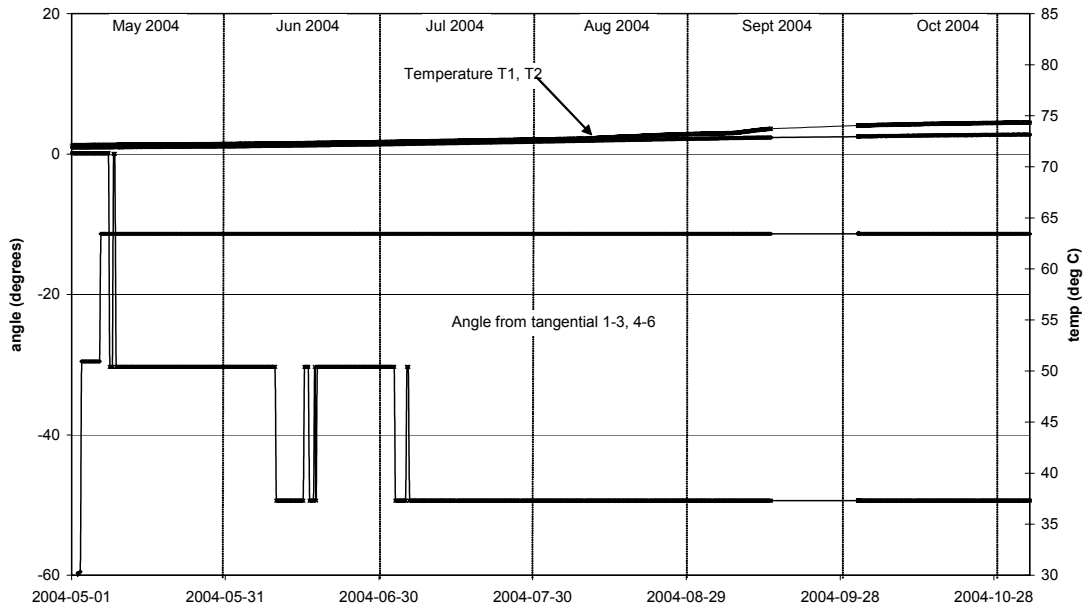
Biaxial stressmeter B1 uncompensated for temperature:



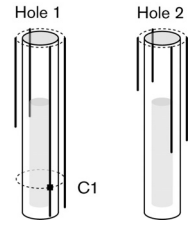
Biaxial stressmeter B1
Maximum stress increase and stress reduction in plane perpendicular to borehole axis



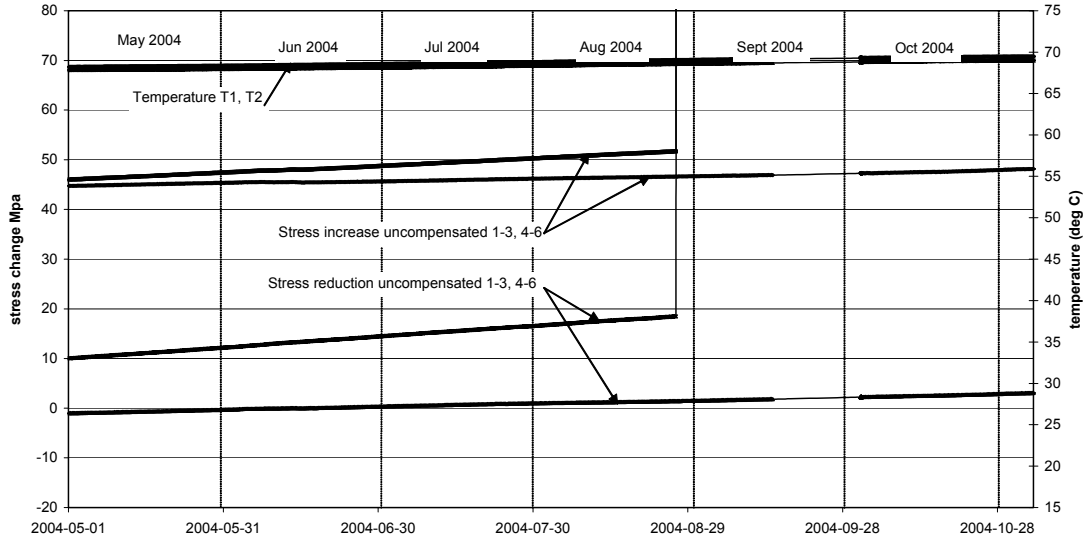
Biaxial stressmeter B1
Orientation of maximum stress increase in plane perpendicular to borehole axis



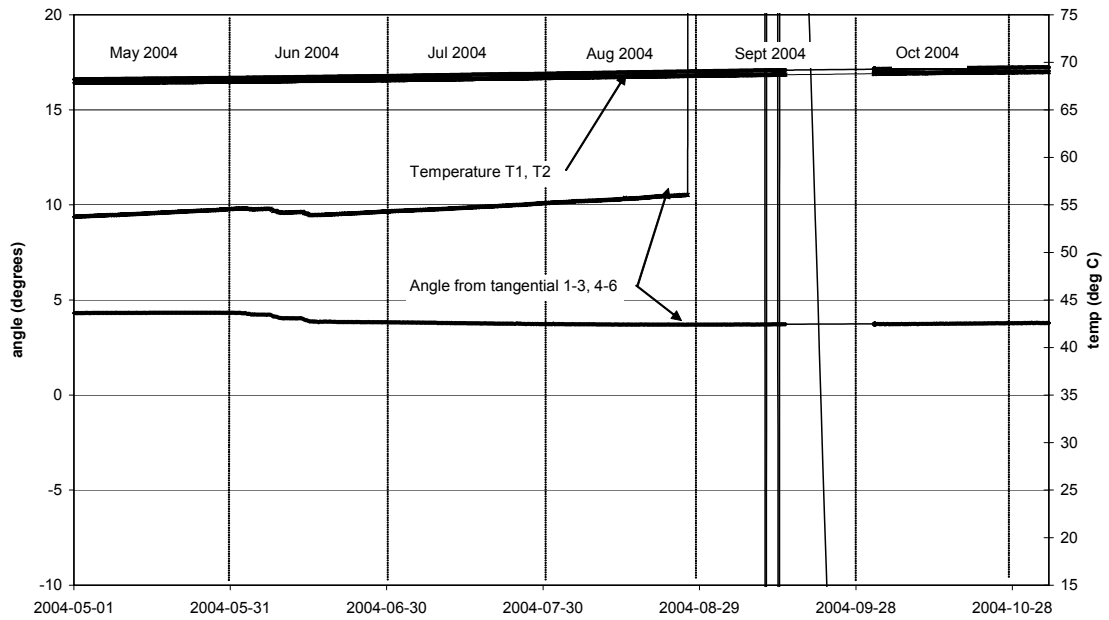
Biaxial stressmeter C1 uncompensated for temperature:



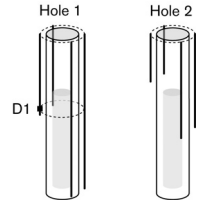
Biaxial stressmeter C1
Maximum stress increase and stress reduction in plane perpendicular to borehole axis



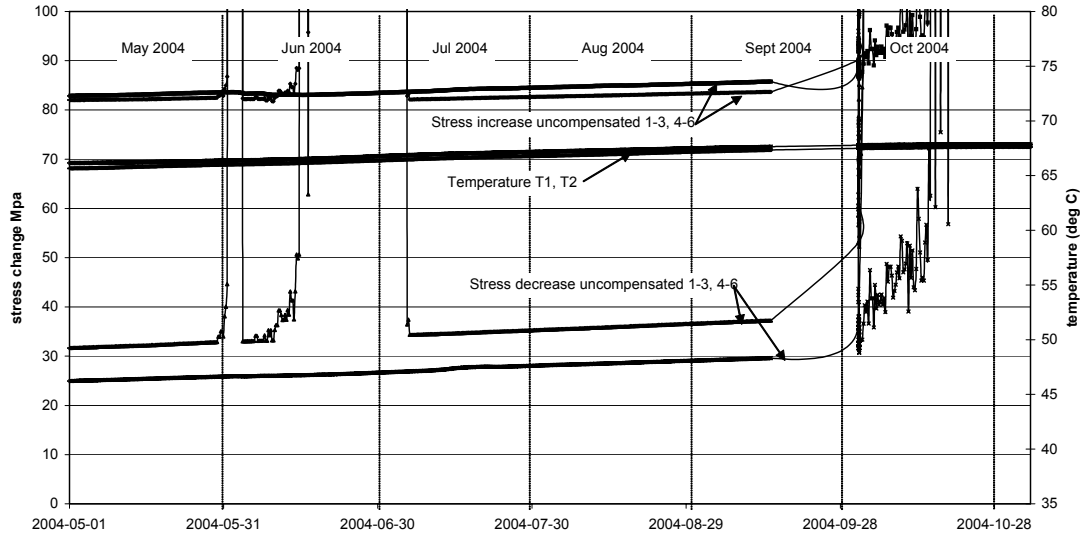
Biaxial stressmeter C1
Orientation of maximum stress increase in plane perpendicular to borehole axis



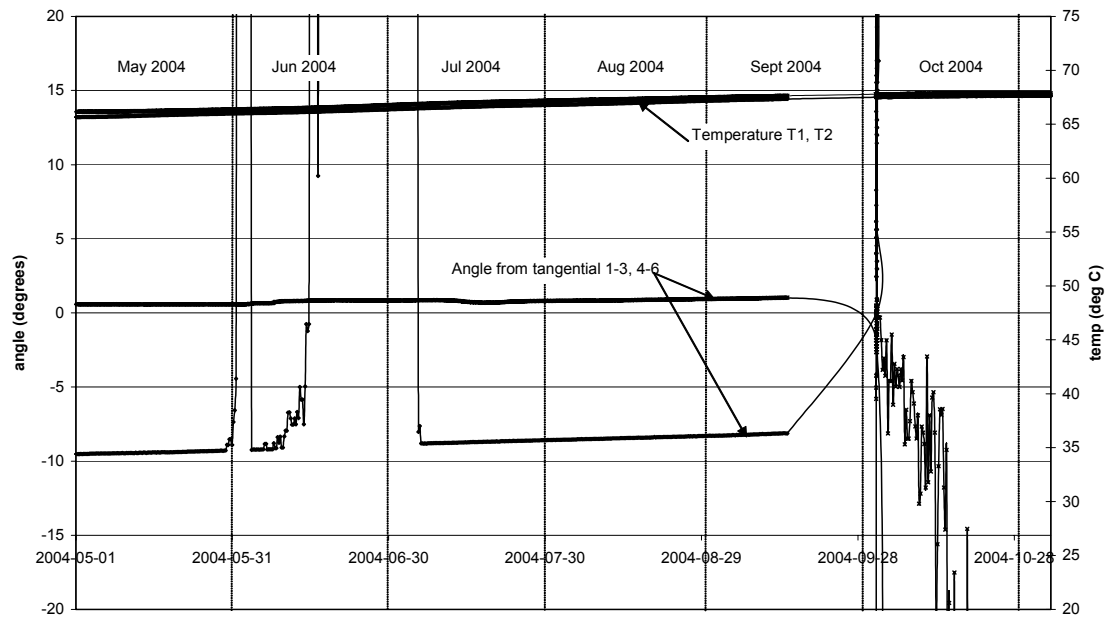
Biaxial stressmeter D1 uncompensated for temperature:



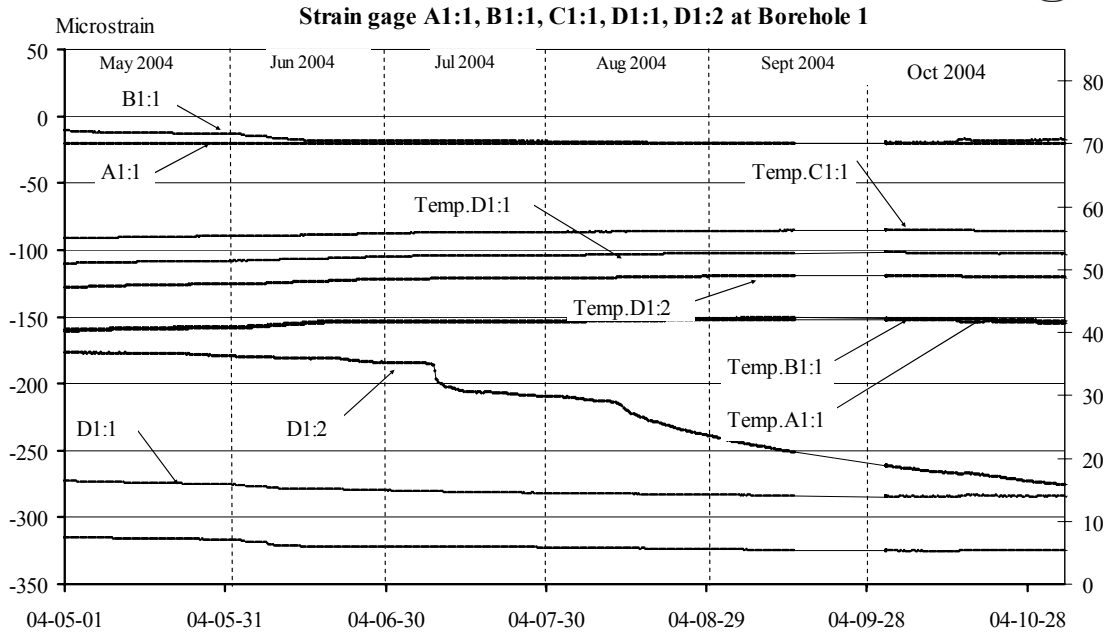
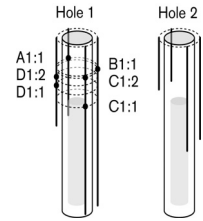
Biaxial stressmeter D1
Maximum stress increase and stress reduction in plane perpendicular to borehole axis



Biaxial stressmeter D1
Orientation of maximum stress increase in plane perpendicular to borehole axis

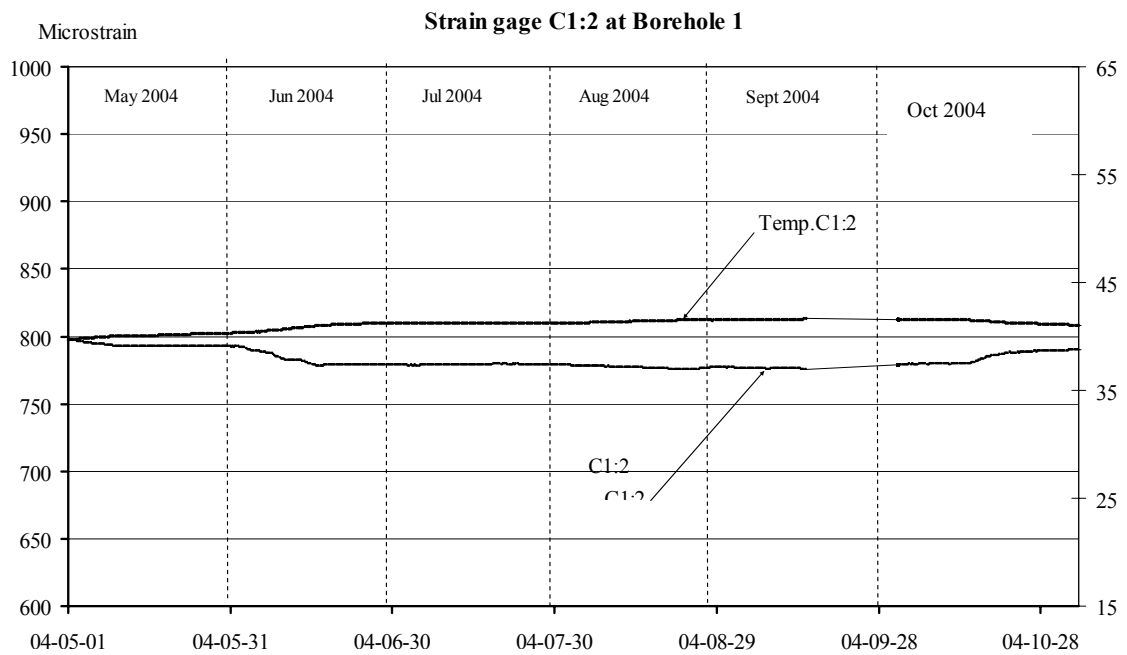


5.1.2 Strainmeter A1:1, B1:1, C1:1, D1:1, D1:2 (temperature compensated)



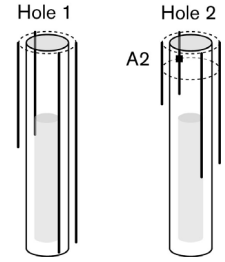
Positive values of microstrain represent elongation

5.1.3 Strainmeter C1:2 (temperature compensated)



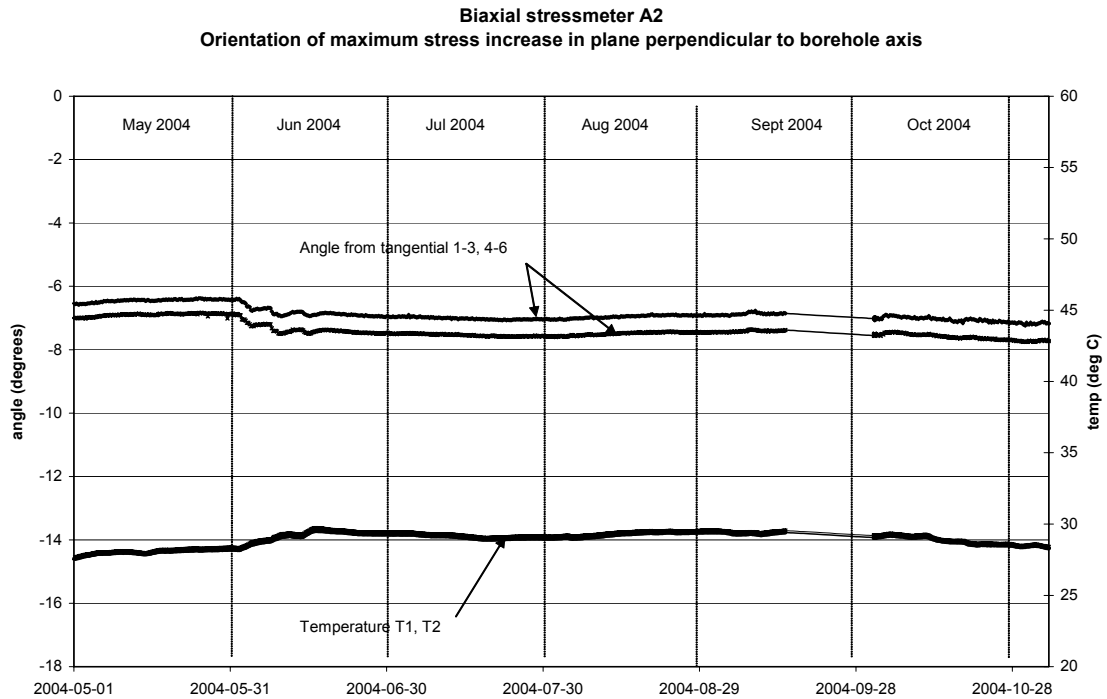
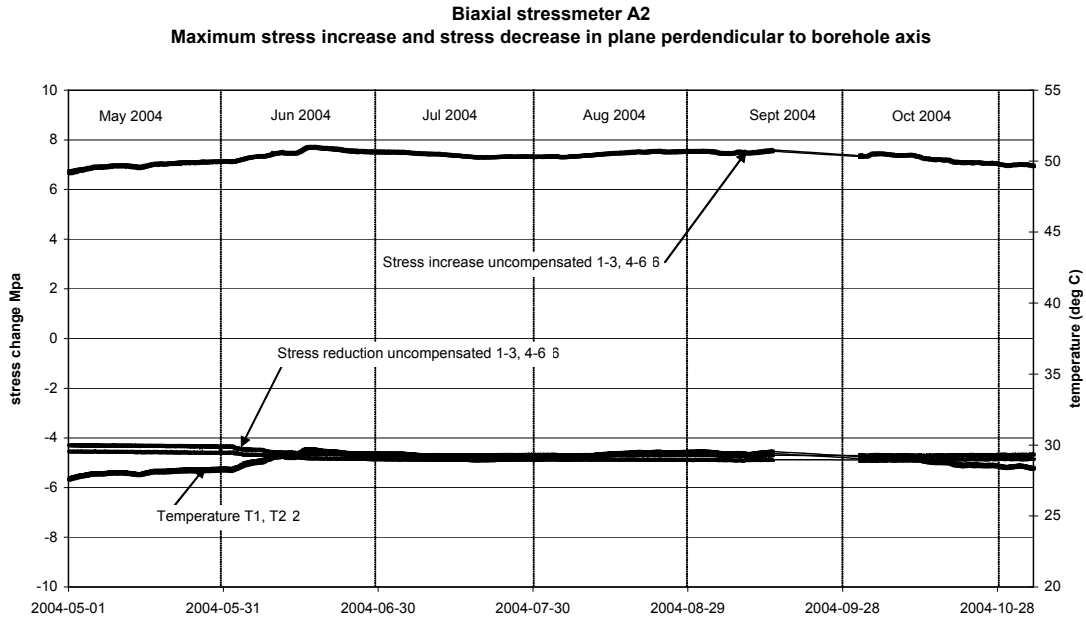
Positive values of microstrain represent elongation

Results of canister hole 2

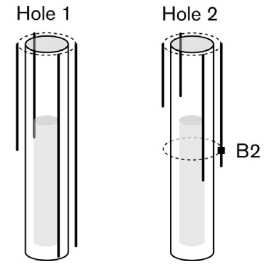


5.1.4 Stress change for each biaxial stressmeter

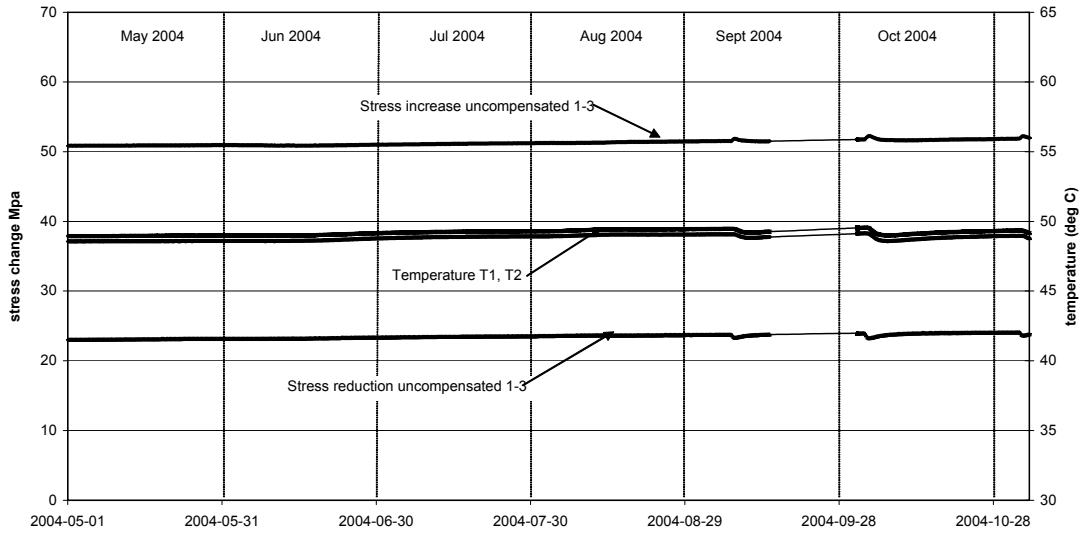
Biaxial stressmeter A2 uncompensated for temperature:



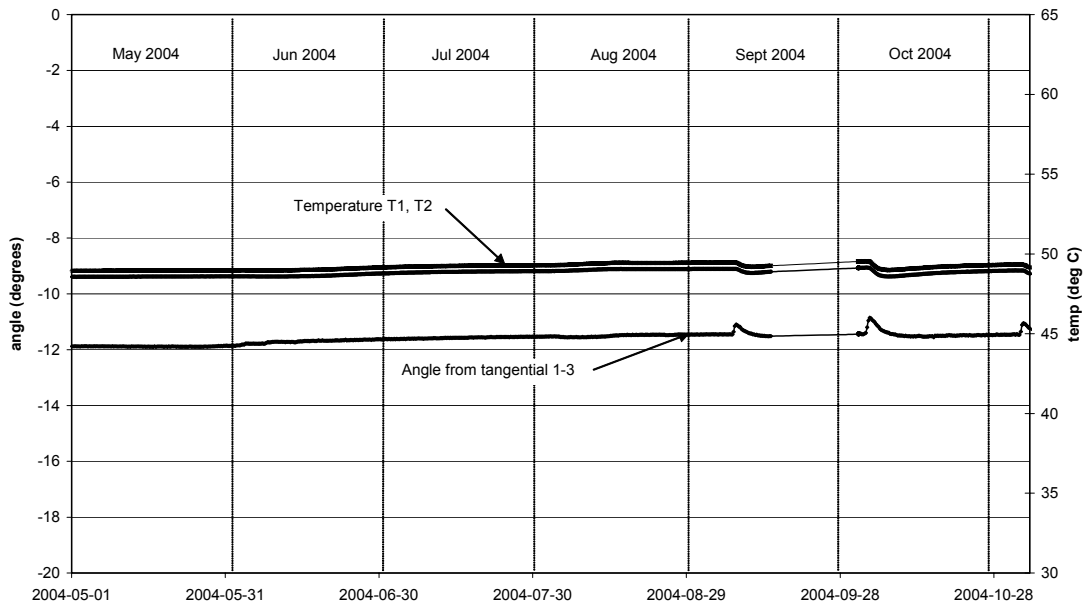
Biaxial stressmeter B2 uncompensated for temperature:



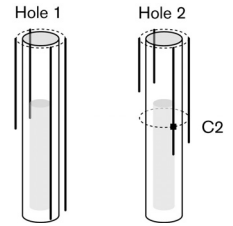
Biaxial stressmeter B2
Maximum stress increase (σ_1) in plane perpendicular to borehole



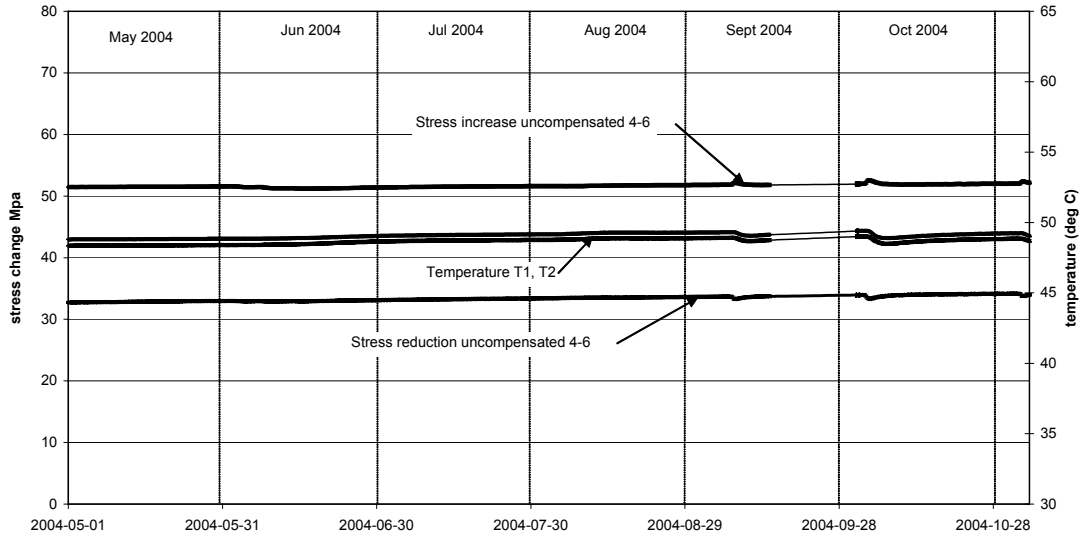
Biaxial stressmeter B2
Orientation of maximum stress increase (σ_1) in plane perpendicular to borehole



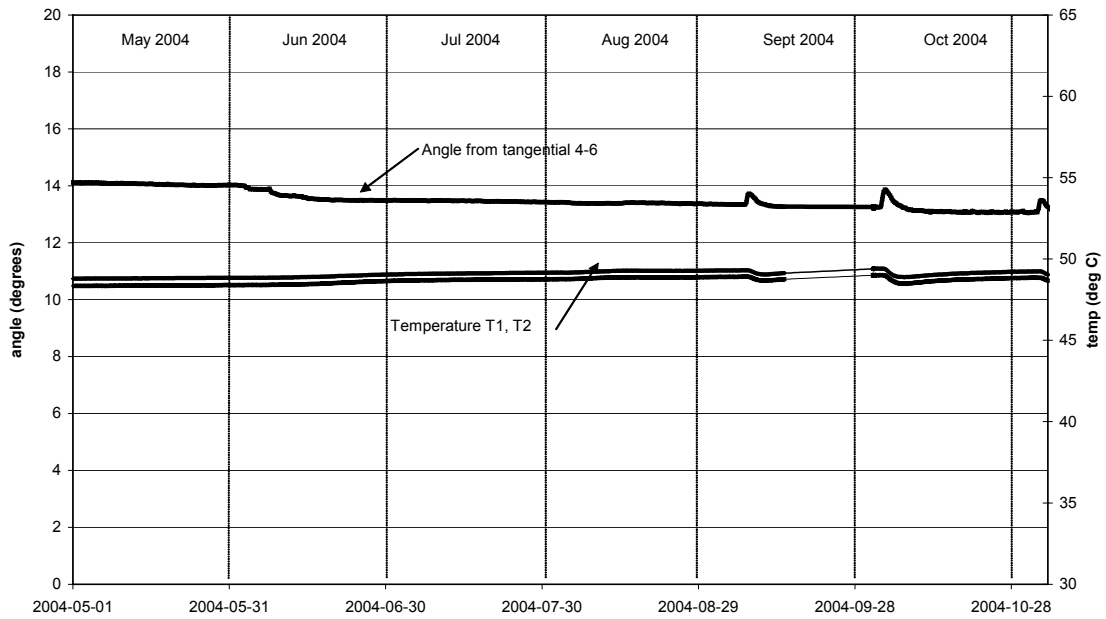
Biaxial stressmeter C2 uncompensated for temperature:



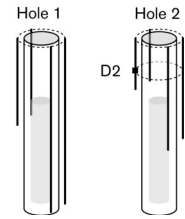
Biaxial stressmeter C2
Maximum stress increase and stress reduction in plane perpendicular to borehole axis



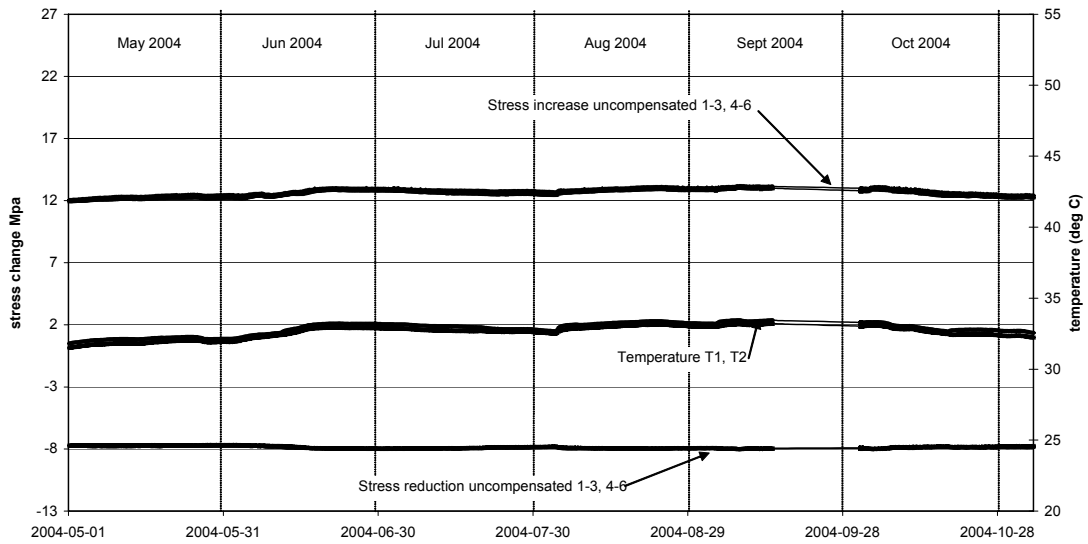
Biaxial stressmeter C2
Orientation of maximum stress increase in plane perpendicular to borehole axis



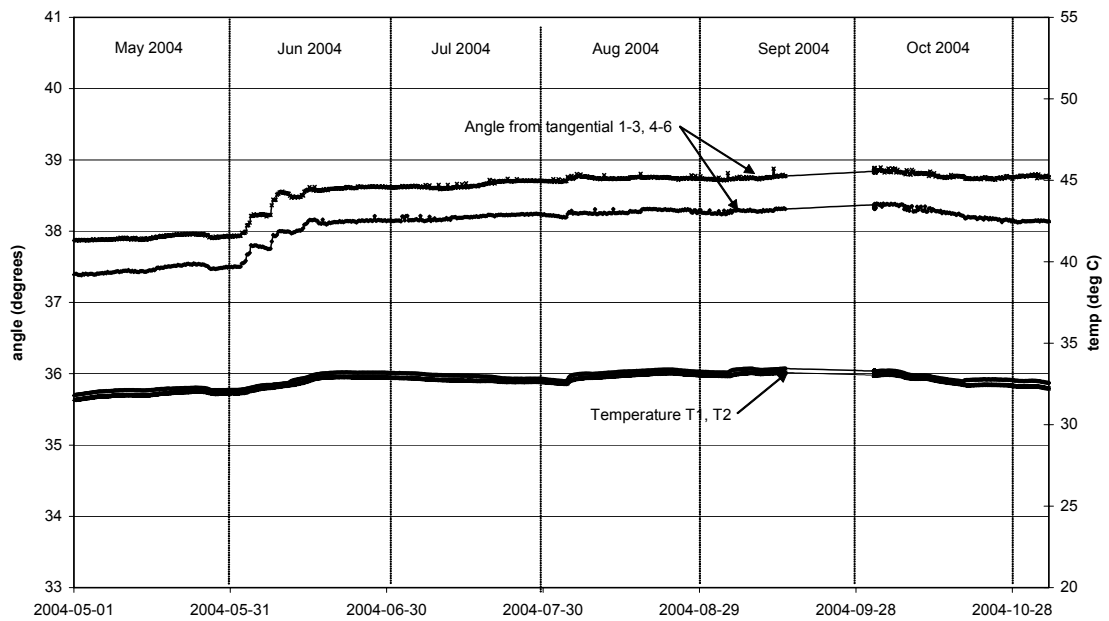
Biaxial stressmeter D2 uncompensated for temperature:



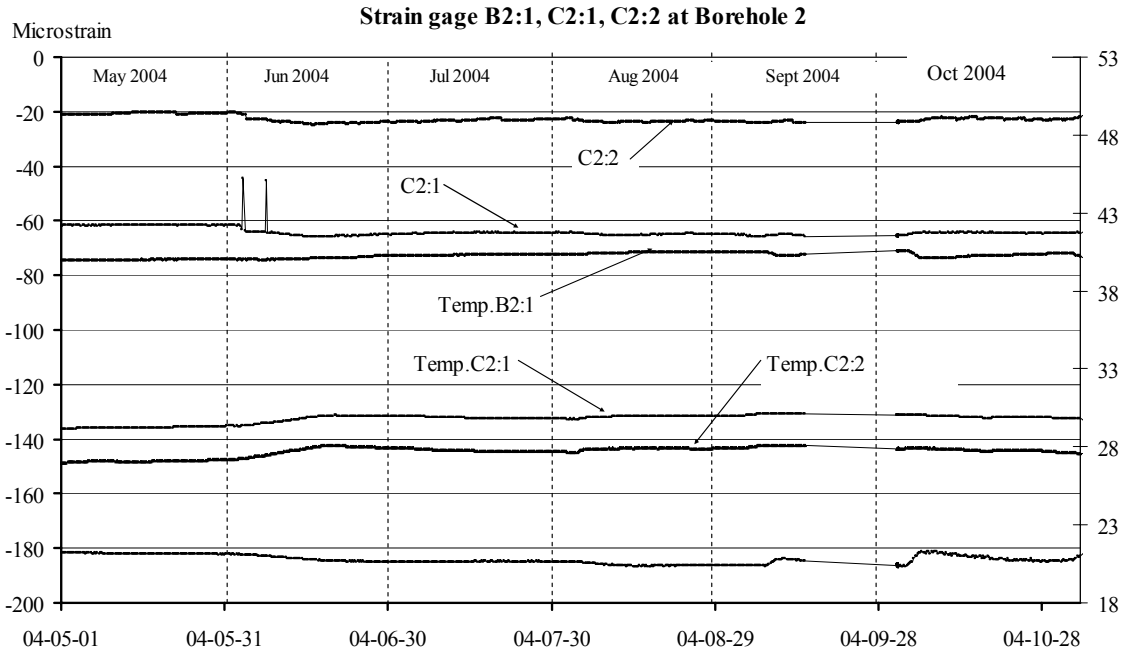
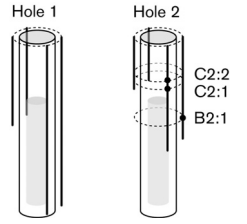
Biaxial stressmeter D2
Maximum stress increase and stress reduction in plane perpendicular to borehole axis



Biaxial stressmeter D2
Orientation of maximum stress increase in plane perpendicular to borehole axis



5.1.5 Strainmeter B2:1, C2:1, C2:2 (temperature compensated)



Positive values of microstrain represent elongation